Reviews and Syntheses: Carbonyl Sulfide as a Multi-scale Tracer for Carbon and Water Cycles

Mary E. Whelan[1,2], Sinikka T. Lennartz[3], Teresa E. Gimeno[4], Richard Wehr[5], Georg Wohlfahrt[6], Yuting Wang[7], Linda M. J. Kooijmans[8], Timothy W. Hilton[2], Sauveur Belviso[9], Philippe Peylin[9], Róisín Commane[10], Wu Sun[11], Huilin Chen[8], Le Kuai[12], Ivan Mammarella[13], Kadmiel Maseyk[14], Max Berkelhammer[15], King-Fai Li[16], Dan Yakir[17], Andrew Zumkehr[2], Yoko Katayama[18], Jérôme Ogée[4], Felix M. Spielmann[6], Florian Kitz[6], Bharat Rastogi[19], Jürgen Kesselmeier[20], Julia Marshall[21], Kukka-Maaria Erkkilä[13], Lisa Wingate[4], Laura K. Meredith[22], Wei He[8], Rüdiger Bunk[20], Thomas Launois[4], Timo Vesala[13,23,24], Johan A. Schmidt[25], Cédric G. Fichot[26], Ulli Seibt[11], Scott Saleska[5], Eric S. Saltzman[27], Stephen A. Montzka[28], Joseph A. Berry[1], J. Elliott Campbell[29]

[1]Carnegie Institution for Science, 260 Panama St., Stanford, CA, USA, 94305
[2]University of California, Merced, 5200 N. Lake Rd., Merced, CA, USA, 95343
[3]GEOMAR Helmholtz-Centre for Ocean Research Kiel, Duesternbrooker Weg 20, Kiel, Germany, 24105
[4]INRA, UMR ISPA, 71 Avenue Edouard Bourleaux, F-33140, Villenave d'Ornon, France
[5]Department of Ecology and Evolutionary Biology, University of Arizona, 1041 E. Lowell St., Tucson, USA, 85721
[6]University of Innsbruck, Institute of Ecology, Sternwartestr. 15, Innsbruck, Austria, 6020
[7]Institute of Environmental Physics, University of Bremen, Otto-Hahn-Allee 1, Bremen, Germany, 28359
[8]Centre for Isotope Research, University of Groningen, Nijenborgh 6, Groningen, The Netherlands, 9747 AG
[9]Laboratoire des Sciences du Climat et de l'Environnement, CEA-CNRS-UVSQ, Orme des Merisiers, Gif-sur-Yvette, France, 91191
[10]Harvard School of Engineering and Applied Sciences, 20 Oxford Street, Cambridge, USA, 2138
[11]Department of Atmospheric and Oceanic Sciences, University of California, Los Angeles, 405 Hilgard Ave., 7127 Math Sciences Building, Los Angeles, CA, USA, 90095-1565
[12]UCLA Joint Institute for Regional Earth System Science and Engineering (JIFRESSE) | Jet Propulsion Laboratory, Caltech, 4800 Oak Groove Dr., M/S 233-200, Pasadena, CA, USA, 91109
[13]Department of Physics, PO Box 68, FI-00014, University of Helsinki, Finland
[14]School of Environment, Earth and Ecosystem Sciences, The Open University, Walton Hall, Milton Keynes, UK, MK17 8NY
[15]Department of Earth and Environmental Sciences, University of Illinois at Chicago, Chicago, IL, USA, 60607
[16]Environmental Sciences, University of California, Riverside, 900 University Ave, Geology 2460, Riverside, USA, CA 92521
[17]Earth and Planetary Sciences, Weizmann Instiutute of Science, 234 Herzl st., Rehovot, Israel, 76100

[18]Institute of Agriculture, Tokyo University of Agriculture and Technology, 3-5-8 Saiwai-cho, Fuchu, Tokyo, Japan, 183-8509

[19]Forest Ecosystems and Society, Oregon State University, 374 Richardson Hall , Corvallis, USA, 97333

5   [20]Max Planck Institute for Chemistry, Department of Multiphase Chemistry, P.O. Box 3060, Mainz, Germany, 55020

[21]Max Planck Institute for Biogeochemistry, Hans-Knöll-Str. 10, Jena, Germany, 7745

[22]School of Natural Resources and the Environment, University of Arizona, 1064 E. Lowell St., Tucson, USA, 85721

10   [23]University of Helsinki, Department of Forest Sciences, PO Box 27, FI-00014, University of Helsinki, Finland

[24]Viikki Plant Science Centre, University of Helsinki, FI-00014, Helsinki, Finland

[25]University of Copenhagen, Department of Chemistry, Universitetsparken 5, Copenhagen, Denmark, DK-2100

15   [26]Department of Earth and Environment, Boston University, 675 Commonwealth Avenue, Boston, MA, USA, 02215

[27]Department of Earth System Science/University of California, Irvine, University of California, Irvine, Irvine, CA, USA, 92697-3100

[28]NOAA/ESRL/GMD, 325 Broadway, Boulder, USA, 80305

20   [29]Environmental Studies Department, UC Santa Cruz, 1156 High St., Santa Cruz, CA, USA, 95064

Correspondence to: Mary E. Whelan (mary.whelan@gmail.com)

Abstract. For the past decade, observations of carbonyl sulfide (OCS or COS) have been investigated

25   as a proxy for carbon uptake by plants. OCS is destroyed by enzymes that interact with CO_2 during

photosynthesis, namely carbonic anhydrase (CA) and RuBisCO, where CA is the more important. The

majority of sources of OCS to the atmosphere are geographically separated from this large plant sink,

whereas the sources and sinks of CO_2 are co-located in ecosystems. The drawdown of OCS can

therefore be related to the uptake of CO_2 without the added complication of co-located emissions

30   comparable in magnitude. Here we review the state of our understanding of the global OCS cycle and

its applications to ecosystem carbon cycle science. OCS uptake is correlated well to plant carbon

uptake, especially at the regional scale. OCS can be used in conjunction with other independent

measures of ecosystem function, like solar-induced fluorescence and carbon and water isotope studies.

More work needs to be done to generate global coverage for OCS observations and to link this powerful

atmospheric tracer to systems where fundamental questions concerning the carbon and water cycle remain.

1 Introduction

Carbonyl sulfide (OCS or COS) observations have emerged as a tool for understanding terrestrial
5 carbon uptake and plant physiology. Some of the enzymes involved in CO_2 assimilation by leaves (mainly carbonic anhydrase, CA) also efficiently destroy OCS, so that leaves consume OCS whenever they are assimilating CO_2 (Protoschill-Krebs and Kesselmeier, 1992; Schenk et al., 2004; Notni et al., 2007). Moreover, because the two molecules diffuse from the atmosphere to the enzymes along a shared pathway, the rates of OCS and CO_2 uptake tend to be closely related (Seibt et al., 2010) — although the
10 rate of OCS is about 1 million times lower than that of CO_2, owing to the ratio of their natural abundances. CO_2 uptake is difficult to measure by itself because the simultaneous respiration of CO_2 is conflated with photosynthetic CO_2 assimilation. The advantage of measuring OCS to estimate CO_2 uptake is that leaves do not produce OCS. Measurements of OCS concentrations and fluxes can therefore generate estimates of photosynthesis, or of other leaf parameters like stomatal conductance, at
15 otherwise inscrutable temporal and spatial scales. This is particularly true at ecosystem, regional, and global scales, where the large respiratory CO_2 fluxes from other plant tissues and other organisms further obscure the photosynthetic CO_2 signal, i.e. gross primary productivity (GPP).

Several independent groups examined OCS and CO_2 observations and came to similar conclusions
20 about links between the plant uptake processes for the two gases. Goldan et al., (1988) were the first to link OCS plant uptake, F_{OCS}, to that of CO_2, F_{CO2}, specifically referring to GPP. Advancing the global perspective, Chin and Davis (1993) thought F_{OCS} was connected to net primary productivity, which includes respiration terms, and this scaling was used in earlier versions of the OCS budget, e.g. Kettle et al., (2002). Sandoval-Soto et al., (2005) re-introduced GPP as the link to F_{OCS}, using available GPP
25 estimates to improve OCS and S budgets, which were their prime interest. Montzka et al. (2007) first proposed to reverse the perspective in the literature and suggested that OCS might be able to supply

3

constraints on gross CO_2 fluxes, with Campbell et al., (2008) probably the first to directly apply it in this way.

Since then, other applications have been developed, including understanding of terrestrial plant
5   productivity since the last ice age (Campbell et al., 2017a), assessment of the current generation of continental-scale carbon models (e.g. Hilton et al., 2017), and better tracing of large-scale atmospheric processes like convection and tropospheric-stratospheric mass transfers. Many of these applications rely on the fact that the largest fluxes of atmospheric OCS are geographically separated: Most atmospheric OCS is generated in surface oceans and is destroyed by terrestrial plants. In practice, these new
10 applications often call for refining the terms of the global budget of OCS.

New observations have been made possible by technological innovation. While OCS is the longest-lived and most abundant sulfur-containing gas in the atmosphere, its low ambient concentration (~0.5 ppb) relative to other important carbon cycle gases makes measurement challenging. For decades, OCS
15 has been a compound of interest as a source of sulfate to the stratosphere. Quantification of OCS in air used to require time-consuming pre-concentration before injection into a gas chromatograph with a mass spectrometer or other detector. Although extended time series were scarce, a set of observations is being generated by the National Oceanic and Atmospheric Administration (NOAA) Global Air Sampling Network (Montzka et al., 2007). A system for measuring flask samples for a range of
20 important low-concentration trace gases was modified slightly in early 2000 to enable reliable measurements for OCS. These observations allowed for the first robust evidence of OCS as a tracer for terrestrial CO_2 uptake on continental to global scales. In 2009, a quantum cascade laser instrument was developed, followed by many improvements in precision and measurement frequency (Stimler et al., 2010a). Current instruments can measure OCS with < 10 parts-per-trillion precision and a frequency of
25 10 Hz (Kooijmans et al., 2016), which is suitable for eddy covariance (Asaf, et al., 2013; Billesbach et al., 2014) although users of these instruments should be mindful to correct OCS spectra for water vapor interactions (Kooijmans et al., 2016; Bunk et al., 2017). On larger spatial scales, many FTIR stations

and 3 satellites currently in operation have recently been used to retrieve spectral signals for OCS in the atmosphere.

This review seeks to synthesize our collective understanding of atmospheric and biospheric OCS, to highlight the innovative new questions that these data will help answer, and to identify the outstanding knowledge gaps that will need to be addressed moving forward. First, we present what information is known from surface level studies. Then we develop a scaled up global OCS budget that suggests a considerable missing source of OCS to the atmosphere. We examine how the existing data has been applied to estimating GPP and other ecosystem variables. Finally, we describe where data is available and submit a community research plan. The ultimate goal of OCS tracer research is to constrain our estimates of global carbon-climate feedbacks. To this end, we need to perform the modeling studies necessary to determine the location, distribution, and feasibility of a tall tower network that would support regional-scale GPP estimates based on OCS uptake. In support of regional studies, our understanding of processes should be refined: in particular, lab-based studies with water or nutrient-stressed plants are needed. On the global scale, our understanding of the OCS budget needs to be reconciled, determining whether a large missing source is from the oceans or from anthropogenic activity. With these advances, OCS could become an essential tracer of plant CO_2 uptake that operates on temporal and spatial scales where there are currently large knowledge gaps.

2 Global OCS budget

The sulfur cycle is arguably the most perturbed element cycle on Earth. Half of sulfur inputs to the atmosphere come from anthropogenic activity (Rice et al., 1981). OCS is the most abundant and stable of all the sulfur-containing gases. Ambient concentrations of OCS are relatively stable in the short term (months), and in the longer term (millennia) may reflect large-scale changes in global plant cover (Aydin et al., 2016).

Much work has been done to characterize OCS exchange over terrestrial and oceanic ecosystems, but important questions remain. Upscaling ecosystem estimates (Sandoval-Soto et al., 2005) and global transport models with atmospheric measurements (Berry et al., 2013, Suntharalingam et al., 2008)

suggest that there may be a large missing source of OCS, sometimes attributed to the tropical oceans; however, individual observations from ocean vessels do not necessarily support this hypothesis (Lennartz et al., 2017). Most oxic soils only contribute a small flux to the overall ecosystem OCS exchange, but some agricultural soils have been shown to contribute large emissions to the atmosphere that offset up to 25% of the total OCS uptake flux (Kitz et al., 2017; Maseyk et al., 2014; Whelan et al., 2016). Process studies with agricultural soils demonstrate a potentially larger source under increasing water content and high soil pore CO_2 (Bunk et al., 2017). No obvious pattern has emerged to explain why some soils exhibit large emissions. Anthropogenic emissions are an important OCS source to the atmosphere, but data for the relevant global industries are incomplete (Zumkehr et al., 2017). Here we analyze our current understanding of global surface-atmosphere OCS exchange and generate new global flux estimates from the bottom up, with no attempt at balancing the atmospheric budget (Fig. 1). In this article, we use the convention that positive flux represents emission to the atmosphere and negative flux represents uptake by the ecosystem.

2.1 Atmosphere

Our understanding of the OCS balance in the atmosphere has evolved as new observations have become available. The major atmosphere-based sinks of OCS are reaction within the troposphere and photolysis in the stratosphere. The tropospheric sink owing to oxidation by OH is estimated to be in the range 82–130 Gg S y^{-1} (Berry et al., 2013; Kettle et al., 2002; Watts, 2000), and the stratospheric sink is in the range 30–80 Gg S y^{-1}, or 50 ± 15 Gg S y^{-1} (Barkley et al., 2008; Chin and Davis, 1995; Crutzen, 1976; Engel and Schmidt, 1994; Krysztofiak et al., 2015; Turco et al., 1980; Weisenstein et al., 1997). Spatial and temporal trends of atmospheric OCS variations also reflect changes of OCS fluxes, including the oceanic and anthropogenic sources, and the biospheric sink.

The spatial and temporal variations in OCS that emerge from observations suggest that seasonality is dominantly influenced by terrestrial uptake in the Northern Hemispheric summer, and by oceanic fluxes in the Southern Hemisphere. The global atmospheric flask sampling network described in Montzka et al. (2007) has served as a basis for understanding the distribution and seasonality of OCS concentrations in

6

both hemispheres at Earth's surface and, from regular aircraft profiles, through much of the troposphere over North America. Improvements in the OCS budget were also derived through inverse modeling of those NOAA observations on a global scale (Berry et al., 2013; Launois et al., 2015b; Suntharalingam et al., 2008). Moreover, lower concentrations were generally found in the terrestrial atmospheric

5   boundary layer compared to the free troposphere during the growing season, and amplitudes of seasonal variability were enhanced at low-altitude stations, particularly those situated in mid-continent (as opposed to coastal marine sites). These lines of evidence all support the notion that OCS is primarily removed from the atmosphere via terrestrial plants during the growing season.

10   Total column measurements of OCS have been made with ground-based Fourier transform spectroscopy (FTS). Within the accuracy of those measurements there was no significant trend detected in stratospheric OCS until 2005. Updates of these records, reanalyzed with methods to increase accuracy (Kremser et al., 2015; Lejeune et al., 2017) do suggest a trend in OCS columns. Kremser et al. found an overall positive tropospheric trend of 0.43–0.73%/y at three sites in the southern hemisphere

15   from 2001 to 2014. However, the increasing trend was interrupted by a sharp decreasing trend from 2008 to 2010. This dip was also observed in the global surface flask measurements (Fig. S2, Campbell et al., 2017a). A similar dip was observed in the stratosphere, but was smaller than in the troposphere. Also, Lejeune et al. (2017) observed changing trends over Jungfraujoch, Switzerland, with a decrease in tropospheric OCS from 1995 to 2002 and an increase from 2002 to 2008; after 2008 there was no

20   significant trend observed. Smaller datasets of OCS vertical profiles could be used to validate these broader trends, e.g. Kato et al. (2011). The generally smaller trends in the stratosphere indicate that the trends are driven by processes within the troposphere (Lejeune et al., 2017). Campbell et al. (2015) presented an inventory of anthropogenic CS_2 (rayon industry) and OCS emissions. The OCS trends observed with FTIR column measurements show close resemblance with global rayon production,

25   which decreased until 1990, then stayed mostly constant until 2002 and increased after that. An increase in OCS concentrations from the mid-20th century with a decline around the 1980s were also recorded in firn air (Montzka et al., 2004).

With the commercially available quantum cascade laser spectrometer (Commane et al., 2013; Kooijmans et al., 2016; Stimler et al., 2010a), continuous atmospheric concentration measurements of OCS allow for regional source and sink studies (Belviso et al., 2016; Kooijmans et al., 2016). In situ vertical profile measurements of OCS have been obtained in the altitude range from 14 to 30 km at

5   tropical and polar latitudes using the SPIRALE, a tunable diode laser spectrometer (Krysztofiak et al., 2015). The uncertainty of the in situ OCS measurements increases with decreasing pressures (higher altitude), ranging from 3.3% below 18 km to more than 30% above 26 km. As more data become available, the OCS budget will become better understood, clarifying the in situ tropospheric and stratospheric sinks for OCS.

10

2.2 Terrestrial ecosystems

Uptake by land plants is thought to represent the most important sink for OCS, estimated to account for 50–82% of the global sink strength, followed by soil (Launois et al., 2015b, and references therein). The yearly average net land flux rate in recent modeling studies of global budgets (i.e. plant and soil uptake

15   minus soil emissions) ranges from -2.5 to -12.9 pmol m^{-2} s^{-1} (Fig. 2). Relative to the many published site-level studies, this is a small range (Fig. 2). The available observations are limited in time and do not cover tropical ecosystems, which contribute almost 60% of global GPP (Beer et al., 2010). The only study reporting year-round OCS flux measurements is from a mixed temperate forest, which was a sink for OCS with a net flux of -4.7 pmol m^{-2} s^{-1} during the observation period (Commane et al., 2015). Daily average

20   OCS fluxes during the peak growing season are available from a larger selection of studies and cover the range from -8 to -23 pmol m-2 s-1, excluding Xu et al., (2002) which found a surprisingly high uptake (−97 ± 11.7 pmol m^{-2} s^{-1}) from the relaxed eddy accumulation method (Fig. 2).

The terrestrial plant OCS uptake has typically been derived by scaling estimates of the plant CO_2 uptake

25   with proportionality coefficients, such as the leaf relative uptake rate ratio (LRU; Sandoval-Soto et al., 2005):

$$F_{OCS} = F_{CO2}[OCS][CO_2]^{-1} LRU \qquad\qquad (1)$$

8

where F_{OCS} is the uptake of OCS into plant leaves, F_{CO2} is CO_2 uptake, [OCS] and $[CO_2]$ are the ambient concentrations of OCS and CO_2, and LRU is the ratio of the OCS to CO_2 uptake, which is a function of plant type and water and light conditions. F_{CO2} is often equated with GPP, however

5 photorespiration in C_3 plants confuses the matter (Wohlfahrt and Gu, 2015). The concept of the LRU has been instrumental, both in calculating the plant OCS sink from estimates of plant CO_2 uptake in global modeling studies and for experimentally estimating GPP from ecosystem-scale OCS flux measurements (e.g. Asaf et al., 2013). For the purpose of this synthesis, we have compiled LRU data (n = 53) from an earlier review and merged them with more recent published studies (Berkelhammer et al.,

10 2014; Stimler et al., 2010b, 2011, 2012). The LRUs compiled in Sandoval-Soto et al., (2005) were partly re-calculated in Seibt et al., (2010) to account for the lower gas concentrations in the sample cuvettes.. As shown in Fig. 3, LRU estimates for C_3 species under well-illuminated conditions are positively skewed, with 95 % of the data between 0.7 to 6.2, which coincides with the expected range of 0.6 to 4.3 predicted by Wohlfahrt et al. (2012) on a theoretical basis. The median, 1.68, is quite close to

15 values reported/used in earlier studies (e.g. Asaf et al., 2013; Berkelhammer et al., 2014) and provides a solid "anchor ratio" for linking C_3 plant OCS uptake and photosynthesis in high light. LRU data are fewer for C_4 species (n = 4) converging to a median of 1.21, reflecting more efficient CO_2 uptake rates compared to C_3 species (Stimler et al., 2011). The causes for the observed variability in Fig. 3, whether reflective of differences in environmental conditions or differences between plant species (e.g. in leaf

20 internal conductance for OCS or in carbonic anhydrase activity), are still poorly understood and hamper the specification of defensible plant functional type-specific LRUs (Sandoval-Soto et al., 2005) and the development of models with non-constant LRU (Wohlfahrt et al., 2012).

As detailed by Seibt et al. (2010) and Wohlfahrt et al. (2012), the LRU remains fairly constant with

25 changes in boundary layer and stomatal conductance but is expected to deviate due to changes in internal OCS conductance and CA activity. The primary environmental driver of LRU is light, and an increase in LRU with decreasing photosynthetically active radiation has been observed at both the leaf (Stimler et al., 2010b, 2011) and ecosystem scale (Maseyk et al., 2014; Commane et al., 2015, Wehr et

al., 2017). This behavior arises because photosynthetic CO_2 assimilation is reduced in low light whereas OCS uptake continues since the reaction with CA is not light dependent (Stimler et al., 2011). Relatively little is known regarding CA activity (Wehr et al., 2017), while changes in stomatal and leaf internal conductances in response to environmental stresses are well known (e.g. Brilli et al., 2011).

5

Despite the limited temporal and spatial coverage, these data suggest that some of the larger global land net sink estimates may be too high (see also Launois et al., 2015b). Soils contain processes that both emit and consume OCS (Sun et al., 2015; Whelan et al., 2016), with a few studies reporting net OCS emission under certain conditions comparable in magnitude to net uptake rates during peak growth (Fig. 2). At present, the processes and drivers underlying these emissions are poorly understood – some evidence points to photo/thermo-production from dead plant matter playing a role (Kitz et al., 2017; Whelan et al., 2016; Whelan and Rhew, 2015). More year-round measurements from a larger number of biomes, in particular those presently underrepresented, are required to provide reliable bottom-up estimates of the total net land OCS flux (see Fig. 1).

15

2.2.1 Grasslands

Grasslands cover ~20% of the terrestrial surface and store ~30% of the world's soil carbon (Hungate et al., 1997; Scurlock and Hall, 1998). Although grasslands store less carbon per area than forests, they are more ubiquitous and contain a larger portion of the terrestrial carbon pool (Parton et al., 1995). Grasslands generally are considered to behave as carbon sinks or be carbon-neutral but appear highly sensitive to drought and heat waves and can rapidly shift from neutrality to a carbon source (Hoover and Rogers, 2016). Studies on the response of grasslands to elevated CO_2 suggest that the sink strength temporarily increases. Because much of this carbon is stored as labile pools, it is unclear whether the effect has long-term consequences (Hungate et al., 1997). The lability of these pools and their dynamics are difficult to study and point to important uncertainties and challenges in projecting the role these ecosystems will play in a changing carbon cycle. Existing work highlights the need for additional studies on primary productivity in grassland ecosystems, which could be addressed with OCS observations.

Studies of OCS exchange in native or restored grasslands have been limited (see Fig. 2). Theoretical deposition velocities for grasses of 0.75 mm s^{-1} were reported by Kuhn et al. (1999) and LRU values of 2.0 were reported by Seibt et al. (2010). In an early field-based study on the topic, Mihalopoulos et al.

5   (1989) noted uptake of OCS when winds passed over a coastal grassland in northwestern France. More recently, Whelan and Rhew (2016) presented chamber-based estimates of ecosystem fluxes from a California grassland with a Mediterranean climate. They found total ecosystem fluxes of -26 pmol m^{-2} s^{-1} during the wet season and -6.1 pmol m^{-2} s^{-1} during the dry season. Individual flux estimates ranged from -75 pmol m^{-2} s^{-1} to +7 pmol m^{-2} s^{-1}, indicating a wide range of possible fluxes. During the dry

10   season, simulated rain led to a reduced sink or an increased source. During the wet season, simulated moisture increased the sink strength. While this study did not separate soil and plant components of the flux, light and dark flux estimates yielded similar sinks, suggesting either a large role for soils in the ecosystem flux or the presence of open stomata under dark conditions. In a similar study, Yi and Wang (2011) undertook chamber measurements over a grass lawn in subtropical China. Ecosystem fluxes of -

15   19.2 pmol m^{-2} s^{-1} were observed. They noted soil fluxes on average of -9.9 pmol m^{-2} s^{-1} that were occasionally greater than 50% of the total ecosystem flux. The large contribution of soils to the grassland OCS flux was attributed to atmospheric water stress on the plants that led to significant stomatal closure and reduced midday uptake by vegetation. More recently, Gerdel et al. (2017) reported daily average ecosystem-scale OCS fluxes of -28.7 ± 9.9 pmol m^{-2} s^{-1} for a productive managed

20   temperature grassland.

Solar radiation has been identified recently as a controlling factor of grassland soil flux. Kitz et al. (2017) used transparent chambers over a temperate grassland soil with plants removed. This study found high production of OCS (up to 60 pmol m^{-2} s^{-1}) and revealed the dominant influence of radiation,

25   as opposed to moisture, on the soil flux. Although positive fluxes from grassland soils have been noted elsewhere with both opaque and transparent chambers (Berkelhammer et al., 2014; Maseyk et al., 2014; Whelan and Rhew, 2016), the magnitude of the OCS emissions from bare soils significantly exceeded measurements made elsewhere. Kitz et al. (2017) highlighted that in grasslands, primary production is

11

devoted to belowground biomass early in the growing season, leading to a situation where exposed soils may be emitting photo-produced OCS simultaneously with high GPP. If unaccounted for, this would lead to an underestimation of the plant component of the total ecosystem OCS flux (Kitz et al., 2017; Whelan and Rhew, 2016).

5

Existing studies suggest a pressing need to understand how soil OCS fluxes evolve in grasslands during seasonal changes in leaf area index (i.e. changes in surface exposure to radiation). This would involve sustained chamber measurements as well as total ecosystem flux measurements. An issue that has not been addressed in previous work, but is critical, is that grasslands tend to include varying mixtures of C_3

10 and C_4 species whose relative abundance and importance to GPP evolves over the season in response to temperature and soil moisture. These different photosynthetic pathways are known to exhibit different LRU values (see Sect. 2.1 introduction) and are expected to have unique ecosystem relative uptake (ERU) values. Therefore, with seasonal variations in climate, there will be changes in photosynthetic pathways and the relative rate that plants uptake OCS and CO_2. On the one hand, this poses a challenge

15 to direct estimations of GPP from OCS; on the other hand, evolving ERU values may provide a unique opportunity to study C_3 and C_4 contributions to GPP.

2.2.2 Forests

Forests mediate land-atmosphere fluxes of carbon and water (Alkama and Cescatti, 2016) and how

20 forests will respond to climate change is an area of active debate (Metcalfe et al., 2017). OCS has the potential to overcome many difficulties in studying the carbon balance of forest ecosystems. To make flux measurements using eddy flux covariance or vertical concentration gradients, tall forest canopies require even taller towers. To partition carbon fluxes, respiration is often quantified at night when photosynthesis has ceased and turbulent airflow is reduced (Reichstein et al., 2005). This method has

25 important uncertainties, e.g. less respiration happens during the day than at night (Wehr et al., 2016). Partitioning with OCS is based on daytime data and does not rely on modeling respiration with limited nighttime flux measurements and associated uncertainty.

12

As expected, forests are daytime net sinks for atmospheric OCS when photosynthesis is occurring in the canopy (Table 1). While the relative uptake of OCS to CO_2 by leaves appears to be stable in high light conditions, the ratio changes in low light when the net CO_2 uptake is reduced (Stimler et al., 2011; Wehr et al., 2017). Forest soil interaction with OCS has been found to be small (Castro and Galloway,

5 1991; Steinbacher et al., 2004; White et al., 2010; Xu et al., 2002; Yi et al., 2007) and straightforward to correct (Wehr et al., 2017). Sun et al. (2016) noted that litter was the most important component of soil OCS flux in an oak woodland, composing up to 90% of the small surface sink. Otherwise, forest ecosystem OCS uptake appears to be dominated by tree leaves, both during the day and at night (Kooijmans et al., 2017).

10

The OCS tracer approach is particularly useful in high humidity or foggy environments like the tropics, where traditional estimates of carbon uptake variables via water vapor exchange are ineffective (Campbell et al., 2017b). So far, all forest OCS investigations on the ecosystem scale have been in the temperate and boreal zones. There are no published studies from the tropical latitudes, though some

15 studies are underway. The application of the OCS tracer in tall canopies poses difficulties because turbulence can be limited in canopies and complicate many traditional methods of trace gas flux measurements (Blonquist et al., 2011; Kooijmans et al., 2017). A possible solution is using the "surface renewal" approach (Paw U et al., 1995), but it has not been attempted for OCS. Regional scale modeling with OCS appears to sidestep site-level problems, as in Hilton et al., (2017). With more OCS

20 observing towers upstream and downstream of large forested areas, OCS may be able to resolve the daily or weekly carbon uptake by forest ecosystems, a large and crucial component in understanding future climate-carbon feedbacks.

2.2.3 Wetlands and peatlands

25 Wetlands cover approximately 6% of the global land area (Lehner and Döll, 2004), but contribute a proportionally larger amount to the source of reduced sulfur gases to the atmosphere. Much of the early work on OCS terrestrial-atmospheric fluxes was conducted in wetlands, perhaps because of the large emissions observed there. Unfortunately, many of these first surveys were conducted with sulfur-free

13

sweep air, significantly biasing the observed net OCS flux compared with that under ambient conditions (Castro and Galloway, 1991). While it appears that all other terrestrial plants are net sinks of OCS, wetland plants may produce OCS or may act as passive conduits for gases produced in the soil (Whelan et al., 2013).

5

OCS fluxes have been measured in a variety of wetland ecosystems, including tundra, coastal salt marshes, tidal flats, mangrove swamps, and freshwater marshes. Observed ecosystem emission rates vary by two orders of magnitude and generally increase with salinity (Fig. 4). OCS emissions in salt marshes usually range from 10 to 300 pmol m^{-2} s^{-1} (Aneja et al., 1981; DeLaune et al., 2002; Li et al., 2016; Steudler and Peterson, 1984, 1985; Whelan et al., 2013), whereas freshwater marshes and tundra bogs have mean emission rates below 10 pmol m^{-2} s^{-1} (DeLaune et al., 2002; Fried et al., 1993) or act as net sinks due to plant uptake (Fried et al., 1993; Liu and Li, 2008; de Mello and Hines, 1994). OCS exchange in brackish wetlands has been reported only in DeLaune et al. (2002), which found similar emission rates compared with saline coastal wetlands.

15

Although plants are generally OCS sinks, wetland plants may appear as OCS sources if their stems act as conduits transmitting OCS produced in the soil to the atmosphere, or OCS may be a by-product of processes related to osmotic management by plants in saline environments. For example, in a *Batis maritima* coastal marsh, vegetated plots were found to have up to four times more OCS emission than soil-only plots (Whelan et al., 2013). The life cycle of wetland plants may also influence their ability to transmit belowground trace gases to the atmosphere, due to variation in the plant structures involved in gas transport, e.g. rooting depth and plant height (Chanton et al., 1997). Growing season plant–soil system OCS emission may greatly exceed that in the non-growing season (Li et al., 2016), but whether this is caused by environmental factors like temperature and soil saturation or by the developmental stage of plants is unclear. Assessing the role of plants in the wetland OCS budget would require careful investigation of OCS transport via plant stems and OCS producing capacity of aboveground plant materials and the rhizosphere.

The contribution of global wetlands to the atmospheric OCS budget needs to be better constrained to assess regional importance and whether wetland OCS emissions will affect other applications of the OCS tracer, e.g. interpretation of historical GPP changes from ice core data when wetlands were more prevalent. Often global ecosystem models do not have the resolution necessary to take into account

5   wetland contributions, though there is a potential for significant effects (Whelan et al., 2013). What happens to wetland OCS exchange following land use change (for example, saltwater intrusion into freshwater marshes)? Would we then be able to discern the effect of sea level rise on the global OCS budget as coastal wetlands are inundated and destroyed? We need to characterize soil and vegetation components of OCS exchange across major wetland types, make longer-term observations of wetland

10   OCS exchange to understand the environmental controls over variability, and implement wetland OCS processes in land biosphere models for regional and global simulations.

2.2.4 Lakes and rivers

Freshwaters are supersaturated with CO_2 (Cole et al., 1994), contributing significant emissions to the global atmospheric carbon budget (Bastviken et al., 2011). The role of lakes and rivers in the global

15   OCS budget is not well known. OCS production and consumption have been studied in ocean waters, and these processes most likely occur similarly in lakes and rivers. In the ocean, OCS is produced photochemically from chromophoric dissolved organic matter (CDOM) (Ferek and Andreae, 1984) and by a light-independent production that has been linked to sulfur radical formation (Flöck et al., 1997; Zhang et al., 1998). Recently, a mechanism for OCS photo-production was described for lake water (Du

20   et al., 2017). Dissolved OCS (Fig. 4) is consumed by hydrolysis at a rate determined by pH, salinity, and temperature (Fig. 5.; Elliott et al., 1989).

OCS is present in freshwaters at much higher concentrations than those found in the ocean (Table 2). This might be due to more efficient mixing in the ocean surface waters compared to lakes. However,

25   Richards et al. (1991) found that the concentration remained at the same level throughout the water column and observed a midsummer OCS concentration minima in 8 of the 11 studied lakes. This latter point was surprising because photochemical production should be highest during the summer months. It

15

has been demonstrated that ocean algae take up OCS, which might explain the low concentrations when light levels are high; however, Blezinger et al. (2000) concluded that the consumption term should be small compared to hydrolysis and photo-production.

5   To our knowledge, there have not yet been any studies on OCS fluxes using direct flux measurement methods over freshwaters. Richards et al. (1991) calculated OCS fluxes from different lakes in Ontario, Canada, based on concentration measurements and wind-speed-dependent gas transfer coefficients, resulting in fluxes of 2–5 pmol OCS m^{-2} s^{-1}. In another study, Richards et al. (1994) found fluxes of 2–34 pmol OCS m^{-2} s^{-1} in salty lakes. These fluxes are 5 to 75 times higher than those measured in the

10   oceans (Lennartz et al., 2017). In addition to direct emissions of OCS from freshwaters, there is also an indirect atmospheric OCS source from carbon disulfide (CS_2) production (Richards et al., 1991, 1994), which can be oxidized into OCS (Wang et al., 2001).

It is easier to take measurements in lakes than on the open ocean while generating more information on

15   the processes that may drive OCS production in both regions. To support this, flux data by eddy covariance (EC) and floating chamber methods from lakes and rivers are required. For proper interpretations of EC fluxes, one needs to monitor other variables in addition to the OCS flux: downwelling and upwelling radiation, wind velocity, friction velocity, CS_2, CO_2, sensible and latent heat fluxes, water temperature, water-surface OCS concentration, pH, and CDOM. These measurements

20   would facilitate understanding of the biotic and abiotic factors driving water–air exchange of OCS and would provide the basis for upscaling aquatic OCS balances.

2.3 Other terrestrial OCS flux components

25   Other ecosystem components contribute to the total OCS exchange in natural systems. The direction of flux is often determined by temperature and moisture conditions. For example, when conditions are hot and dry, abiotic processes in soil or biotic production in bryophytes can sometimes overtake consumption, resulting in an OCS source to the atmosphere (Gimeno et al., 2017; Whelan et al., 2016). Under specific circumstances, these additional fluxes may be important regionally or at the site level.

16

2.3.1 Soils

The contribution of soils to the atmospheric budget of OCS has been studied for a few decades in both the field and the laboratory. The soil–atmosphere exchange of OCS has been measured in a range of
5   environments, and these measurements show that soil is predominantly a sink for OCS in non-wetland soils. Wetland (anoxic) soils are typically a source of OCS, but OCS production has also been observed in some agricultural oxic soils.

In the field, reported oxic soil OCS fluxes range from near zero up to -10 pmol m^{-2} s^{-1}, with average
10   uptake rates typically between 0 and 5 pmol m^{-2} s^{-1} (see Fig. 7). Higher uptake fluxes of -10 – -20 pmol m^{-2} s^{-1} have been observed in a grassland soil (Whelan and Rhew, 2016), wheat field soils (Kanda et al., 1995; Maseyk et al., 2014), unplanted rice paddies (Yi et al., 2008) and bare lawn soil (Yi and Wang, 2011). However, under warm and dry conditions, fluxes approached zero in grasslands (Berkelhammer et al., 2014; Whelan and Rhew, 2016) and an oak woodland (Sun et al., 2016). The highest reported
15   fluxes are nearly -40 pmol m^{-2} s^{-1}, following simulated rainfall in a grassland (Whelan and Rhew, 2016). Sun et al. (2016) also reported a rapid response to re-wetting following a rainstorm in a dry Mediterranean woodland.

Variations in soil OCS fluxes measured in the field have been linked to temperature, soil water content,
20   nutrient status, and CO_2 fluxes. Uptake rates have been found to increase with temperature (White et al., 2010; Yi et al., 2008) but also decrease with temperature such that OCS fluxes approached zero or shifted to emissions at temperatures around 15–20˚C (Maseyk et al., 2014; Steinbacher et al., 2004; Whelan and Rhew, 2016). It can be difficult to separate the effects of temperature and soil water content in the field, and seasonal decreases in OCS fluxes may also be associated with lower soil water content
25   (Steinbacher et al., 2004; Sun et al., 2016). Uptake rates have also been found to be stimulated by nutrient addition in the form of fertilizer or lime (Melillo and Steudler, 1989; Simmons, 1999).

17

Several studies have found that OCS uptake is also positively correlated with rates of soil respiration, or CO_2 production (Yi et al., 2007), but these relationships vary with temperature (Sun et al., 2016, 2017) or soil water content (Maseyk et al., 2014). The relationship with respiration is attributed to the role of microbial activity in OCS consumption, and similar covariance has been seen between OCS and H_2

5 uptake (Belviso et al., 2013), which is also a microbially driven process. Berkelhammer et al. (2014) and Sun et al. (2017) have also found that the OCS/CO_2 flux ratio has a non-linear relationship with temperature, such that the ratio decreases (becomes more negative) at lower temperatures but is constant at higher temperatures. The links between OCS and CO_2 production extend to the litter layer (Kesselmeier and Hubert, 2002; Sun et al., 2016). Kesselmeier and Hubert (2002) observed both OCS

10 uptake and emission by beech leaf litter that was related to microbial respiration rates, a finding that may indicate OCS production within an elevated CO_2 environment, and Sun et al. (2016) determined that most of the soil OCS uptake in an oak woodland occurred in the litter layer.

Extensive laboratory studies have added further insight into the mechanisms underlying soil OCS

15 exchange, demonstrating that OCS uptake is mainly governed by biological activity and physical constraints. Kesselmeier et al. (1999), van Diest and Kesselmeier (2008), and Whelan et al. (2016) characterized the response of several controlling variables such as atmospheric OCS mixing ratios, temperature and soil water content or water-filled pore space, demonstrating clear temperature and soil water content optima for OCS consumption. These optima vary with soil type but indicate water

20 limitation at low soil water content and diffusion resistance at high soil water content, and are responses characteristic of biological processes. Additionally, other organism-mediated or abiotic processes in the soil, such as photo- or thermal degradation of soil organic matter (Whelan and Rhew, 2015), can play an important role in terrestrial–atmospheric OCS exchange. Under typical conditions, most soil is a small sink of OCS, probably due to the prevalence of carbonic anhydrase in microbial communities

25 (Kesselmeier et al., 1999).

Soil OCS emissions are usually associated with anoxic wetland soils (Aneja et al., 1981; Kanda et al., 1992; Whelan et al., 2013; Yi et al., 2008), due to the strong activity of sulfate reduction metabolism in

anoxic environments (Schlesinger and Bernhardt, 2012). Much early work on the subject used sulfur-free sweep air leading to biased results, and few soil-only field measurements with ambient air exist, e.g. Whelan et al., (2013) found fluxes ranging from 1 to 27 pmol m^{-2} s^{-1}. We integrate a "global" estimate of wetland fluxes in Sect. 2.7. Temperature and redox potential are major abiotic drivers

5   controlling OCS production from wetland soils. Temperature probably drives the observed seasonal variation of OCS production, with higher fluxes in the summer than winter (Whelan et al., 2013). Soil redox potential is an indicator of soil oxidation-reduction status and is positively related to oxygen content in the soil column (Patrick and DeLaune, 1977).

10   OCS exchange rates in wetland soils may also depend on transport in the soil column. Tidal flooding inhibits OCS emission from wetland soils, perhaps due to decreasing gas diffusivity with increasing soil saturation rather than changes in OCS production rates (Whelan et al., 2013). If OCS produced by microbes accumulates in isolated soil pore spaces during inundation, subsequent ventilation can lead to abrupt release of OCS, which may appear as high variability in surface OCS emissions. However, the

15   interaction between production and transport processes in driving OCS exchange variability remains poorly understood. Known abiotic contributions, e.g. the role of solubility, are detailed in Sect. 2.3.3 Abiotic processes.

Recent field and laboratory studies have shown that OCS production is also occurring in oxic soils.

20   Substantial OCS production has been observed in a temperate grassland under both wet and dry conditions (Kitz et al., 2017) and in a wheat field under dry conditions (Maseyk et al., 2014). Related strongly to temperature (Maseyk et al., 2014) and radiation (Kitz et al., 2017), OCS fluxes of up to +30 and +60 pmol m^{-2} s^{-1} were observed in the wheat field and grassland, respectively. These production rates are similar, or even exceed, those seen in waterlogged environments. OCS fluxes from rice

25   paddies were ca. +10 pmol m^{-2} s^{-1}, but sometimes exceeded +40 pmol m^{-2} s^{-1} (Kanda et al., 1992; Yi et al., 2008), and from vegetated salt marshes are +40–+120 pmol m^{-2} s^{-1} (Aneja et al., 1981; Whelan et al., 2013). However, saline wetlands cover a small portion of the Earth's surface (roughly 10^4 km^2) whereas agricultural areas are widespread (more than 10^7 km^2).

Soil OCS production has been investigated through laboratory incubations (Bunk et al., 2017; Whelan et al., 2016; Whelan and Rhew, 2015), revealing that most soils experience abiotic OCS emissions. Whelan et al. (2016) measured OCS soil fluxes from six disparate study sites: Soils from a temperate

5   forest, a tropical forest, a savannah, and two agricultural fields > 800 km apart all exhibited net OCS emissions under hot and dry conditions. Desert soil samples generated no emissions and only small OCS uptake. Whelan and Rhew (2015) compared sterilized to living soil samples from the agricultural study site originally investigated in Maseyk et al. (2014), finding that all samples emitted considerable amounts of OCS under high ambient temperature and radiation, with even higher emissions after

10 sterilization. Recently, Bunk et al. (2017) showed that net OCS emissions can occur from agricultural soils at all water contents.

The recent evidence of soil OCS emissions led Launois et al. (2015b) to include an emissions term in their soil flux estimates by upscaling biome-specific emissions. For global fluxes, Launois et al. (2015b)

15 used ranges typically measured for anoxic soil emissions reported by Whelan et al. (2013), which had dependencies on temperature and flooded state. Using a map of estimated anoxic soils used for methane emission estimates (Wania et al., 2010), OCS production was assessed and allowed to vary by ±30% in optimization. Typically, peatlands were probable net emitters of OCS, with a mean value of 25 pmol m^{-2} s^{-1}. Some ecosystems, such as rice paddies, shift from a net source to net sink depending on the

20 flooding state of the soil. Because the reported range of fluxes was centered on 0, Launois et al. (2015b) considered these fields to have net emissions of zero. Peatlands are mainly located in the northernmost regions (above 60˚ N) and were expected to contribute about 101 ±30% Gg S y^{-1} to total emissions combining the wetland extent from Wania et al., (2010) and the estimated mean peatland flux. Seasonality was also indirectly included in soil fluxes because frozen soil was assumed to have a 0 net

25 OCS flux. In the simulation, emission estimates dominated in some extratropical regions of the Northern Hemisphere, turning them into a net source of OCS in late autumn and winter.

20

Recently, two mechanistic models for soil OCS exchange have been developed using diffusion–reaction equations (Ogée et al., 2016; Sun et al., 2015). Both models resolve the vertical transport and the source and sink terms of OCS in soil layers. OCS uptake is represented with the Michaelis–Menten enzyme kinetics, dependent on the OCS concentration in each soil layer, whereas OCS production is assumed to

5   follow an exponential relationship with soil temperature, consistent with field observations (Maseyk et al., 2014). Although diffusion across soil layers neither produces nor consumes OCS, by altering the OCS concentration profile it affects the concentration-dependent uptake of OCS. The mechanistic models that resolve the diffusion process thus have the advantage over empirical models of more realistic evaluation of OCS exchange. The models demonstrate good skill in simulating observed

10   features of soil OCS exchange, such as the responses of OCS uptake to soil water content (Ogée et al., 2016; Sun et al., 2015) and temperature (Ogée et al., 2015) and the transition from OCS sink to source at high soil temperature (Sun et al., 2015). It is hoped that future studies may integrate the mechanistic frameworks of soil OCS exchange into global land models (e.g. Community Land Model or Simple Biosphere Model) to simulate soil OCS fluxes for a better estimate of the global soil OCS budget.

15

2.3.2 Microbial communities

Microbes are key drivers of OCS exchange in terrestrial ecosystem components such soil (Sect. 2.3.2) and in association with plants and other non-vascular photoautotrophic communities (2.3.1). Cyanobacteria, micro-algae, bacteria, and fungi can contribute to net OCS uptake (Gries et al., 1994;

20   Kusumi et al., 2011; Ogawa et al., 2013; Protoschill-Krebs et al., 1995; Smith and Kelly, 1988, Bunk et al., 2017). *Fusarium* and *Trichoderma* spp. that have been isolated from the surfaces of sandstones from ancient monuments and forest soil exhibited OCS uptake (Li et al., 2010; Masaki et al., 2016). Cultured bacteria have been observed to consume OCS, including *Thiobacillus thioparus*, *Mycobacterium* spp., and *Streptomyces* spp. (Kusumi et al., 2011; Ogawa et al., 2016; Smith and Kelly, 1988). Some free-

25   living saprophyte Sordariomycete fungi and *Actinomycetale* bacteria, dominant in many soils, are also capable of degrading OCS (Harman et al., 2004; Nacke et al., 2011). Bacterial OCS degradation in sterilized soil inoculated with *Mycobacterium* sp. showed surprising ability to take up OCS (Kato et al., 2008). In addition, cell-free extract of *Acidianus* sp. also showed significant catalysed hydrolysis of

21

OCS (Smeulders et al., 2011). Performing fungi inhibition experiments in whole soils, Bunk et al., (2017) showed that fungi might be the dominant player in soil OCS uptake.

Both bacteria and fungi, purified from soil environments or from culture collections, show degradation

5 of OCS at atmospheric concentrations. For example, *Mycobacterium* spp. purified from soil and *Dietzia maris* NBRC15801[T] and *Streptomyces ambofaciens* NBRC12836[T] showed significant OCS degradation (Kato et al., 2008; Ogawa et al., 2016), and purified saprotrophic fungi such as *Fusarium solani* and *Trichoderma* spp. were found to decrease atmospheric OCS (Li et al., 2010; Masaki et al., 2016). In addition to the uptake of OCS at atmospheric concentrations, OCS degradation of ppm-level

10 concentrations has been detected in various fungi and bacteria purified from various environments. For example, 38 out of 43 fungi isolated from soil degraded 30 ppm OCS in around 24 hours without any prior acclimation to the high OCS concentrations (Masaki et al., 2016). A change in activity between ambient or ppt-level and ppb-level OCS concentrations suggests that different microbial communities are responsible for OCS consumption in the high and low concentration regimes (Conrad and Meuser,

15 2000).

Biotic OCS production is a possibility: in bacteria, novel enzymatic pathways have been described that degrade thiocyanate and isothiocyanate and render OCS as a byproduct (Bezsudnova et al., 2007; Hussain et al., 2013; Katayama et al., 1992; Welte et al., 2016). Evidence for OCS emissions following

20 SCN⁻ degradation has been observed from a range of environmental samples from aquatic and terrestrial origins, indicating a wide distribution of OCS-emitting microorganisms in nature (Yamasaki et al., 2002). Hydrolysis of isothiocyanate, another breakdown product of glucosinolates (Hanschen et al., 2014), by the SaxA protein also yields OCS, as shown in phytopathogenic *Pectobacterium* sp. (Welte et al., 2016). Some Actinomycetales bacteria and Mucoromycotina fungi, both commonly found in soils,

25 are also known to emit OCS, but the origin and pathway remains to be elucidated (Masaki et al., 2016; Ogawa et al., 2016).

2.3.3 Non-vascular and epiphytic phototrophic communities

Many land surfaces host photoautotrophic communities known as cryptogamic covers, assemblies of bryophytes (mosses, liverworts, and hornworts), lichens, algae, and cyanobacteria. In contemporary terrestrial ecosystems, these communities contribute significantly to the biogeochemical cycling of

5 carbon and nitrogen (e.g. Lindo et al., 2013; Maestre et al., 2013), but global estimates of OCS uptake by these communities currently do not exist. Unlike vascular plants, bryophytes and lichens lack responsive stomata and protective cuticles to control water losses. As a result, their tissue hydration and physiological activity oscillate more dramatically with variations in ambient moisture than neighbouring vascular plants. In these organisms, photosynthetic CO_2 uptake is limited by moisture availability and

10 diel and seasonal variations in light. OCS uptake, on the other hand, continues in the dark even when photosynthesis ceases (Gimeno et al., 2017; Gries et al., 1994; Kuhn et al., 1999; Kuhn and Kesselmeier, 2000).

At the global scale, our findings so far suggest that quantifying the contribution of cryptogamic covers

15 to the OCS budget is not a straightforward task. This is because CO_2 and OCS fluxes are not necessarily coupled in lichens and bryophytes, and therefore OCS exchange cannot be modeled following the same approach as for vascular plants. Fortunately, the emission component from these organisms seems to be primarily driven by temperature (Gimeno et al., 2017) and the geographical extent of their contribution is limited to areas where cryptogamic covers constitute a non-negligible biomass fraction or contribute

20 significantly to other ecosystem biogeochemical cycles (Elbert et al., 2012). A first approach toward estimating the contribution of these communities would require compiling sensitivity parameters (to air moisture, temperature, and other variables as in Porada et al., 2014) to predict OCS exchange from climatic drivers for dominant species, functional types, or even whole communities from these regions.

25 In addition to the contribution of cryptogamic covers to OCS uptake, there exist hyperdiverse microbial communities that colonise the surface of plant leaves or the "phyllosphere" (Vacher et al., 2016). The phyllosphere is an extremely large habitat (estimated in 1 billion km^2) hosting microbial population densities ranging from 10^5 to 10^7 cells cm^{-2} of leaf surface (Vorholt, 2012). With respect to

23

OCS, it has already been shown that plant-fungal interactions can cause OCS emissions (Bloem et al., 2012). Assuming that these epiphytic microbes are capable of consuming and emitting OCS, they likely play a role in ecosystem OCS budgets.

2.3.4 Abiotic processes

Several abiotic processes can affect surface fluxes of OCS. OCS can dissolve in water and adsorb and desorb on solid surfaces. Emission to the atmosphere can also be generated by swings in redox potential and thermal- or photo-degradation of organic matter, both in soil and in the surface ocean.

Hydrolysis of OCS in water occurs slowly relative to the time scales of typical flux observations (Fig. 6). The temperature dependence of OCS solubility was modeled and described by Equation 20 in Sun et al., (2015): For a OCS concentration in air of 500 ppt, in equilibrium at ambient temperatures, the OCS dissolved in water will be less than 0.5 pmol OCS/mol H_2O (Fig. 5). Some portion of the dissolved OCS is destroyed by hydrolysis, following data generated by Elliott et al. (1989). For the rate-limiting step of hydrolysis in near-room-temperature water, the pseudo-first order rate constant is around 2×10^{-5} s^{-1}. The hydrolysis of OCS gains significance over hours, and especially in ice cores (Aydin et al., 2014, 2016).

Under typical environmental conditions, OCS adsorption and desorption is near steady state. OCS adsorbs onto various mineral surfaces at ambient temperatures and can be desorbed at higher temperatures (Devai and DeLaune, 1997). This characteristic is exploited for analysis of OCS in air: An air sample can be directed through a tube containing an adsorbent material, then desorbed at a detector in a laboratory (Pandey and Kim, 2009; Steudler and Kijowski, 1984). This approach is less sensitive than whole-air analyses by mass spectrometer (Montzka et al., 2007) or quantum cascade laser (Stimler et al., 2010a). A rigorous investigation of OCS adsorption onto soil surfaces has yet to be conducted. In some ecosystems with large temperature swings, temperature-regulated sorption cannot be ruled out as playing a small role in observed fluxes.

OCS consumption and production in precipitation does not play a significant role in OCS ecosystem fluxes. Two precipitation studies found both snow and rain were supersaturated with OCS (Belviso et al., 1989; Mu et al., 2004). Mu et al. suggested that this excess OCS may be due to photochemical reactions with sulfur-containing compounds scavenged by the water droplets. These reactions can

5 continue after the precipitation is deposited and re-generate the highly supersaturated OCS state after 24 hours of irradiation. The highest observed OCS concentration in precipitation was 48 ng OCS/L or 14 pmol OCS/mol H_2O. The densest cloud water content is about 3 gH_2O m^{-3}. For 1 m^3 of air, there are $2*10^{-12}$ excess moles of OCS. For 1 m^3 of dry ambient air at 500 ppt OCS, there are $2*10^{-8}$ moles OCS. This potential flux is described further in Campbell et al., (2017b). Even in the densest supersaturated

10 clouds, the OCS in the air would represent 99.99% of the OCS present.

Redox potential has long been known to play a role in the production of reduced sulfur gases, including OCS. All wetland soils observed in the field produced OCS (see Fig. 4). OCS was emitted from soils in lab studies where redox was manipulated (Devai and DeLaune, 1995). Watts (2000) divided all soils

15 into "oxic" and "anoxic," where low-oxygen soils generally produced OCS. However, recent studies question this simple framework.

Most oxic soils investigated act as small sinks of OCS (see review in Fig. 3 of Whelan et al., 2013), but a few oxic soils observed under field and laboratory conditions have released large amounts of OCS

20 under high temperatures or light conditions (Kitz et al., 2017; Maseyk et al., 2014; Whelan et al., 2016). This is attributed to the thermal- and photo-decomposition of organic matter (Whelan and Rhew, 2015). Whelan et al. (2016) determined that dried soils will exhibit net OCS emission following an exponential curve with temperature. Of six soils from vastly different ecosystems, only the sample from a desert showed no emissions when air-dried and heated. Sterilized soils exhibited a higher baseline of OCS

25 emissions, suggesting that OCS production was abiotic and some of the OCS produced was consumed by in situ microbes (Whelan and Rhew, 2015). It could be that soils containing organic matter will emit OCS under hot and dry conditions, but that most ecosystems never experience the low soil moisture and

high temperature combination in the field. Regardless, it is necessary to take this flux contribution into account when modeling potential soil OCS fluxes (Sun et al., 2015).

2.4 Ocean

5   A missing source of about 600–800 Gg S y^{-1} in the atmospheric budget of OCS has recently been identified by several top-down approaches (Berry et al., 2013; Glatthor et al., 2015; Kuai et al., 2015; Suntharalingam et al., 2008; Wang et al., 2016). Satellite data have shown that tropospheric OCS is elevated above the North Indian and northwest tropical Pacific oceans, and inverse models using enhanced oceanic emissions reproduced a similar pattern (Kuai et al., 2015). Global oceanic emissions

10   would need to amount to 800–1000 Gg S y^{-1} to fully account for this missing source. The oceans are known to contribute to the atmospheric budget of OCS via direct OCS emissions and indirect emissions of two short-lived gases: CS_2 and, potentially, dimethyl sulfide (DMS), most likely photochemical products of biogenic compounds (Fig. 8) (Chin and Davis, 1993; Watts, 2000; Kettle et al., 2002). However, large uncertainties are still associated with current estimates of marine fluxes (Launois et al.,

15   2015a; Lennartz et al., 2017, and references therein) and has led to diverging conclusions on whether oceanic emissions represent the missing source of OCS. Bottom-up emission estimates from global oceans have been obtained from simulations with models of different levels of complexity. Lennartz et al. (2017, 130±80 Gg S y^{-1}) predict highest emissions in high latitudes consistent with previous observations, whereas Launois et al. (2015a, 813 Gg S y^{-1}) predict highest emissions in the tropical

20   oceans with the 3D oceanic model NEMO-PISCES. The latter corroborates the emissions needed to account for the missing source, but requires OCS surface water concentrations one order of magnitude higher than the majority of open ocean observations. The discrepancies between bottom-up oceanic emission estimates, and between top-down and bottom-up approaches, indicate the need to reduce uncertainties in the global marine OCS flux from direct and indirect sources, requiring new field

25   measurements and process studies.

2.4.1 Surface ocean OCS measurements

Although in situ measurements of OCS in the surface ocean remain relatively scarce, they span a range of oceanic regimes and seasons. Observations of OCS in the surface water of the Atlantic, Pacific, Indian Ocean, and Southern Ocean revealed a consistent concentration range of ~10–100 pmols per liter in the surface mixed layer on daily averages, across different methods. Largest differences are found between coastal and estuaries (nanomolar range) and open oceans (picomolar range) (Table 3). A publicly accessible database of ship-based measurements in water and the marine boundary layer should receive the highest priority. Because vertical profiles of OCS concentrations are even more scarce and OCS enrichment in the sea-surface microlayer remains a general unknown, high-resolution measurements over time and depth in open and coastal waters are required to show how OCS concentrations vary over diel cycles and along transects from open to coastal waters. The consistent range of observed OCS concentrations determines the magnitude for direct oceanic emissions, but uncertainty remains due to our limited ability to globally extrapolate production processes in models.

2.4.2 Marine production and removal processes

The primary sources of OCS in the ocean are photochemical and light-independent (dark) processes (Von Hobe et al., 2001; Uher and Andreae, 1997), and the primary sink is hydrolysis (Fig. 6; Elliott et al., 1989). Although evidence indicates that these three processes can regulate OCS concentrations in the ocean surface mixed layer, diverging studies on the magnitude and global significance of marine emissions of OCS have recently highlighted that considerable uncertainties remain in the quantification of these source and sink terms (Launois et al., 2015a; Lennartz et al., 2017).

The OCS photo-production term remains poorly constrained. Global estimates of photo-production for the surface mixed layer can range by as much as 40-fold depending on the methodology used (Fig. 9). While some discrepancies can be attributed to distinct limitations within each methodology, it is evident that at the heart of the problem lies a limited knowledge of the magnitude, spectral characteristics, and spatial and temporal variability of the spectral apparent quantum yield (AQY) for OCS photo-production in the ocean. Here, we propose that refining estimates and uncertainty bounds for OCS

27

photo-production could be facilitated by (1) a comprehensive study of the variability of the spectrally resolved AQYs across contrasting marine environments, determined using laboratory-based photochemical experiments done under very controlled illumination conditions; (2) the use of a photochemical model that utilizes AQYs, fully accounts for the spectral and depth dependence of

5 photochemical processes in the surface ocean, and facilitates calculations on a global scale by capturing the variability in solar irradiance and chromophoric dissolved organic matter (Fichot and Miller, 2010); and (3) the cross-validation of the depth-resolved modeled rates with direct in situ measurements of photo-production rates and/or with rates derived from field observations of surface OCS concentrations (e.g. Lennartz et al., 2017).

10

Dark production remains similarly poorly constrained. Despite evidence for the role of biological processes (Flöck and Andreae, 1996) and for the involvement of radicals (Pos et al., 1998), only one parameterization is currently used in models of dark production (Von Hobe et al., 2001). Neither the direct precursor nor the global applicability of this parameterization is known. The acquisition of

15 vertical profiles of OCS concentrations within and below the euphotic zone would help reduce this uncertainty. Continuous concentration measurements from research vessels can be used to calculate dark production rates assuming an equilibrium between hydrolysis and dark production during nighttime. Different processes undoubtedly require further dedicated process studies to assess their importance. Despite these unknowns, the current gap in the OCS budget is larger than the estimated

20 ocean emissions, including uncertainties from process parameterization and in situ observations.

2.4.3 Indirect marine emissions

Indirect marine emissions from oxidation of the precursor gases CS_2 and potentially DMS were hypothesized to be on the same order as or larger than direct ocean emissions of OCS (Chin and Davis, 1993; Watts, 2000; Kettle et al., 2002). Production and loss processes of CS_2 in seawater are less well

25 constrained than OCS production, and they include photo-production (Xie et al., 1998), evidence for biological production (Xie et al., 1999), and a slow chemical sink (Elliott, 1990).

Measurements of CS_2 in the surface ocean are very scarce, but comprise several transects in the Atlantic and Pacific oceans with concentrations in the lower picomolar range. Significantly larger concentrations have been found in coastal waters (Uher, 2006, and references therein). A molar yield of CS_2 to OCS of 0.81–0.93 was established by Stickel et al. (1993) and Chin and Davis (1993), resulting in OCS

5   emissions from CS_2 with an uncertainty of 20–80 Gg S y^{-1}. This uncertainty arises from the uncertainty in the emissions, not the molar yield, for which a globally constant factor is used. In laboratory experiments, Hynes et al. (1988) found that the OCS yield from CS_2 increases with decreasing temperatures, suggesting larger OCS production from CS_2 at high latitudes. To better constrain oceanic emissions of OCS from CS_2, we suggest expanding surface concentration observations across various

10   biogeochemical regimes and seasons; using field observations, laboratory studies, and process models to characterize production processes and identify drivers and rates; and applying a temporally and spatially varying conversion factor when calculating resulting OCS emissions.

The mechanism and atmospheric relevance of OCS production from DMS remains highly uncertain.

15   The production of OCS from the oxidation of DMS by OH has been observed in several chamber experiments, all of which used the same technique and experimental chamber (Barnes et al., 1994, 1996; Patroescu et al., 1998; Arsene et al., 1999, 2001) with a molar yield of $0.7 \pm 0.2\%$. These studies were carried out at precursor levels far exceeding those in the atmosphere (ppm), so the potential exists for radical–radical reactions that do not occur in nature. In addition, experiments took place in a quartz

20   chamber on time scales that have potential for wall-mediated surface or heterogeneous reactions and using only a single total pressure and temperature (1000 mbar, 298 K). The global DMS oxidation source of OCS was estimated by Barnes et al. (1994) as 50.1–140.3 Gg S y^{-1}, and subsequent budgets contain only revisions according to updated DMS emissions (Kettle et al., 2002; Watts, 2000). We suggest that the uncertainty in the production of OCS from DMS is underestimated, given the

25   uncertainty in the pressure/temperature dependence of OCS production via this mechanism, and the uncertainty of the applicability of the chamber results to the atmosphere. Until these issues are resolved, we recommend that this term be removed as a source from future budgets, but retained as an

29

uncertainty. Validating the atmospheric applicability of the reported yields would require experiments at lower concentrations in a system that eliminates (or permits quantification) of wall-induced reactions.

2.5 Anthropogenic sources

Anthropogenic sources have been used to interpret changes in atmospheric OCS observations in space
5   and time (Campbell et al., 2015, 2017a; Zumkehr et al., 2017). These sources include direct emissions of OCS as well as indirect sources caused by anthropogenic emissions of CS_2. The dominant anthropogenic source is from rayon production (Campbell et al., 2015), while other large anthropogenic sources include coal combustion, aluminum smelting, pigment production, shipping, tire wear, vehicle emissions, and coke production (Blake et al., 2008; Chin and Davis, 1993; Du et al., 2016; Lee and
10   Brimblecombe, 2016; Watts, 2000). Temporally and spatially explicit inventories have been created for use in OCS atmospheric transport models (Campbell et al., 2015; Zumkehr et al., 2017).

Bottom-up analysis of the global anthropogenic inventory estimates a source of 500 ± 220 Gg S y^{-1} for the year 2012. The large uncertainty is primarily due to limited observations of emission factors,
15   particularly for the rayon, pulp, and paper industries. An independent approach using a top-down method estimated that the average source for the years 2011 through 2013 was 230 to 350 Gg S y^{-1} (Campbell et al., 2015). One possible reason for the gap between these estimates is that the top-down study used a constrained optimization approach in which the optimization was limited to the a priori range, which at the time of that study was 150 to 364 Gg S y^{-1}. These two estimates are considerably
20   larger than the older gridded inventory estimate of 180 Gg S y^{-1} (Kettle et al., 2002), which was used in all recent global atmospheric modeling studies. Also, the Kettle inventory failed to capture the concentration of global emissions in China that is revealed in the updated inventory. The upward revision of the anthropogenic source suggests that some of the missing source in the global budget could be accounted for by anthropogenic emissions.
25

The spatial and temporal trends in these inventories have multiple implications for applying OCS as a carbon cycle tracer. First, most of the anthropogenic source is located in China, while most of the

30

atmospheric OCS monitoring is located in North America (Campbell et al., 2015). The spatial separation allows regional applications of OCS to North America to control for most of the anthropogenic influence through observed boundary conditions (Campbell et al., 2008; Hilton et al., 2015, 2017). Second, the anthropogenic source has large inter-annual variations (Campbell et al., 2015),

5   which suggests that applications of the OCS tracer to inter-annual carbon cycle analysis will require careful consideration of anthropogenic variability.

Several airborne campaigns have observed increases in OCS concentrations in air masses from nearby burning events (Blake et al., 2008). Biomass burning is generally accounted as a separate category. The

10   most recent estimate of the biomass burning sources is 116 ± 52 Gg S y^{-1}, which includes contributions from biofuels, open burning, and agriculture residue that are 63%, 26%, and 11% of the total, respectively (Campbell et al., 2015).

2.6 Volcanic sources

Extensive sampling of degassing magma, volcanic fumaroles, and geothermal fluids has shown that

15   OCS is also emitted into the atmosphere by volcanism. Although OCS can be released at room temperature by volcanic ash (Rasmussen et al., 1982), measurements from both air and ground showed that OCS was conserved in the atmospheric plume emitted by the Erebus volcano up to tens of kilometers downwind of the volcanic source (Oppenheimer et al., 2010). This finding is consistent with our current understanding of the chemical reactivity of OCS in the troposphere.

20

The first compilation of OCS/CO_2 ratios in volcanic gases of various volcanoes was published in the mid-1980s (Belviso et al., 1986). In light of the variability of the OCS/CO_2 ratio in volcanic gases, it was possible to evaluate the volcanic contribution of eruptive and non-eruptive volcanoes from their respective estimated CO_2 emissions. The authors gathered data from 11 volcanoes covering nearly the

25   whole range of volcanic temperatures (100–1100°C) and encompassing the main types of terrestrial volcanisms. They reported a statistically significant linear relationship between the logarithm of the OCS/CO_2 ratios and the reciprocal of the emission temperature of the gases, and pointed out that this

31

experimental relationship was consistent with thermodynamical calculations. Although most of the results showed that the OCS/CO_2 ratio of volcanic gases was closely related to their emission temperature, samples collected at Merapi Volcano did not match well with the linear model. A revised temperature dependence of $\log[OCS/CO_2]$ is shown in Fig. 10. The compilation of measurements from 14 volcanoes shows that the former relationship (red dots and line) overestimated by up to an order of magnitude the OCS/CO_2 ratio of volcanic gases with emission temperatures from 110°C to 400°C typical of extra-eruptive volcanoes, whereas for temperatures over 700°C, typical of eruptive and post-eruptive volcanoes, the former model underestimated the ratios by less than an order of magnitude. For a more complete description of the outgassing state of active volcanoes the reader is referred to Belviso et al. (1986). In the latter, the extra-eruptive volcanoes already represented a negligible proportion of the total OCS volcanic source strength: now they can definitely be discarded from the inventory of volcanic emissions. The range of the preferred global volcanic CO_2 emission estimates of the five studies reviewed by Gerlach (2011) being 0.15–0.26 Pg y^{-1}, or 0.205 ± 0.055 Pg y^{-1}, and assuming that the mean OCS/CO_2 molar ratio of gases emitted by eruptive and post-eruptive volcanoes is 2.3×10^{-4} (for emission temperatures in the range 525°C–1130°C), the revised annual volcanic input of OCS into the troposphere is estimated to be in the range 25–43 Gg S y^{-1}, in accordance with former estimates (Belviso et al., 1986, and references therein).

2.7 Bottom-up OCS budget

We calculate a "bottom up" global balance of OCS with several approaches. In Table 4, we provide estimates of OCS fluxes into (positive) and out of (negative) the atmosphere. The derivation of the values provided in the table are discussed below.

First, we compare estimates of OCS terrestrial uptake based on carbon cycle assessments with actual observations. We build a budget for terrestrial biomes that relies on observations where available, and on estimates of carbon uptake where no data exists, as has been done previously with less available information (Campbell et al., 2008; Kettle et al., 2002; Suntharalingam et al., 2008). In Table 5, the estimated OCS uptake is first calculated from a GPP estimate and Eq. 1, then the net OCS flux is

32

appraised by taking into account observed or estimated soil fluxes for each biome. The contribution of wetlands and cryptogamic cover is treated separately. Eq. (1) relates GPP to OCS uptake, with [CO_2] and [OCS] assumed to be 400 ppm and 500 ppt, respectively, and LRU is 1.16 ± 0.2 for C_4 plants (Stimler et al. 2010b) and 1.99 ± 1.44 for C_3 plants (Fig. 1). We further assume a 100-day growing

5   season with 12 h of light per day for the purposes of converting between annual estimates of GPP and field measurements calculated in s^{-1} units, though this obviously does not represent the diversity of biomes' carbon assimilation patterns. Additionally, we assume that plants in tropical and desert biomes photosynthesize using the C_4 pathway. The result is presented in Table 4. Anticipated fluxes from soils and plants are then combined, scaled to the area of the biome extent, and presented in Table 4 as annual

10   contributions to the atmospheric OCS budget.

To determine the role of cryptogamic communities to the atmospheric OCS loading, we leverage work that has already been done on the carbon balance and Eq. (1). According to Elbert et al. (2012), the annual contribution of cryptogamic covers is 3.9 Pg C. A [OCS] of 500 ppt, a [CO_2] of 400 ppm, and a

15   LRU of 1.1 ± 0.5, yields $-8 - -21$ Gg S y^{-1}.

Lakes and rivers could be important for regional OCS studies, especially in the northern latitudes. Lakes cover only about 3% of the Earth's surface (Downing et al., 2006), but in the boreal zone lakes cover on average 7% of land area. In some parts of Finland (Raatikainen and Kuusisto, 1990) and Northern

20   Canada (Spence et al., 2003) they occupy up to 20% and 30% of the landscape, respectively. Among the admittedly few studies, no observations support lakes and rivers as a consistent OCS sink. To estimate the maximum possible source of lakes to the atmospheric OCS burden, we perform a simple estimation of the global OCS flux following the approach in MacIntyre et al. (1995) as

25   $F_{OCS} = k(c_{aq} - c_{eq})$ (2)

where gas transfer coefficient, k, is assumed to be constant 0.54 m d^{-1} (Read et al., 2012); OCS concentration in the water, c_{aq}, taken as minimum 90 pmol L^{-1} or as maximum 1.1 nmol L^{-1} (Richards et al., 1991); and OCS concentration in the surface water if it was in equilibrium with the above air, c_{eq},

calculated using Henry's law at global average temperature of 15°C and global atmospheric OCS mixing ratio of 500 ppt. Accounting for the number of ice-free days in a year and total lake surface area per latitude, the range of possible burden of OCS from lakes to the atmosphere is reported here as 0.8 to 12 Gg S y^{-1}.

5

As a first guess at the contribution of wetlands to the global OCS budget, we use a range of OCS flux observations in pmol OCS m^2 s^{-1} for fresh and saline wetlands: -15 (de Mello and Hines, 1994) to +27 (Liu and Li, 2008) for freshwater wetlands and -9.5 (Li et al., 2016) to +60 (Whelan et al., 2013) for saltwater wetlands (Fig. 4). Marine and inland wetlands cover 552 and 9299 10^3 km^2, respectively

10 (Dixon et al., 2016; Lehner and Döll, 2004). Performing a simple scaling exercise results in contributions of -140 to 250 and -5 to 33 Gg S y^{-1} for fresh and saltwater wetlands, respectively, yielding a total range of -150 to 290 (Table 4). This scaling calculation does not take into account diurnal flux variation, tidal variation, temperature, and many other factors.

15 Examining Table 4, we find a large missing source of at least 1200 Gg S y^{-1}, up to 4100 Gg S y^{-1}. It has been suggested that ocean OCS production has been underestimated (Berry et al., 2013), but some research points to unaccounted anthropogenic sources closing the budget gap (Zumkehr et al., 2017). This suggests that the uncertainty on our ocean OCS production and/or the industry inventories do not capture their true range of OCS fluxes. Additionally, there is a possibility that the plant sink is

20 overestimated or that there is an unidentified source. More observations in the ocean OCS source region and from industrial processes, particularly in Asia, are needed to further assess their actual magnitude and variation (Suntharalingam et al., 2008). Current leaf-based investigations need to be expanded to include water or nutrient-stressed plants, perhaps revealing lower OCS plant uptake. Despite the large uncertainties of the global OCS budget, many applications of the OCS tracer have been attempted with

25 success.

3 Applications

3.1 Global and regional GPP estimates

Terrestrial photosynthetic carbon fluxes (GPP) are a key source of uncertainty in climate prediction (Ciais et al., 2014). Efforts to estimate GPP using models disagree in their diagnoses of global (Piao et al., 2013) and regional (Parazoo et al., 2015) GPP magnitude and regional spatial distribution in North America (Huntzinger et al., 2012), the Amazon (Restrepo-Coupe et al., 2017), and Southeast Asia (Ichii et al., 2013). This demonstrates a critical gap in understanding of the terrestrial carbon cycle and suggests a need for independent information, such as that provided by OCS observations, to further constrain models.

There are two approaches to performing this application. One uses a biosphere model to simulate the CO_2 and OCS biospheric fluxes with the mechanism described above, which is the so-called "bottom up" method. Berry et al. (2013) employed the Simple Biosphere Model (SiB3) to estimate coupled CO_2 and OCS land fluxes, and designed an experiment to examine the different responses in photosynthesis and respiration under different soil hydrology and water stress. Berry et al. compared the drawdown of CO_2 and OCS under different conditions and in different regions and the results indicated that additional information on separating the responses of photosynthesis and respiration to environmental forcing could be provided with the help of OCS. Launois et al. (2015) and Campbell et al. (2017a) used a simpler approach to simulate OCS fluxes from several land surface models, based on the simulated GPP and LRU. They further used an atmospheric transport model to evaluate the potential biases in the simulated GPP and respiration fields, comparing simultaneously the simulated OCS and CO_2 concentrations to observed atmospheric mixing ratios (see Sect. 3.1.1). Recent work by Hilton et al. (2017) combined both approaches to constrain the spatial distribution of GPP in North America.

The second method relies on obtaining the biosphere fluxes of CO_2 and OCS from gradients in measured atmospheric concentrations using inverse modeling, which is the "top-down" method. Atmospheric inverse modeling with CO_2 measurements alone is only able to constrain the total net flux of CO_2 and it is unable to distinguish between the underlying fluxes arising from photosynthesis and

35

respiration. Adding atmospheric OCS measurements to the analysis will allow gross carbon fluxes to be calculated, from which biospheric responses to climate variations can be better described. Currently, there is a need for more surface measurements to carry out this method on large spatial scales. Using satellite observations sensitive to the mid or upper troposphere cannot well distinguish spatial variations

5 of surface fluxes, e.g. exactly where a potential ocean source is located.

There are uncertainties shared by both approaches. While OCS observations show promise as an independent GPP tracer, there are smaller terrestrial OCS sources and sinks from soils (Kesselmeier et al., 1999; Kettle et al., 2002; Maseyk et al., 2014; Ogée et al., 2016; Sun et al., 2015; Whelan et al.,

10 2015) and industrial activities (Campbell et al., 2015; Kettle et al., 2002; Zumkehr et al., 2017) that must be considered (see Sect. 2). For studies relying on LRU, laboratory and field work has shown that LRU varies under different conditions, such as low light (Stimler et al., 2010b). Although there are uncertainties in the OCS sources and sinks, OCS observations are useful even with an unbalanced global budget because the uncertainty introduced by LRU variation and potential soil OCS emissions is

15 much smaller than the uncertainty of our current understanding of regional carbon balance (Hilton et al., 2015).
Here we describe the work that is underway or has already been done to use OCS observations to glean more information about ecosystem functioning, specifically GPP, on different spatial and temporal scales. With the bottom up approach, generating maps of OCS uptake over land has given us an idea of

20 the spatial distribution and magnitude of GPP, allowing us to evaluate the representation of carbon uptake in our current suite of biosphere models. We also explore the potential of using OCS to understand carbon cycle changes under extreme events. With the suite of OCS satellite data available, we describe studies that have examine OCS with the "top down" approach. Finally, we examine GPP estimates on very long temporal scales using the OCS ice core record.

25 **3.1.1 Evaluating biosphere models**

There are uncertainties in evaluating biosphere models using OCS without carefully chosen OCS component fluxes, especially at small spatial scales. However, on the regional scale, Hilton et al. (2017)

36

showed that the spatial placement of GPP dominates other uncertainty sources in the GPP tracer approach. Using aircraft OCS observations from the NOAA Global Greenhouse Gas Reference Networks aircraft program (http://www.esrl.noaa.gov/gmd/ccgg/aircraft/index.html, an update of results published in Montzka et al., 2007), they derived OCS plant fluxes from differing GPP models' spatial
5   placement of North American GPP and used a chemical transport model to compare these to the aircraft observations. The study used multiple estimates of OCS soil fluxes, OCS anthropogenic fluxes, and continental boundary fluxes, supporting three different approaches to modeling the relationship of OCS and CO_2 plant uptake. Each of these contributes uncertainty to using OCS as a GPP tracer. By using these multiple estimates of each uncertainty, Hilton et al. (2017) quantitatively estimated each
10   uncertainty source as well as the sources' combined, comprehensive uncertainty.

Models that placed the largest GPP in the Upper Midwest of the United States produced OCS plant fluxes that matched well against aircraft observations for all estimates of OCS soil flux, OCS anthropogenic flux, and transport model boundary conditions. OCS plant fluxes derived from GPP
15   models that place the largest GPP in the Southeast United States were not able to match aircraft-observed OCS for any combination of secondary OCS fluxes. While inconsistent with some modeled GPP estimates, placement of the strongest North American GPP in the Upper Midwest is consistent with new ecosystem models from the Coupled Model Intercomparison Project Phase 6 (CMIP6) (Eyring et al., 2016) with enhanced agroecosystem processes and emerging space-based estimates from SIF
20   (Guanter et al., 2014). This result is encouraging for the potential of OCS to provide a directly observable tracer for GPP at regional scales.

State-of-the-art global land surface models, such as those used in CMIP6, show large differences in the simulated GPP in terms of mean value, phase, and amplitude, hampering accurate investigations into
25   carbon-climate feedbacks. Launois et al. (2015b) analyzed the potential of existing atmospheric OCS mixing ratio measurements (discrete samples from NOAA), together with CO_2, to evaluate model GPP biases. They used the simulated GPP from three global land surface models (ORCHIDEE, CLM4CN and LPJ; simulations from the TRENDY intercomparison (Sitch et al., 2015)) and an atmospheric

transport model, LMDz. Vegetation uptake of OCS was derived as a linear function of GPP using LRU, the ratio of OCS to CO_2 deposition velocities, from Seibt et al. (2010). Non-photosynthetic sinks (oxic soils, atmospheric oxidation), biogenic sources (oceans and anoxic soils), and anthropogenic sources of OCS were also included in the transport simulations. The amplitude and phase of the seasonal variations

5 of atmospheric OCS appear to be mainly controlled by the vegetation OCS sink. This allows for bias recognition in the spatial and temporal patterns of the GPP. For instance, the ORCHIDEE GPP at high northern latitudes is overestimated, as revealed by a too-large OCS seasonal cycle at the Alert station (ALT, Canada) (Fig. 11). Similarly, the seasonal variations of the GPP in CLM4CN appear to be out of phase for the northernmost ecosystems, showing a maximum carbon uptake too early in spring. Both

10 model biases could only be deduced from the OCS diagnostic, although they are also suggested by the CO_2 evaluation. These results highlight the potential of current in situ OCS measurement to reveal model GPP and respiration biases; however, they rely on the robustness of the global OCS modeling framework and in particular the choice of the LRU values (assumed constant in time) and the parameterization of soil OCS uptake (i.e. with small seasonal variations).

15 **3.1.2 Extreme events and the carbon cycle**

Climate extremes have strong impacts on ecosystems by rapidly altering the stable state (Reichstein et al., 2013). OCS observations can be used to discern how extreme events affect the carbon cycle. Taking drought as an example, the mechanisms affecting carbon balance triggered by droughts can be described conceptually; however, the individual processes are difficult to quantify with CO_2 measurements alone.

20 Most studies conclude that drought ought to decrease an ecosystem's respiration rates and photosynthetic production. However, the net effect of drought is challenging to assess, and different studies can be contradictory (Phillips et al., 2009). Figure 12 shows the impacts of drought on the ecosystem CO_2 and OCS exchange. With a mild drought (Fig. 12, blue arrows), the soil surface might dry out, reducing soil respiration and thus total ecosystem respiration. Plant roots would still be able to

25 reach enough water, GPP would be unchanged or decreases slightly, and the net ecosystem production would increase. For a severe drought (Fig. 12, red arrows), GPP would be reduced because plants close stomata in order to conserve water, and the net ecosystem production would likely decrease.

38

Additionally, some studies have shown an increased GPP during drought events, resulting from increased availability of sunlight (Huete et al., 2006; Saleska et al., 2007), which makes the overall effect even more complex.

5   Adding OCS to climate extremes studies would provide additional information on the biospheric processes. During drought events (Fig. 12), the OCS uptake changes along with GPP, since both processes are controlled by stomatal conductance. That results in an unchanged or slightly decreased OCS uptake during a mild drought and a largely reduced OCS uptake in a severe drought. With a given ratio between GPP and OCS uptake, the changes in GPP can be quantified for both mild and severe
10   droughts.

3.1.3 Top-down global OCS budget

More precisely quantified OCS surface fluxes should improve our knowledge of terrestrial photosynthesis and hence GPP (Sandoval-Soto et al., 2005). Improved knowledge of the global OCS budget will help constrain OCS surface flux components (vegetation, soil, ocean, anthropogenic).
15   Current OCS surface flux budgets are mostly bottom-up estimates derived from leaf-scale or terrestrial-scale experiments (Berry et al., 2013; Campbell et al., 2008; Kettle et al., 2002; Suntharalingam et al., 2008). In addition to a better global OCS budget, atmospheric OCS measurements can also be used to further constrain bottom-up or mechanistic estimates. Such "top-down" estimates use observed spatial and temporal gradients of OCS in the atmosphere to adjust an independent estimate of surface fluxes
20   (usually called the "prior" estimate).

Only a few top-down attempts have been made with the sparse flask sampling network results (i.e. mainly from NOAA). Launois et al. (2015b) used the measurements at 10 surface stations to optimize global scalars of all surface OCS flux components in order to obtain a closed global OCS budget (i.e.
25   sources and sink that are compatible with the atmospheric budget) and to highlight the main contributing surface flux components to the trend and seasonal cycle of atmospheric OCS as well as to the inter-hemispheric gradient.

39

Recent satellite-based OCS measurements can be used to derive top-down estimates at continental to regional scales. Kuai et al. (2015) proposed to estimate the OCS surface flux from NASA's Tropospheric Emission Spectrometer (TES) ocean-only observations using a Bayesian inversion

5 technique, which can be thought of as a time-independent version of the 4D-VAR assimilation (Liu et al., 2016). Their results implied a large ocean OCS source over the Indo-Pacific region, and the total ocean source budget was consistent with the global budget proposed by Berry et al. (2013). A similar conclusion was obtained by Glatthor et al. (2015), who showed that the OCS global seasonal cycle observed by MIPAS was more consistent with the seasonal cycles modeled using the Berry et al. global

10 budget than using the global budget proposed earlier by Kettle et al. (2002).

Among the four satellite OCS products, only TES OCS data have been used for OCS surface flux inversions. As the TES OCS product is limited to over ocean only, the inversion of the OCS terrestrial sinks in Kuai et al. (2015) may be subject to large uncertainties. Thus, for consistency, TES OCS over

15 land may be highly desired. Spectral retrieval over land requires exact details of surface properties, including surface altitude, temperature, emissivity, reflectance, snow cover, etc., which have been considered in the IASI OCS retrieval (Camy-Peyret et al., 2017; Vincent and Dudhia, 2017). A similar retrieval algorithm for TES OCS is currently under development. The accuracy of the surface flux inversion can be further improved by using simultaneous OCS observations from more satellites, e.g.

20 TES and MIPAS, to provide more constraints on the horizontal and vertical OCS distribution in different parts of atmosphere. Satellite products need to be compared to tower or airborne data, perhaps determining how well the upper troposphere can reflect surface fluxes. This effort is furthered by better estimates of surface fluxes, in particular observations of OCS emissions from the oceans in areas where we assume a large source region might exist (Kuai et al., 2015). Thus better "bottom-up" surface flux

25 estimates constrained by more numerous atmospheric observations can provide powerful constraints on OCS surface fluxes, and thus GPP.

3.1.4 Long-term changes in carbon uptake

Measurements of OCS in Antarctic ice core and firn air samples have been used to explore long-term trends in GPP. Ice core samples from the West Antarctic Ice Sheet Divide were used to produce a 54,300 year OCS record and an order of magnitude estimate of the change in GPP during the last glacial/interglacial transition (Aydin et al., 2016). Atmospheric OCS declined by 80 to 100 ppt during the last glacial/interglacial transition. Interpretation of these measurements with a simple box model suggests that GPP roughly doubled during the transition. This order of magnitude estimate is consistent with an ecosystem model that simulates 44% growth in GPP over the same period (Prentice et al., 2011).

The ice core OCS record has also been used to explore change in GPP in the Little Ice Age. Ice core observations over the last 2,000 years show relative maxima at the peak of the Little Ice Age (Aydin et al., 2008). These OCS observations were used to estimate growth in GPP and combined with other data to estimate the temperature sensitivity of pre-industrial CO_2 fluxes for the terrestrial biosphere (Rubino et al., 2016).

Analysis of firn air samples was used to estimate GPP trends in the industrial era. Firn air measurements and one-dimensional firn models have been used to show an increase in atmospheric OCS during most of the industrial era, with a decadal period of decline beginning in the 1990s (Montzka et al., 2004, 2007). The trend in the firn record has been interpreted to largely reflect the increase in industrial emissions, but it also suggests an increase in GPP during the 20th century of 31 ± 5%, which is consistent with some global ecosystem models (Campbell et al., 2017a). Understanding of GPP in the current industrial era is needed to provide a benchmark for future projections from earth system models, given that they have highly uncertain carbon-climate feedbacks in climate projections (Friedlingstein et al., 2013).

41

3.2 OCS to probe variables other than GPP

Although OCS has been studied mostly as a proxy for photosynthesis, OCS uptake by vegetation is actually governed mechanistically by (i) the series of diffusive conductances of OCS into the leaf, and (ii) the reaction rate coefficient for OCS destruction by CA (Wohlfahrt et al., 2012). CA is present both in plant leaves and soils, although soil uptake tends to be proportionally much lower than plant uptake. Over soils, OCS uptake provides information about CA activities within diverse microbial communities. OCS uptake over plants integrates information about the sequential components of the diffusive conductance (the leaf boundary layer, stomatal, and mesophyll conductances) and about CA activity, all important aspects of plant and ecosystem function. Stomatal conductance in particular is a prominent research focus in its own right, as it couples the carbon and water cycles via transpiration and photosynthesis.

Stomatal conductance is typically determined from combined estimates of transpiration, water vapor concentration, and leaf temperature. That approach can be particularly challenging at the canopy scale, where transpiration is difficult to distinguish from non-stomatal water fluxes (i.e. evaporation from soil and canopy surfaces) and to upscale from sap flux measurements (Wilson et al., 2001). Use of OCS uptake involves the similar, but more tractable challenge of distinguishing the canopy OCS uptake from soil OCS uptake or emission via soil surface chamber measurements, as in Wehr et al. (2017). Use of OCS uptake may also be less sensitive to errors in leaf temperature, which is difficult to define and quantify at the canopy scale—though leaf temperature may still enter the problem via estimation of mesophyll conductance and CA activity.

The use of OCS to study stomatal conductance is therefore promising, but it is so far represented mostly by a single study: Wehr et al. (2017) used OCS uptake to derive canopy stomatal conductance and hence transpiration in a temperate forest. Eddy covariance and soil chamber measurements were combined to quantify canopy OCS uptake, whose diel and seasonal patterns turned out to be predictable (to within 3%) from independent estimates of the stomatal, mesophyll, and boundary layer conductances under the assumption of constant CA activity. Stomatal conductance was the rate-limiting

42

diffusive step, and so its diel and seasonal patterns were retrievable from the canopy OCS uptake to within 6% of independent estimates based on sensible and latent heat flux measurements (Fig. 13). These findings support the underlying theoretical basis describing OCS uptake by the vegetation, even if the canopy is treated as a single "big leaf", and suggest that OCS may be a useful probe of stomatal

5   conductance. Traditionally, stomatal conductance is indirectly observed by measuring the transpiration water flux from the leaf when stomata are open. OCS would be especially useful in humid environments or at night, when transpiration is too small to use other methods that rely on sap flow or heat flux (Campbell et al., 2017b). However, an independent estimate of CA activity would be required.

10   A powerful and more general approach would be to combine OCS measurements with other constraints in an ecosystem model framework. OCS uptake can serve as a glue that binds other measurable quantities within a model, because OCS is related to: (a) GPP, via all three diffusive conductances and CA activity; (b) transpiration, via the boundary layer and stomatal conductances; and (c) the ^{18}O isotope compositions of CO_2 and H_2O, via CA activity. The ^{18}O connection results from the fact that CA

15   promotes the exchange of oxygen isotopes between CO_2 and liquid water in the leaves (Stimler et al., 2011). Solar-induced fluorescence measurements could also be synergistic, as they relate to the photochemical aspect of photosynthesis, while OCS uptake relates to the gas transport aspect.

Further study of vegetative OCS uptake along these lines has the potential to elucidate ecosystem

20   function, including the mechanistic basis of the OCS-GPP relationship (for example, OCS and CO_2 data can be used to optimize biosphere parameters such as the Ball-Berry slope and intercept (Ball et al., 1987; Collatz et al., 1991)). Practical use of OCS as a GPP proxy will require improved quantitative understanding of how the diffusive conductances and CA activity mediate that relationship.

25   Microbial CA activity is thought to be the driver of OCS consumption in soils as it is in leaves. This has been supported by experiments using CA-specific inhibitors (Kesselmeier et al., 1999). Using CA-specific enzymatic parameters for OCS, Ogée et al. (2016) showed that the observed OCS uptake rates found in several soils were coherent with the microbial biomass and expected internal CA concentration

in microbial cells. A number of enzymes besides CA have affinity to OCS as a substrate, such as RuBisCO (Lorimer & Pierce, 1989), carbon monoxide dehydrogenase (Ensign, 1995), nitrogenase (Seefeldt et al., 1995), OCS hydrolase (Ogawa et al., 2013), and CS_2 hydrolase (Smeulders et al., 2011), but their impact on total soil OCS consumption has not been assessed. One possible method of

5   determining the importance of these other enzymes involves OCS isotope measurements. OCS-S isotope fractionation by COSase was determined and compared with the value of intact cell of *T. thioparus* from which this enzyme was purified (Ogawa et al., 2017). The values were also examined and compared among the purified bacteria from soil isolated by Kato et al. (2008) (Kamezaki et al., 2016).

10

Studies of soil CA are also relevant to a second carbon cycle tracer, $CO^{18}O$. As noted above, CA accelerates the rate of oxygen isotope exchange during CO_2 hydration in leaf and soil water pools, whose oxygen isotope composition can differ markedly because of differences in pool size and evaporation rates. Leaf and soil CO_2 fluxes carry in turn very different oxygen isotopic signatures, thus

15   serving to help partition carbon exchange. Similar knowledge gaps surround the role of CA in driving soil $CO^{18}O$ exchange as for OCS, making studies that simultaneously address both tracers especially valuable. For example, if the same enzyme pools (CA or other enzymes) catalyze soil reaction rates for both OCS and CO_2, the two tracers can be used in parallel to simultaneously assess CA activity in soils and foliage for better determination of GPP at local to global scales. This CA-based coupling between

20   OCS and $CO^{18}O$ provides a unique gene-to-trace gas model system to develop methods to link soil genomics with ecosystem function.

Significant progress can be made in filling knowledge gaps regarding the microbial drivers for soil OCS uptake by combining culture-dependent and independent approaches with readily available genomic

25   databases and tools. For example, culture-independent studies should attempt to determine whether microbial community structure and/or the abundance and diversity of genes encoding for CA or other enzymes (or their expression) are predictive for OCS consumption. In fact, recent soil surveys adopting these approaches have identified potential links between OCS consumption and the abundance of fungi

(Sauze et al., 2017) and β-CA expression by *Actinobacteria* (Meredith et al., in prep). Culture-dependent studies that broaden the collection of microbial isolates assessed for OCS activity are needed to constrain the activities of CA classes and other enzymes for OCS. These efforts may enable trait-based prediction of soil OCS uptake rates from microbial community composition. Future work in this area will not only help build a mechanistic understanding of soil OCS dynamics but also provide insight into the ecological role of microbial CA and OCS consumption in soil microbial populations.

3.3 OCS as a tracer for the origins of air masses

The sources of OCS are geographically separate from the terrestrial biosphere sink, and OCS observations in the right time and location may be used to better understand atmospheric transport of other substances, like water or isoprene. A parcel of air that has most recently mixed with the ocean-influenced atmosphere will generally have more OCS than a parcel that has interacted with, for example, a forested system. In this way, the possible path that a parcel has taken can be suggested by swings in OCS concentration.

The association of GPP and OCS uptake was first observed in large-scale regional studies, and the data presented in Campbell et al. (2008) showed a large difference of OCS concentrations between the free troposphere and the planetary boundary layer over vegetated North America. Decreases of OCS have also been associated with higher levels of biogenic volatile organic compounds over the northeastern United States, and the potential for OCS as an inverted tracer for the exposure of an air mass to the biosphere was investigated (de Gouw et al., 2009). Commane et al., (2013) were able to correlate changes in wind patterns and associated air mass origins with swings in OCS concentrations.

Currently, large OCS datasets like those generated with satellites have good spatial coverage, but are most sensitive to the OCS concentration in the upper atmosphere. In order to use OCS to probe meteorological questions data sets need to be generated with appropriate resolution with regard to altitude and frequency of observations, for example, from flights crossing the planetary boundary layer or through areas of convection.

4 Available datasets

To use the OCS GPP tracer to its full potential, surface OCS estimates over land and ocean are needed to evaluate ocean and ecosystem fluxes to the atmosphere at the global scale. Current satellite retrievals are sensitive to OCS concentrations much higher in the troposphere, and FTIR or tower data have limited coverage. Currently, the most used surface OCS dataset is from the NOAA Flask Network, where gas samples are often collected twice a day. Coordinating satellite retrievals with ground-based measurement efforts is important to realize greater data coverage and accuracy.

4.1 OCS satellite data products

Currently, global OCS concentrations have been retrieved from a few satellite instruments, including NASA's TES (Kuai et al., 2014), the Canadian Space Agency's Atmospheric Chemistry Experiment– Fourier Transform Spectrometer (ACE-FTS) (Boone et al., 2005), the European Space Agency's MIPAS (Glatthor et al., 2017) and the Infrared Atmospheric Sounding Interferometer (IASI) (Camy-Peyret et al., 2017; Vincent and Dudhia, 2017). Among these instruments, TES and IASI are nadir-viewing instruments (i.e. looking downwards from space towards the surface), while ACE-FTS and MIPAS are limb scanners (i.e. looking through the atmosphere tangentially), measuring spectra of the atmospheric tracers. Nadir measurements are less prone to cloud interference and provide good horizontal spatial resolution but coarse vertical resolution. In contrast, limb measurements provide better vertical resolution and higher sensitivity to tracer concentrations, but they are subject to a higher probability of cloud interference and poorer line-of-sight spatial resolution. Accurate limb measurements are generally limited to altitudes above the upper troposphere. Currently there are no satellite measurements that are strongly sensitive to OCS concentrations near the surface, where they are most needed to evaluate surface fluxes.

The standard TES OCS product is an average between 200 and 900 hPa, with maximum sensitivity to the mid-tropospheric value (Kuai et al., 2014). Currently, the TES OCS retrievals are available over ocean only for latitudes below 40°, where the signal-to-noise ratio is higher (due to larger thermal contrasts) and the surface spectral emissivity can be easily specified. Comparisons with collocated

airborne and ground measurements show that the current TES OCS data has an accuracy of 50–80 ppt, and the accuracy is improved to ~7 ppt when averaged over one month (Kuai et al., 2014).

IASI retrieves a single value for the total column OCS. Recently, Vincent and Dudhia (2017) reported
5   the pole-to-pole global OCS retrieved from the IASI measurements, regardless of surface types. Their preliminary test showed that the seasonally averaged IASI OCS data vary consistent with ground measurements.

MIPAS retrievals from 7 to 25 km characterize the average OCS concentration in a thin layer (a few
10   kilometers thick) around the corresponding tangent height. Currently, the MIPAS OCS product provides pole-to-pole OCS concentrations at multiple levels in the upper troposphere and the stratosphere, which show an accuracy of ~50 ppt against balloon-borne measurements (Glatthor et al., 2017).

The ACE-FTS OCS reported concentrations in the lower stratosphere are known to be 15% lower than
15   the balloon-borne measurements (Velazco et al., 2011) and ~100 ppt lower than MIPAS OCS (Glatthor et al., 2017).

Fig. 14a shows the tropospheric OCS patterns obtained using TES Level-2 swath OCS retrievals in 2006, averaged over four seasons (March to May, June to August, September to November, and
20   December to February). The TES swath data have been averaged to 5° longitude × 4° latitude grid boxes, but due to low TES spatial sampling, these OCS patterns have been further smoothed to a 20° × 20° spatial resolution. Only those swath data that pass quality flags, such as high signal-to-noise ratio, cloud clearance, and high goodness-to-fit (Kuai et al., 2014), are used in the grid box averages. The tropospheric OCS variability ranges from 520 to 570 ppt over the latitudes between ±40°. There is
25   constant high OCS abundance over the tropics for all seasons, especially over the Indo-Pacific region and the Caribbean Sea, indicating the effect of tropical convection, which brings high-OCS air near the ocean surface to the mid-troposphere and may be due to an OCS ocean source. In contrast, over the

47

Cold Tongue region in the eastern Pacific, the observed OCS is low due to the strong subsidence over there.

For comparison, Fig. 14b shows the seasonal upper tropospheric OCS patterns at 250 hPa obtained
5   using MIPAS Level-2 swath OCS retrievals from 2002 to 2011. The MIPAS swath data have been averaged to the same TES 5° longitude × 4° latitude grid boxes and have also been smoothed to a 20°×20° spatial resolution. MIPAS also provides OCS abundance over the polar region, but we focus only on the tropical region to facilitate comparison. Similar to TES, the MIPAS retrievals also reveal high OCS abundance over the tropics. However, MIPAS also shows significantly higher OCS
10   abundance in subtropical regions compared to the TES observations, indicating the effect of poleward transport in the upper troposphere. The MIPAS observations also reveal lower OCS abundance over the continents, especially over South America and Africa. These continental OCS-low areas strongly suggest the effects of vegetation sinks, which unfortunately are not seen in TES observations because of the unavailability of TES retrievals over land.
15

Fig. 14c shows two-month averages of the day-time total column OCS obtained using IASI OCS retrievals in 2014. IASI also provides total column OCS over the polar region, which we do not discuss here. IASI has much higher spatial sampling than TES, and the patterns shown in Fig. 14c have a high spatial resolution of 0.5° × 0.5°. The IASI OCS observations over land generally agree with the MIPAS
20   observations, showing large sinks over South America and Africa. The high spatial resolution also helps reveal more clearly the land OCS sources over Asia, which are not seen in TES nor MIPAS observations. Furthermore, the relatively low OCS abundance over the Inter-Tropical Convergence Zone is only apparent in IASI data.

25   Figure 15 shows the summertime (June–August) latitudinal distribution of OCS observed by MIPAS (Glatthor et al., 2017). The distributions in other seasons are similar due to the long atmospheric OCS lifetime. In the troposphere, the tropical OCS is ~520 ppt, while the polar OCS is ~480 ppt. The vertical transport by convection over the Indo-Pacific region is clearly seen. The main source of OCS is in the

troposphere and it is destroyed in the stratosphere; the abundance above the tropopause decreases rapidly as altitude increases. The mid-stratospheric OCS is significantly higher in the tropical region than in the polar region because of the upwelling Brewer-Dobson branch at the equator that transports OCS from the lower stratosphere upward. Furthermore, the OCS abundance is significantly lower (close to zero) over the winter poles due to downwelling over the polar vortex.

OCS is an important tool to constrain GPP, and more resources are needed to improve the accuracy of current satellite products. Measurement campaigns need to be put in motion that will allow us to measure OCS reliably from space. The next generations of high-quality satellite instruments may target measuring OCS in the lower troposphere and/or near the boundary layer with better land surface coverage, which would improve the surface flux inversion. Optimal requirements of the instrumental designs (e.g. maximum spectral resolutions, maximum footprint dimensions, minimum signal-to-noise ratios, and choice of orbits) to achieve a lower tropospheric sensitivity can be tested using a set of representative atmospheric conditions, such as those provided by NASA's Observing System Simulation Experiments.

4.2 FTIR data

Ground-based FTIR retrievals of OCS are sensitive to the altitudes between surface and 30 km, and can therefore more directly capture the variations near the surface compared to the satellite data. There are two networks of FTIR spectrometers: the Network for the Detection of Atmospheric Composition Change (NDACC), recording the mid-infrared spectra including the OCS bands, and the Total Carbon Column Observing Network (TCCON) mainly focus on the near-infrared without OCS bands, but some of the TCCON sites are expending the measurements to the OCS bands. The FTIR remote sensing measurement is an indirect measurement, and therefore needs to be calibrated to in-situ observations to have the same scale when combining the datasets, e.g. Wang et al.,(2016) added an offset when comparing FTIR retrievals and HIAPER Pole-to-Pole Observations (HIPPO) to the same model.

OCS concentrations can be retrieved for all historical spectra and some additional data are available by request [to whom?]. Published datasets exist for the periods 1993–1997 (Griffith et al., 1998), 1978–2002 (Rinsland et al., 2002), 2001–2014 (Kremser et al., 2015), 2005–2012 (Wang et al., 2016), and 1995–2015 (Lejeune et al., 2017) and by an airborne Fourier spectrometer for the period 1978–2005

5 (Coffey and Hannigan, 2010). As with comparing in situ atmospheric observations, it is important to note how disparate datasets are calibrated.

4.3 Tower and airborne data

OCS measurements from aircraft began in the late 1980s, using both *in situ* and flask collection with

10 subsequent analysis by GC-MS (e.g. Bandy et al., 1992, 1993; Hoell et al., 1993; Thornton et al., 1996; Blake et al., 2008, etc). Data are available from two kinds of airborne sampling: survey flights, and atmospheric chemistry projects. The airborne survey flight data are designed to sample background air at set locations on a regular basis over long time periods and are part of the NOAA ESRL GMD Carbon Cycle Aircraft Network (Montzka et al., 2007). These data include sampling from 1999 at a range of

15 locations. These data have been used extensively in analysis of the continental US carbon budget (e.g. Campbell et al., 2008; Hilton et al., 2017) but sample sites outside the continental US are also available. Larger spatial scale/shorter time interval survey flights include the HIPPO (2009-2011) and ATom (2016-2018) airborne programs that predominantly sample OCS over remote marine locations. Atmospheric chemistry flights are designed to understand chemical processing and pollution transport

20 and include sampling as part of pollution transport across the Pacific (e.g. Pacific Exploratory Mission-West A (PEM-A), Thornton et al., 1996) or Transport and Chemical Evolution over the Pacific experiment (TRACE-P), which sampled Asian outflow dominated by anthropogenic OCS emissions in 2001, (Blake et al., 2004). Other projects included sampling of OCS over continents (e.g. over the US in 2004; Blake et al., 2008).

25

OCS measurements have been made from tall towers using flask and subsequent analysis by GC-MS. Most long-term tall tower observations have been conducted as part of the NOAA ESRL GMD Carbon

Cycle Tower Network (Montzka et al., 2007). These data from 11-12 sites include continuous sampling from 2000 to present at a daily or twice daily time basis for much of the record.

4.4 Ecosystem-level data

Three approaches have been used to quantify ecosystem fluxes of OCS: chamber measurements, gradient measurements, and eddy flux covariance measurements. While researchers have been quantifying OCS measurements with chambers for decades, most field outings prior to 1990 used dynamic chambers with sulfur-free sweep air, artificially inducing high emissions (Castro and Galloway, 1991). Chamber measurements made in ambient OCS conditions tend to show uptake in most non-wetland plants and soils, with a few important exceptions (Kitz et al., 2017; Maseyk et al., 2014).

Eddy covariance measurements have been used in a variety of ecosystems, generally finding the expected uptake of OCS (Asaf et al., 2013; Billesbach et al., 2014; Commane et al., 2015; Wehr et al., 2017). An OCS analyzer capable of measuring ambient OCS and CO_2 concentrations at 10 Hz has become commercially available (Kooijmans et al., 2016; Commane et al., 2013; Stimler et al., 2010a). With this powerful new tool, traditional methods of partitioning carbon fluxes over ecosystems can be directly compared to using OCS data as a proxy for GPP in situ. Few studies have made use of the gradient method (Berresheim and Vulcan, 1992). See Sect. 2.1 for specific studies.

4.5 Oceanic measurements

OCS measurements in the surface ocean comprise ca. 6,000 ship-based measurements. These samples are usually taken at a depth of 0–5m below the ocean surface and analyzed with gas chromatography using different detectors (mass-spectrometry, flame photometry) or off-axis integrated cavity output spectrometry. Table 3 gives an overview on available measurements. No central database for ship-based OCS measurements is available at the moment, but one is desired to derive global patterns and facilitate model comparison. Measurements of the precursor gas CS_2 are scarcer than OCS measurements. Samples for CS_2 are taken usually in a similar way to OCS samples from the same depth range. They

51

are mainly analyzed using gas chromatography and mass-spectrometry detection. Approximately 1,500 measurements are available.

4.6 Ice core records

Several ice cores have been analyzed for OCS concentrations. Aydin et al. (2014, 2016) developed the necessary corrections to take into account OCS hydrolysis within the ice core bubbles. Some ice core material is not suitable for OCS analysis because the environment was too warm for long periods and OCS was continuously hydrolyzed for thousands of years. The discussion in Aydin et al. (2016) identifies the records that are derived from more ideal conditions.

5 Conclusion

There are many questions yet to be answered about OCS fluxes between the Earth surface and the atmosphere. On the global scale, there is a large missing source or overestimated sink of OCS. This may be from incomplete knowledge of the tropical ocean source, incomplete observations of anthropogenic sources, or an unlikely overestimation of the plant sink. The few ocean water OCS measurements have not revealed a large enough OCS source to close the budget gap. This review concludes that the DMS source contribution for ocean OCS estimations should be considered only as a source of uncertainty until further reaction chamber experiments can be performed under conditions more similar to ambient air. Anthropogenic OCS estimates would benefit greatly from CS_2 and OCS observations from rayon factories, particularly in Asia. Unaccounted for domestic coal combustion in Asia may also play a significant role. To challenge the robustness of the very large plant sink, observing OCS uptake in plants that are water or nutrient stressed may show OCS exchange closer to the natural environment.

Other questions become more important on the regional scale. NOAA aircraft profiles were intended to be conducted from many different sites across the U.S. If this were realized it could help substantially with the COS budget for this region, and inform us about COS from different processes that would likely be relevant on larger scales. We will need to quantify soil OCS fluxes in periodically hot and dry regions, excluding deserts. Several boreal regions must take into account OCS fluxes from lakes and

freshwater as well as bryophytes and lichen. Upcoming studies in tall forests require a more in-depth treatment of cryptogamic cover and other canopy-dwelling organisms, e.g. lichen.

Our overall understanding of the elements of the budget are summarized in Table 6. While there is still
5 much work to be done, our collective knowledge has developed enough to warrant substantial investment in infrastructure to make OCS measurements from a coordinated network of tall towers, supporting and supported by satellite observations. Several types of observations are needed to link the observed ground fluxes and the atmospheric satellite fluxes, for example, FTIR measurements and AirCore campaigns. The OCS tracer gives us information on the instantaneous and integrated carbon
10 flux into plants. For regional and global-scale studies, it can be used to answer questions about large-scale perturbations and carbon-climate feedbacks, e.g. regional droughts. Most importantly, the OCS tracer can be applied in regions where current satellite coverage is poor, such as the Tropics. Creating a global OCS data product and a coordinated tall tower network generating continuous, calibrated concentration data will promote a massive advancement in our understanding of global
15 carbon feedbacks and their effect on the water cycle.

15   **References**

Alkama, R. and Cescatti, A.: Biophysical climate impacts of recent changes in global forest cover, Science, 351, 600–604, 2016.
Aneja, V. P., Overton, J. H., and Aneja, A. P.: Emission Survey of Biogenic Sulfur Flux from Terrestrial Surfaces, JAPCA J. Air Waste Ma., 31, 256–258, 1981.

20   Arsene, C., Barnes, I., and Becker, K. H.: FT-IR product study of the photo-oxidation of dimethyl sulfide: Temperature and O_2 partial pressure dependence, Phys. Chem. Chem. Phys., 1, 5463–5470, 1999.
Arsene, C., Barnes, I., Becker, K. H., and Mocanu, R.: FT-IR product study on the photo-oxidation of dimethyl sulphide in the presence of NOx—temperature dependence, Atmos. Environ., 35, 3769–

25   3780, 2001.
Asaf, D., Rotenberg, E., Tatarinov, F., Dicken, U., Montzka, S. A., and Yakir, D.: Ecosystem photosynthesis inferred from measurements of carbonyl sulphide flux, Nat. Geosci., 6, 186–190, 2013.
Aydin, M., Williams, M. B., Tatum, C., and Saltzman, E. S.: Carbonyl sulfide in air extracted from a

30   South Pole ice core: a 2000 year record, Atmos. Chem. Phys., 8, 7533–7542, 2008.

Aydin, M., Fudge, T. J., Verhulst, K. R., Nicewonger, M. R., Waddington, E. D., and Saltzman, E. S.: Carbonyl sulfide hydrolysis in Antarctic ice cores and an atmospheric history for the last 8000 years, J. Geophys. Res.-Atmos., 119, 2014JD021618, 2014.

Aydin, M., Campbell, J. E., Fudge, T. J., Cuffey, K. M., Nicewonger, M. R., Verhulst, K. R., and Saltzman, E. S.: Changes in atmospheric carbonyl sulfide over the last 54,000 years inferred from measurements in Antarctic ice cores, J. Geophys. Res.-Atmos., 121, 2015JD024235, 2016.

Ball, J. T., Woodrow, I. E., and Berry, J. A.: A model predicting stomatal conductance and its contribution to the control of photosynthesis under different environmental conditions, in: Progress in Photosynthesis Research, Vol. 4, edited by: Biggins, J., Martinus Nijhoff, the Netherlands, 221–224, 1987.

Bandy, A. R., Thornton, D. C., Scott, D. L., Lalevic, M., Lewin, E. E. and Driedger, A. R.: A time series for carbonyl sulfide in the northern hemisphere, J. Atmos. Chem., 14, 527–534, 1992.

Bandy, A. R., Thornton, D. C. and Driedger, A. R.: Airborne measurements of sulfur dioxide, dimethyl sulfide, carbon disulfide, and carbonyl sulfide by isotope dilution gas chromatography/mass spectrometry, J. Geophys. Res., 98, 23423–23433, 1993.

Barkley, M. P., Palmer, P. I., Boone, C. D., Bernath, P. F., and Suntharalingam, P.: Global distributions of carbonyl sulfide in the upper troposphere and stratosphere, Geophys. Res. Lett., 35, L14810, 2008.

Barnes, I., Becker, K. H., and Patroescu, I.: The tropospheric oxidation of dimethyl sulfide: A new source of carbonyl sulfide, Geophys. Res. Lett., 21, 2389–2392, 1994.

Barnes, I., Becker, K. H., and Patroescu, I.: FTIR product study of the OH initiated oxidation of dimethyl sulphide: Observation of carbonyl sulphide and dimethyl sulphoxide, Atmos. Environ., 30, 1805–1814, 1996.

Bastviken, D., Tranvik, L. J., Downing, J. A., Crill, P. M., and Enrich-Prast, A.: Freshwater methane emissions offset the continental carbon sink, Science, 331, 50, 2011.

Beer, C., Reichstein, M., Tomelleri, E., Ciais, P., Jung, M., Carvalhais, N., Rödenbeck, C., Arain, M. A., Baldocchi, D., and Bonan, G. B.: Terrestrial gross carbon dioxide uptake: global distribution and covariation with climate, Science, 329, 834–838, 2010.

Belviso, S., Nguyen, B. C., and Allard, P.: Estimate of carbonyl sulfide (OCS) volcanic source strength deduced from OCS/CO_2 ratios in volcanic gases, Geophys. Res. Lett., 13, 133–136, 1986.

Belviso, S., Mihalopoulos, N., and Nguyen, B. C.: The supersaturation of carbonyl sulfide (OCS) in rain waters, Atmos. Environ., 21, 1363–1367, 1989.

Belviso, S., Schmidt, M., Yver, C., Ramonet, M., Gros, V., and Launois, T.: Strong similarities between night-time deposition velocities of carbonyl sulphide and molecular hydrogen inferred from semi-continuous atmospheric observations in Gif-sur-Yvette, Paris region, Tellus B, 65, doi:10.3402/tellusb.v65i0.20719, 2013.

Belviso, S., Reiter, I. M., Loubet, B., Gros, V., Lathière, J., Montagne, D., Delmotte, M., Ramonet, M., Kalogridis, C., Lebegue, B., Bonnaire, N., Kazan, V., Gauquelin, T., Fernandez, C., and Genty, B.: A top-down approach of surface carbonyl sulfide exchange by a Mediterranean oak forest ecosystem in southern France, Atmos. Chem. Phys., 16, 14909–14923, 2016.

Berkelhammer, M., Asaf, D., Still, C., Montzka, S., Noone, D., Gupta, M., Provencal, R., Chen, H., and Yakir, D.: Constraining surface carbon fluxes using in situ measurements of carbonyl sulfide and carbon dioxide, Global Biogeochem. Cy., 28, 161–179, 2014.

Berresheim, H. and Vulcan, V. D.: Vertical distributions of COS, CS_2, DMS and other sulfur compounds in a loblolly pine forest, Atmos. Environ. A-Gen., 26, 2031–2036, 1992.

Berry, J., Wolf, A., Campbell, J. E., Baker, I., Blake, N., Blake, D., Denning, A. S., Kawa, S. R., Montzka, S. A., Seibt, U., Stimler, K., Yakir, D., and Zhu, Z.: A coupled model of the global cycles of carbonyl sulfide and CO_2: A possible new window on the carbon cycle, J. Geophys. Res.-Biogeo., 118, 842–852, 2013.

Bezsudnova, E. Y., Sorokin, D. Y., Tikhonova, T. V., and Popov, V. O.: Thiocyanate hydrolase, the primary enzyme initiating thiocyanate degradation in the novel obligately chemolithoautotrophic halophilic sulfur-oxidizing bacterium *Thiohalophilus thiocyanoxidans*, BBA-Proteins Proteom., 1774, 1563–1570, 2007.

Billesbach, D. P., Berry, J. A., Seibt, U., Maseyk, K., Torn, M. S., Fischer, M. L., Abu-Naser, M., and Campbell, J. E.: Growing season eddy covariance measurements of carbonyl sulfide and CO_2 fluxes: COS and CO_2 relationships in Southern Great Plains winter wheat, Agric. Forest Meteorol., 184, 48–55, 2014.

Blake, N. J., Streets, D. G., Woo, J.-H., Simpson, I. J., Green, J., Meinardi, S., Kita, K., Atlas, E., Fuelberg, H. E., Sachse, G., Avery, M. A., Vay, S. A., Talbot, R. W., Dibb, J. E., Bandy, A. R., Thornton, D. C., Rowland, F. S. and Blake, D. R.: Carbonyl sulfide and carbon disulfide: Large-scale distributions over the western Pacific and emissions from Asia during TRACE-P, J. Geophys. Res., 109, D15S05, 2004.

Blake, N. J., Campbell, J. E., Vay, S. A., Fuelberg, H. E., Huey, L. G., Sachse, G., Meinardi, S., Beyersdorf, A., Baker, A., Barletta, B., Midyett, J., Doezema, L., Kamboures, M., McAdams, J., Novak, B., Rowland, F. S., and Blake, D. R.: Carbonyl sulfide (OCS): Large-scale distributions over North America during INTEX-NA and relationship to CO_2, J. Geophys. Res.-Atmos., 113, doi:10.1029/2007JD009163, 2008.

Blezinger, S., Wilhelm, C., and Kesselmeier, J.: Enzymatic consumption of carbonyl sulfide (COS) by marine algae, Biogeochemistry, 48, 185–197, 2000.

Bloem, E., Haneklaus, S., Kesselmeier, J., and Schnug, E.: Sulfur fertilization and fungal infections affect the exchange of H_2S and COS from agricultural crops. J. Agricultural and Food Chemistry, 60, 7588-7596, 2012.

Blonquist, J. M., Montzka, S. A., Munger, J. W., Yakir, D., Desai, A. R., Dragoni, D., Griffis, T. J., Monson, R. K., Scott, R. L., and Bowling, D. R.: The potential of carbonyl sulfide as a proxy for gross primary production at flux tower sites, J. Geophys. Res.-Biogeo., 116, 1–18, 2011.

Boone, C. D., Nassar, R., Walker, K. A., Rochon, Y., McLeod, S. D., Rinsland, C. P., and Bernath, P. F.: Retrievals for the atmospheric chemistry experiment Fourier-transform spectrometer, Appl. Optics, 44, 7218–7231, 2005.

Brilli, F., Hörtnagl, L., Hammerle, A., Haslwanter, A., Hansel, A., Loreto, F., and Wohlfahrt, G.: Leaf and ecosystem response to soil water availability in mountain grasslands, Agric. Forest Meteorol., 151, 1731–1740, 2011.

Bunk, R., Behrendt, T., Yi, Z., Andreae, M. O., and Kesselmeier, J.: Exchange of carbonyl sulfide (OCS) between soils and atmosphere under various CO_2 concentrations, J. Geophys. Res.-Biogeo., 2016JG003678, 2017.

56

Campbell, J. E., Carmichael, G. R., Chai, T., Mena-Carrasco, M., Tang, Y., Blake, D. R., Blake, N. J., Vay, S. A., Collatz, G. J., Baker, I., Berry, J. A., Montzka, S. A., Sweeney, C., Schnoor, J. L., and Stanier, C. O.: Photosynthetic control of atmospheric carbonyl sulfide during the growing season, Science, 322, 1085–1088, 2008.

5   Campbell, J. E., Whelan, M. E., Seibt, U., Smith, S. J., Berry, J. A., and Hilton, T. W.: Atmospheric carbonyl sulfide sources from anthropogenic activity: Implications for carbon cycle constraints, Geophys. Res. Lett., doi:10.1002/2015GL063445, 2015.

Campbell, J. E., Berry, J. A., Seibt, U., Smith, S. J., Montzka, S. A., Launois, T., Belviso, S., Bopp, L. and Laine, M.: Large historical growth in global terrestrial gross primary production, Nature,
10   544(7648), 84–87, 2017a.

Campbell, J.E., Whelan, M.E., Berry, J.A., Hilton, T.W., Zumkehr, A., Stinecipher, J., Lu, Y., Kornfeld, A., Seibt, U., Dawson, T.E., Montzka, S.A., Baker, I.T., Kulkarni, S., Wang, Y., Herndon, S.C., Zahniser, M.S., Commane, R., Loik, M.E.: Coast redwood sink of atmospheric carbonyl sulfide provides a new biogeochemical tracer for coastal fog-mediated processes, J Geophys Res Biogeosci,
15   2017b.

Camy-Peyret, C., Liuzzi, G., Masiello, G., Serio, C., Venafra, S., & Montzka, S. A.: Assessment of IASI capability for retrieving carbonyl sulphide (OCS), J Quant Spectrosc Ra, 201, 197–208, 2017.

Castro, M. S. and Galloway, J. N.: A comparison of sulfur-free and ambient air enclosure techniques for measuring the exchange of reduced sulfur gases between soils and the atmosphere, J. Geophys. Res.,
20   96, 15427–15437, 1991.

Chanton, J. P., Whiting, G. J., Blair, N. E., Lindau, C. W., and Bollich, P. K.: Methane emission from rice: Stable isotopes, diurnal variations, and CO_2 exchange, Global Biogeochem. Cy., 11, 15–27, 1997.

Chin, M. and Davis, D. D.: Global sources and sinks of OCS and CS_2 and their distributions, Global
25   Biogeochem. Cy., 7, 321–337, 1993.

Chin, M. and Davis, D. D.: A reanalysis of carbonyl sulfide as a source of stratospheric background sulfur aerosol, J. Geophys. Res., 100(D5), 8993–9005, 1995.

Chiodini, G., Cioni, R., Raco, B., and Scandiffio, G.: Carbonyl sulphide (OCS) in geothermal fluids: An example from the Larderello field (Italy), Geothermics, 20, 319-327, 1991.

30   Ciais, P., Sabine, C., Bala, G., Bopp, L., Brovkin, V., Canadell, J., Chhabra, A., DeFries, R., Galloway, J., Heimann, M.. and Others: Carbon and other biogeochemical cycles, in: Climate Change 2013: The Physical Science Basis., Cambridge University Press, Cambridge, pp. 465–570, 2014.

Coffey, M. T. and Hannigan, J. W.: The temporal trend of stratospheric carbonyl sulfide, J. Atmos. Chem., 67, 61, 2010.

35   Cole, J. J., Caraco, N. F., Kling, G. W., and Kratz, T. K.: Carbon dioxide supersaturation in the surface waters of lakes, Science, 265, 1568–1570, 1994.

Collatz, G. J., Ball, J. T., Grivet, C., and Berry, J. A.: Physiological and environmental regulation of stomatal conductance, photosynthesis and transpiration: a model that includes a laminar boundary layer, Agr. Forest Meteorol., 54, 107–136, 1991.

40   Commane, R., Herndon, S. C., Zahniser, M. S., Lerner, B. M., McManus, J. B., Munger, J. W., Nelson, D. D., and Wofsy, S. C.: Carbonyl sulfide in the planetary boundary layer: Coastal and continental influences, J. Geophys. Res.-Atmos., 118, 8001–8009, 2013.

Commane, R., Meredith, L. K., Baker, I. T., Berry, J. A., Munger, J. W., Montzka, S. A., Templer, P. H., Juice, S. M., Zahniser, M. S., and Wofsy, S. C.: Seasonal fluxes of carbonyl sulfide in a midlatitude forest, P. Natl. Acad. Sci. USA, 112, 14162–14167, 2015.

Conrad, R. and Meuser, K.: Soils contain more than one activity consuming carbonyl sulfide, Atmos. Environ., 34, 3635–3639, 2000.

Crutzen, P. J.: The possible importance of CSO for the sulfate layer of the stratosphere, Geophys. Res. Lett., 3, 73–76, 1976.

Cutter, G. A., Cutter, L. S., and Filippino, K. C.: Sources and cycling of carbonyl sulfide in the Sargasso Sea, Limnol. Oceanogr., 49, 555–565, 2004.

de Gouw, J. A., Warneke, C., Montzka, S. A., Holloway, J. S., Parrish, D. D., Fehsenfeld, F. C., Atlas, E. L., Weber, R. J., and Flocke, F. M.: Carbonyl sulfide as an inverse tracer for biogenic organic carbon in gas and aerosol phases, Geophys. Res. Lett., 36(5), L05804, 2009.

DeLaune, R. D., Devai, I., and Lindau, C. W.: Flux of reduced sulfur gases along a salinity gradient in Louisiana coastal marshes, Estuar. Coast. Shelf S., 54, 1003–1011, 2002.

de Mello, W. Z. and Hines, M. E.: Application of static and dynamic enclosures for determining dimethyl sulfide and carbonyl sulfide exchange in Sphagnum peatlands: Implications for the magnitude and direction of flux, J. Geophys. Res., 99, 14601–14607, 1994.

Deprez, P. P., Franzmann, P. D., and Burton, H. R.: Determination of reduced sulfur gases in antarctic lakes and seawater by gas chromatography after solid adsorbent preconcentration, J. Chromatogr. A, 362, 9–21, 1986.

Devai, I. and DeLaune, R. D.: Formation of volatile sulfur compounds in salt marsh sediment as influenced by soil redox condition, Org. Geochem., 23, 283–287, 1995.

Devai, I. and DeLaune, R. D.: Trapping Efficiency of Various Solid Adsorbents for Sampling and Quantitative Gas Chromatographic Analysis of Carbonyl Sulfide, Anal. Lett., 30, 187–198, 1997.

Dixon, M. J. R., Loh, J., Davidson, N. C., Beltrame, C., Freeman, R., and Walpole, M.: Tracking global change in ecosystem area: The Wetland Extent Trends index, Biol. Conserv., 193, 27–35, 2016.

Downing, J. A., Prairie, Y. T., Cole, J. J., Duarte, C. M., Tranvik, L. J., Striegl, R. G., McDowell, W. H., Kortelainen, P., Caraco, N. F., Melack, J. M., and Middleburg, J. J.: The global abundance and size distribution of lakes, ponds, and impoundments, Limnol. Oceanogr., 51, 2388–2397, 2006.

Du, Q., Zhang, C., Mu, Y., Cheng, Y., Zhang, Y., Liu, C., Song, M., Tian, D., Liu, P., Liu, J., Xue, C., Ye, C.: An important missing source of atmospheric carbonyl sulfide: Domestic coal combustion, Geophys Res Lett, 43(16), 8720–8727, 2016.

Du, Q., Mu, Y., Zhang, C., Liu, J., Zhang, Y., and Liu, C.: Photochemical production of carbonyl sulfide, carbon disulfide and dimethyl sulfide in a lake water, J. Environ. Sci. , 51, 146–156, 2017.

Elbert, W., Weber, B., Burrows, S., Steinkamp, J., Büdel, B., Andreae, M. O., and Pöschl, U.: Contribution of cryptogamic covers to the global cycles of carbon and nitrogen, Nat. Geosci., 5, 459–462, 2012.

Elliott, S.: Effect of hydrogen peroxide on the alkaline hydrolysis of carbon disulfide, Environ. Sci. Technol., 24, 264–267, 1990.

Elliott, S., Lu, E., and Rowland, F. S.: Rates and mechanisms for the hydrolysis of carbonyl sulfide in natural waters, Environ. Sci. Technol., 23, 458–461, 1989.

Engel, A. and Schmidt, U.: Vertical profile measurements of carbonylsulfide in the stratosphere, Geophys. Res. Lett., 21, 2219–2222, 1994.

Ensign, S. A.: Reactivity of carbon monoxide dehydrogenase from Rhodospirillum rubrum with carbon dioxide, carbonyl sulfide, and carbon disulfide, Biochemistry, 34, 5372–5378, 1995.

5 Eyring, V., Bony, S., Meehl, G. A., Senior, C. A., Stevens, B., Stouffer, R. J., and Taylor, K. E.: Overview of the Coupled Model Intercomparison Project Phase 6 (CMIP6) experimental design and organization, Geosci. Model Dev., 9, 1937–1958, 2016.

Ferek, R. J. and Andreae, M. O.: Photochemical production of carbonyl sulphide in marine surface waters, Nature, 307(5947), 148–150, 1984.

10 Fichot, C. G. and Miller, W. L.: An approach to quantify depth-resolved marine photochemical fluxes using remote sensing: Application to carbon monoxide (CO) photoproduction, Remote Sens. Environ., 114, 1363–1377, 2010.

Fischer, M. L., Torn, M. S., Billesbach, D. P., Doyle, G., Northup, B., and Biraud, S. C.: Carbon, water, and heat flux responses to experimental burning and drought in a tallgrass prairie, Agric. Forest
15 Meteorol., 166, 169–174, 2012.

Flöck, O. R. and Andreae, M. O.: Photochemical and non-photochemical formation and destruction of carbonyl sulfide and methyl mercaptan in ocean waters, Mar. Chem., 54, 11–26, 1996.

Flöck, O. R., Andreae, M. O., and Dräger, M.: Environmentally relevant precursors of carbonyl sulfide in aquatic systems, Mar. Chem., 59, 71–85, 1997.

20 Fried, A., Klinger, L. F., and Iii, D. J. E.: Atmospheric carbonyl sulfide exchange in bog microcosms, Geophys. Res. Lett., 20, 129–132, 1993.

Friedlingstein, P., Meinshausen, M., Arora, V. K., Jones, C. D., Anav, A., Liddicoat, S. K., and Knutti, R.: Uncertainties in CMIP5 climate projections due to carbon cycle feedbacks, J. Climate, 27, 511–526, 2013.

25 Fritz, M. and Bachofen, R.: Volatile organic sulfur compounds in a meromictic alpine lake, Acta Hydroch. Hydrob., 28, 185–192, 2000.

Gerdel, K., Spielmann, F.M., Hammerle, A., and Wohlfahrt G.: Eddy covariance carbonyl sulfide flux measurements with a quantum cascade laser absorption spectrometer, Atmos. Meas. Tech., 10, 3525-3537, 2017.

30 Gerlach, T.: Volcanic versus anthropogenic carbon dioxide, Eos Trans. Amer. Geophys. Union, 92, 201–202, 2011.

Gimeno, T. E., Ogée, J., Royles, J., Gibon, Y., West, J. B., Burlett, R., Jones, S. P., Sauze, J., Wohl, S., Benard, C., Genty, B., and Wingate, L.: Bryophyte gas-exchange dynamics along varying hydration status reveal a significant carbonyl sulphide (COS) sink in the dark and COS source in the light, New
35 Phytol., 215, 965–976, 2017.

Glatthor, N., Höpfner, M., Baker, I. T., Berry, J., Campbell, J. E., Kawa, S. R., Krysztofiak, G., Leyser, A., Sinnhuber, B.-M., Stiller, G. P., Stinecipher, J., and von Clarmann, T.: Tropical sources and sinks of carbonyl sulfide observed from space, Geophys. Res. Lett., 42, 10082–10090, doi: 10.1002/2015GL066293, 2015.

40 Glatthor, N., Höpfner, M., Leyser, A., Stiller, G. P., von Clarmann, T., Grabowski, U., Kellmann, S., Linden, A., Sinnhuber, B.-M., Krysztofiak, G., and Walker, K. A.: Global carbonyl sulfide (OCS) measured by MIPAS/Envisat during 2002–2012, Atmos. Chem. Phys., 17(4), 2631–2652, 2017.

59

Gries, C., Iii, T. H. N., and Kesselmeier, J.: Exchange of reduced sulfur gases between lichens and the atmosphere, Biogeochemistry, 26, 25–39, 1994.

Griffith, D. W. T., Jones, N. B., and Matthews, W. A.: Interhemispheric ratio and annual cycle of carbonyl sulfide (OCS) total column from ground-based solar FTIR spectra, J. Geophys. Res.-Atmos., 103, 8447–8454, 1998.

Guanter, L., Zhang, Y., Jung, M., Joiner, J., Voigt, M., Berry, J. A., Frankenberg, C., Huete, A. R., Zarco-Tejada, P., Lee, J.-E., Moran, M. S., Ponce-Campos, G., Beer, C., Camps-Valls, G., Buchmann, N., Gianelle, D., Klumpp, K., Cescatti, A., Baker, J. M., and Griffis, T. J.: Global and time-resolved monitoring of crop photosynthesis with chlorophyll fluorescence, P. Natl. Acad. Sci. USA, 111, E1327–33, 2014.

Hanschen, F. S., Lamy, E., Schreiner, M., and Rohn, S.: Reactivity and stability of glucosinolates and their breakdown products in foods, Angew. Chem. Int. Edit., 53, 11430–11450, 2014.

Harman, G. E., Howell, C. R., Viterbo, A., Chet, I., and Lorito, M.: Trichoderma species — opportunistic, avirulent plant symbionts, Nat. Rev. Microbiol., 2, 43–56, 2004.

Hilton, T. W., Zumkehr, A., Kulkarni, S., Berry, J., Whelan, M. E., and Campbell, J. E.: Large variability in ecosystem models explains uncertainty in a critical parameter for quantifying GPP with carbonyl sulphide, Tellus B, 67, doi:10.3402/tellusb.v67.26329, 2015.

Hilton, T. W., Whelan, M. E., Zumkehr, A., Kulkarni, S., Berry, J. A., Baker, I. T., Montzka, S. A., Sweeney, C., Miller, B. R., and Campbell, J. E.: Peak growing season gross uptake of carbon in North America is largest in the Midwest USA, Nat. Clim. Change, doi:10.1038/nclimate3272, 2017.

Hoell, J. M., Davis, D. D., Gregory, G. L., McNeal, R. J., Bendura, R. J., Drewry, J. W., Barrick, J. D., Kirchhoff, V. W. J. H., Motta, A. G., Navarro, R. L., Dorko, W. D. and Owen, D. W.: Operational overview of the NASA GTE/CITE 3 airborne instrument intercomparisons for sulfur dioxide, hydrogen sulfide, carbonyl sulfide, dimethyl sulfide, and carbon disulfide, J. Geophys. Res., 98, 23291–23304, 1993.

Hoover, D. L. and Rogers, B. M.: Not all droughts are created equal: The impacts of interannual drought pattern and magnitude on grassland carbon cycling, Glob. Change Biol., 22, 1809–1820, 2016.

Huete, A. R., Didan, K., Shimabukuro, Y. E., Ratana, P., Saleska, S. R., Hutyra, L. R., Yang, W., Nemani, R. R., and Myneni, R.: Amazon rainforests green-up with sunlight in dry season, Geophys. Res. Lett., 33, L06405, 2006.

Hungate, B. A., Holland, E. A., Jackson, R. B., Stuart Chapin, F., Mooney, H. A., and Field, C. B.: The fate of carbon in grasslands under carbon dioxide enrichment, Nature, 388, 576–579, 1997.

Huntzinger, D. N., Post, W. M., Wei, Y., Michalak, A. M., West, T. O., Jacobson, A. R., Baker, I. T., Chen, J. M., Davis, K. J., Hayes, D. J., Hoffman, F. M., Jain, A. K., Liu, S., McGuire, A. D., Neilson, R. P., Potter, C., Poulter, B., Price, D., Raczka, B. M., Tian, H. Q., Thornton, P., Tomelleri, E., Viovy, N., Xiao, J., Yuan, W., Zeng, N., Zhao, M., and Cook, R.: North American Carbon Program (NACP) regional interim synthesis: Terrestrial biospheric model intercomparison, Ecol. Model., 232, 144–157, 2012.

Hussain, A., Ogawa, T., Saito, M., Sekine, T., Nameki, M., Matsushita, Y., Hayashi, T., and Katayama, Y.: Cloning and expression of a gene encoding a novel thermostable thiocyanate-degrading enzyme from a mesophilic alphaproteobacteria strain THI201, Microbiology, 159, 2294–2302, 2013.

60

Hynes, A. J., Wine, P. H., and Nicovich, J. M.: Kinetics and mechanism of the reaction of hydroxyl with carbon disulfide under atmospheric conditions, J. Phys. Chem.-US, 92, 3846–3852, 1988.

Ichii, K., Kondo, M., Lee, Y.-H., Wang, S.-Q., Kim, J., Ueyama, M., Lim, H.-J., Shi, H., Suzuki, T., Ito, A., Kwon, H., Ju, W., Huang, M., Sasai, T., Asanuma, J., Han, S., Hirano, T., Hirata, R., Kato, T., Li, S.-G., Li, Y.-N., Maeda, T., Miyata, A., Matsuura, Y., Murayama, S., Nakai, Y., Ohta, T., Saitoh, T. M., Saigusa, N., Takagi, K., Tang, Y.-H., Wang, H.-M., Yu, G.-R., Zhang, Y.-P., and Zhao, F.-H.: Site-level model–data synthesis of terrestrial carbon fluxes in the CarboEastAsia eddy-covariance observation network: toward future modeling efforts, J. Forestry Res., 18, 13–20, 2013.

Iordan, S. L., Kraczkiewicz-Dowjat, A. J., Kelly, D. P., and Wood, A. P.: Novel eubacteria able to grow on carbon disulfide, Arch. Microbiol., 163, 131–137, 1995.

Jung, M., Reichstein, M., Margolis, H. A., Cescatti, A., Richardson, A. D., Arain, M. A., Arneth, A., Bernhofer, C., Bonal, D., Chen, J., Gianelle, D., Gobron, N., Kiely, G., Kutsch, W., Lasslop, G., Law, B. E., Lindroth, A., Merbold, L., Montagnani, L., Moors, E. J., Papale, D., Sottocornola, M., Vaccari, F., and Williams, C.: Global patterns of land-atmosphere fluxes of carbon dioxide, latent heat, and sensible heat derived from eddy covariance, satellite, and meteorological observations, J. Geophys. Res. Biogeo., 116, doi: 10.1029/2010JG001566, 2011.

Kamezaki K., Hattori S., Ogawa T., Toyoda, S., Kato H., Katayama Y. Yoshida N. 2016. Sulfur isotopic fractionation of carbonyl sulfide during degradation by soil bacteria. Environ. Sci. Technol. 50:3537-3544.

Kamyshny, A., Goifman, A., Rizkov, D., and Lev, O.: Formation of carbonyl sulfide by the reaction of carbon monoxide and inorganic polysulfides, Environ. Sci. Technol., 37, 1865–1872, 2003.

Kanda, K. I., Tsuruta, H., and Minami, K.: Emission of dimethyl sulfide, carbonyl sulfide, and carbon bisulfide from paddy fields, Soil Sci. Plant Nutr., 38, 709–716, 1992.

Kanda, K.-I., Tsuruta, H., and Minami, K.: Emissions of biogenic sulfur gases from maize and wheat fields, Soil Sci. Plant Nutr., 41, 1–8, 1995.

Katayama, Y., Narahara, Y., Inoue, Y., Amano, F., Kanagawa, T., and Kuraishi, H.: A thiocyanate hydrolase of *Thiobacillus thioparus*. A novel enzyme catalyzing the formation of carbonyl sulfide from thiocyanate, J. Biol. Chem., 267, 9170–9175, 1992.

Kato, H., Saito, M., Nagahata, Y., and Katayama, Y.: Degradation of ambient carbonyl sulfide by Mycobacterium spp. in soil, Microbiology, 154, 249–255, 2008.

Kato H., Igarashi Y., Dokiya Y., Katayama Y. (2011) Vertical distribution of carbonyl sulfide at Mt.Fuji, Japan. Water Air Soil Pollution DOI 10.1007/s11270-011-0847-0

Kesselmeier, J. and Hubert, A.: Exchange of reduced volatile sulfur compounds between leaf litter and the atmosphere, Atmos. Environ., 36, 4679–4686, 2002.

Kesselmeier, J., Teusch, N., and Kuhn, U.: Controlling variables for the uptake of atmospheric carbonyl sulfide by soil, J. Geophys. Res., 104, 11577–11584, 1999.

Kettle, A. J., Kuhn, U., Von Hobe, M., Kesselmeier, J., Liss, P. S., and Andreae, M. O.: Comparing forward and inverse models to estimate the seasonal variation of hemisphere-integrated fluxes of carbonyl sulfide, Atmos. Chem. Phys. Discuss., 2, 577–621, 2002.

Kitz, F., Gerdel, K., Hammerle, A., Laterza, T., Spielmann, F. M., and Wohlfahrt, G.: In situ soil COS exchange of a temperate mountain grassland under simulated drought, Oecologia, 183, 851–860, 2017.

Kooijmans, L. M. J., Uitslag, N. A. M., Zahniser, M. S., Nelson, D. D., Montzka, S. A., and Chen, H.: Continuous and high precision atmospheric concentration measurements of COS, CO2, CO and H2O using a quantum cascade laser spectrometer (QCLS), Atmos. Meas. Tech., 9, 5293-5314, 2016.

Kooijmans, L. M. J., Maseyk, K., Seibt, U., Sun, W., Vesala, T., Mammarella, I., Kolari, P., Aalto, J., Franchin, A., Vecchi, R., Valli, G. and Chen, H.: Canopy uptake dominates nighttime carbonyl sulfide fluxes in a boreal forest, Atmos. Chem. Phys., 17, 11453–11465, 2017.

Kremser, S., Jones, N. B., Palm, M., Lejeune, B., Wang, Y., Smale, D., and Deutscher, N. M.: Positive trends in Southern Hemisphere carbonyl sulfide, Geophys. Res. Lett., 42, doi: 10.1002/2015GL065879, 2015.

Krysztofiak, G., Té, Y. V., Catoire, V., Berthet, G., Toon, G. C., Jégou, F., Jeseck, P., and Robert, C.: Carbonyl sulphide (OCS) variability with latitude in the atmosphere, Atmos. Ocean, 53, 89–101, 2015.

Kuai, L., Worden, J., Kulawik, S. S., Montzka, S. A., and Liu, J.: Characterization of Aura TES carbonyl sulfide retrievals over ocean, Atmos. Meas. Tech., 7, 163–172, 2014.

Kuai, L., Worden, J. R., Campbell, J. E., Kulawik, S. S., Li, K.-F., Lee, M., Weidner, R. J., Montzka, S. A., Moore, F. L., Berry, J. A., Baker, I., Denning, A. S., Bian, H., Bowman, K. W., Liu, J., and Yung, Y. L.: Estimate of carbonyl sulfide tropical oceanic surface fluxes using Aura Tropospheric Emission Spectrometer observations, J. Geophys. Res.-Atmos., 120, doi: 10.1002/2015JD023493, 2015.

Kuhn, U. and Kesselmeier, J.: Environmental variables controlling the uptake of carbonyl sulfide by lichens, J. Geophys. Res.-Atmos., 105, 26783–26792, 2000.

Kuhn, U., Ammann, C., Wolf, A., Meixner, F. X., Andreae, M. O., and Kesselmeier, J.: Carbonyl sulfide exchange on an ecosystem scale: soil represents a dominant sink for atmospheric COS, Atmos. Environ., 33, 995–1008, 1999.

Kusumi, A., Li, X. S., and Katayama, Y.: Mycobacteria isolated from angkor monument sandstones grow chemolithoautotrophically by oxidizing elemental sulfur, Front. Microbiol., 2, 104, 2011.

Launois, T., Belviso, S., Bopp, L., Fichot, C. G., and Peylin, P.: A new model for the global biogeochemical cycle of carbonyl sulfide – Part 1: Assessment of direct marine emissions with an oceanic general circulation and biogeochemistry model, Atmos. Chem. Phys., 15, 2295–2312, 2015a.

Launois, T., Peylin, P., Belviso, S., and Poulter, B.: A new model of the global biogeochemical cycle of carbonyl sulfide – Part 2: Use of carbonyl sulfide to constrain gross primary productivity in current vegetation models, Atmos. Chem. Phys., 15, 9285–9312, 2015b.

Lee, C.-L. and Brimblecombe, P.: Anthropogenic contributions to global carbonyl sulfide, carbon disulfide and organosulfides fluxes, Earth-Sci. Rev., 160, 1–18, 2016.

Lehner, B. and Döll, P.: Development and validation of a global database of lakes, reservoirs and wetlands, J. Hydrol., 296, 1–22, 2004.

Lejeune, B., Mahieu, E., Vollmer, M. K., Reimann, S., Bernath, P. F., Boone, C. D., Walker, K. A., and Servais, C.: Optimized approach to retrieve information on atmospheric carbonyl sulfide (OCS) above the Jungfraujoch station and change in its abundance since 1995, J. Quant. Spectrosc. Ra., 186, 81–95, 2017.

Lennartz, S. T., Marandino, C. A., Von Hobe, M., Cortes, P., Quack, B., Simo, R., Booge, D., Pozzer, A., Steinhoff, T., Arevalo-Martinez, D. L., Kloss, C., Bracher, A., Röttgers, R., Atlas, E., and

Krüger, K.: Direct oceanic emissions unlikely to account for the missing source of atmospheric carbonyl sulfide, Atmos. Chem. Phys., 17, 385–402, 2017.

Lindo, Z., Nilsson, M.-C., and Gundale, M. J.: Bryophyte-cyanobacteria associations as regulators of the northern latitude carbon balance in response to global change, Glob. Change Biol., 19, 2022–2035, 2013.

Li, X. S., Sato, T., Ooiwa, Y., Kusumi, A., Gu, J.-D., and Katayama, Y.: Oxidation of elemental sulfur by *Fusarium solani* strain THIF01 harboring endobacterium *Bradyrhizobium* sp, Microb. Ecol., 60, 96–104, 2010.

Li, X., Zhu, Z., Yang, L., and Sun, Z.: Emissions of biogenic sulfur gases (H_2S, COS) from *Phragmites australis* coastal marsh in the Yellow River estuary of China, Chinese Geogr. Sci., 26, 770–778, 2016.

Liu, J. and Li, X.: Sulfur cycle in the typical meadow *Calamagrostis angustifolia* wetland ecosystem in the Sanjiang Plain, Northeast China, J. Environ. Sci., 20, 470–475, 2008.

Liu, J., Bowman, K. W., and Lee, M.: Comparison between the Local Ensemble Transform Kalman Filter (LETKF) and 4D-Var in atmospheric CO_2 flux inversion with the Goddard Earth Observing System-Chem model and the observation impact diagnostics from the LETKF, J. Geophys. Res. D: Atmos., 121, doi: 10.1002/2016JD025100, 2016.

Lorimer, G. H. and Pierce, J.: Carbonyl sulfide: an alternate substrate for but not an activator of ribulose-1,5-bisphosphate carboxylase, J. Biol. Chem., 264, 2764–2772, 1989.

MacIntyre, S., Wanninkhof, R., and Chanton, J. P.: Trace gas exchange across the air–water interface in freshwaters and coastal marine environments, in: Biogenic trace gases: Measuring emissions from soil and water, Matson, P. A., and Harriss, R. C., eds., Blackwell, p. 52–97, 1995.

Maestre, F. T., Escolar, C., de Guevara, M. L., Quero, J. L., Lázaro, R., Delgado-Baquerizo, M., Ochoa, V., Berdugo, M., Gozalo, B., and Gallardo, A.: Changes in biocrust cover drive carbon cycle responses to climate change in drylands, Glob. Change Biol., 19, 3835–3847, 2013.

Masaki, Y., Ozawa, R., Kageyama, K., and Katayama, Y.: Degradation and emission of carbonyl sulfide, an atmospheric trace gas, by fungi isolated from forest soil, FEMS Microbiol. Lett., 363, doi:10.1093/femsle/fnw197, 2016.

Maseyk, K., Berry, J. A., Billesbach, D., Campbell, J. E., Torn, M. S., Zahniser, M., and Seibt, U.: Sources and sinks of carbonyl sulfide in an agricultural field in the Southern Great Plains, P. Natl. Acad. Sci. USA, 111, 9064–9069, 2014.

Melillo, J. M. and Steudler, P. A.: The effect of nitrogen fertilization on the COS and CS_2 emissions from temperature forest soils, J. Atmos. Chem., 9, 411–417, 1989.

Meredith, L. K., Ogée, J., Boye, K., Singer, E., Wingate, L., von Sperber, C., Sengupta, A., Whelan, M.E., Pang, E., Keiluweit, M., Brüggemann, N., Berry, J., Welander, P.V.: Soil exchange rates of COS and $CO^{18}O$ shift with the diversity of microbial communities and their carbonic anhydrase enzymes, In prep.

Metcalfe, D. B., Ricciuto, D., Palmroth, S., Campbell, C., Hurry, V., Mao, J., Keel, S. G., Linder, S., Shi, X., Näsholm, T., Ohlsson, K. E. A., Blackburn, M., Thornton, P. E., and Oren, R.: Informing climate models with rapid chamber measurements of forest carbon uptake, Glob. Change Biol., 23, 2130–2139, 2017.

Mihalopoulos, N., Bonsang, B., Nguyen, B. C., Kanakidou, M., and Belviso, S.: Field observations of carbonyl sulfide deficit near the ground: Possible implication of vegetation, Atmos. Environ., 23, 2159–2166, 1989.

Montzka, S. A., Aydin, M., Battle, M., Butler, J. H., Saltzman, E. S., Hall, B. D., Clarke, A. D.,
5   Mondeel, D., and Elkins, J. W.: A 350-year atmospheric history for carbonyl sulfide inferred from Antarctic firn air and air trapped in ice, J. Geophys. Res., 109, doi:10.1029/2004JD004686, 2004.

Montzka, S. A., Calvert, P., Hall, B. D., Elkins, J. W., Conway, T. J., Tans, P. P., and Sweeney, C.: On the global distribution, seasonality, and budget of atmospheric carbonyl sulfide (COS) and some similarities to CO_2, J. Geophys. Res.- Atmos., 112, doi:10.1029/2006JD007665, 2007.

10   Mu, Y., Geng, C., Wang, M., Wu, H., Zhang, X., and Jiang, G.: Photochemical production of carbonyl sulfide in precipitation, J. Geophys. Res.-Atmos., 109, doi:10.1029/2003JD004206, 2004.

Nacke, H., Thürmer, A., Wollherr, A., Will, C., Hodac, L., Herold, N., Schöning, I., Schrumpf, M., and Daniel, R.: Pyrosequencing-based assessment of bacterial community structure along different management types in German forest and grassland soils, PLoS One, 6, e17000, 2011.

15   Notni, J., Schenk, S., Protoschill-Krebs, G., Kesselmeier, J. and Anders, E., 2007. The missing link in COS metabolism: A model study on the reactivation of carbonic anhydrase from its hydrosulfide analogue. ChemBioChem, 8(5), pp.530-536.

Notsu, K. and Toshiya, M.: Chemical monitoring of volcanic gas using remote FT-IR spectroscopy at several active volcanoes in Japan, Appl. Geochem, 25, 505–512, 2010.

20   Ogawa, T., Noguchi, K., Saito, M., Nagahata, Y., Kato, H., Ohtaki, A., Nakayama, H., Dohmae, N., Matsushita, Y., Odaka, M., Yohda, M., Nyunoya, H., and Katayama, Y.: Carbonyl sulfide hydrolase from *Thiobacillus thioparus* strain THI115 is one of the β-carbonic anhydrase family enzymes, J. Am. Chem. Soc., 135, 3818–3825, 2013.

Ogawa, T., Kato, H., Higashide, M., Nishimiya, M., and Katayama, Y.: Degradation of carbonyl sulfide
25   by Actinomycetes and detection of clade D of β-class carbonic anhydrase, FEMS Microbiol. Lett., doi:10.1093/femsle/fnw223, 2016.

Ogawa T., Hattori S., Kamezaki K., Kato H., Yoshida N., Katayama Y. Isotopic fractionation of sulfur in carbonyl sulfide by carbonyl sulfide hydrolase of *Thiobacillus thioparus* THI115. Microbes and Environments, 32, 367-375, 2017.

30   Ogée, J., Sauze, J., Kesselmeier, J., Genty, B., Van Diest, H., Launois, T., and Wingate, L.: A new mechanistic framework to predict OCS fluxes from soils, Biogeosciences, 13, 2221-2240, 2016.

Oppenheimer, C., Kyle, P., Eisele, F., Crawford, J., Huey, G., Tanner, D., Kim, S., Mauldin, L., Blake, D., Beyersdorf, A., Buhr, M., and Davis, D.: Atmospheric chemistry of an Antarctic volcanic plume, J. Geophys. Res., 115, D04303, 2010.

35   Pandey, S. K. and Kim, K.-H.: A review of methods for the determination of reduced sulfur compounds (RSCs) in air, Environ. Sci. Technol., 43, 3020–3029, 2009.

Parazoo, N. C., Bowman, K., Fisher, J. B., Frankenberg, C., Jones, D. B. A., Cescatti, A., Pérez-Priego, Ó., Wohlfahrt, G., and Montagnani, L.: Terrestrial gross primary production inferred from satellite fluorescence and vegetation models, Glob. Change Biol., 20, 3103–3121, 2014.

40   Parazoo, N. C., Barnes, E., Worden, J., Harper, A. B., Bowman, K. B., Frankenberg, C., Wolf, S., Litvak, M., and Keenan, T. F.: Influence of ENSO and the NAO on terrestrial carbon uptake in the Texas-northern Mexico region, Global Biogeochem. Cy., 29, 1247–1265, 2015.

Parton, W. J., Scurlock, J. M. O., Ojima, D. S., Schimel, D. S., Hall, D. O., and SCOPEGRAM Group Members: Impact of climate change on grassland production and soil carbon worldwide, Glob. Change Biol., 1, 13–22, 1995.

Patrick, W. H., Jr. and DeLaune, R. D.: Chemical and biological redox systems affecting nutrient availability in the coastal wetlands, Geoscience and Man, 18, 137, 1977.

Patroescu, I. V., Barnes, I., Becker, K. H., and Mihalopoulos, N.: FT-IR product study of the OH-initiated oxidation of DMS in the presence of NOx, Atmos. Environ., 33, 25–35, 1998.

Paw U, K.T., Qiu, J., Su, H.-B, Watanabe, T., Brunet, Y.: Surface renewal analysis: a new method to obtain scalar fluxes, Agric. For. Meteorol., 74(1), 119–137, 1995.

Phillips, O. L., Aragão, L. E. O. C., Lewis, S. L., Fisher, J. B., Lloyd, J., López-González, G., Malhi, Y., Monteagudo, A., Peacock, J., Quesada, C. A., van der Heijden, G., Almeida, S., Amaral, I., Arroyo, L., Aymard, G., Baker, T. R., Bánki, O., Blanc, L., Bonal, D., Brando, P., Chave, J., de Oliveira, A. C. A., Cardozo, N. D., Czimczik, C. I., Feldpausch, T. R., Freitas, M. A., Gloor, E., Higuchi, N., Jiménez, E., Lloyd, G., Meir, P., Mendoza, C., Morel, A., Neill, D. A., Nepstad, D., Patiño, S., Peñuela, M. C., Prieto, A., Ramírez, F., Schwarz, M., Silva, J., Silveira, M., Thomas, A. S., Steege, H. T., Stropp, J., Vásquez, R., Zelazowski, P., Alvarez Dávila, E., Andelman, S., Andrade, A., Chao, K.-J., Erwin, T., Di Fiore, A., Honorio C, E., Keeling, H., Killeen, T. J., Laurance, W. F., Peña Cruz, A., Pitman, N. C. A., Núñez Vargas, P., Ramírez-Angulo, H., Rudas, A., Salamão, R., Silva, N., Terborgh, J., and Torres-Lezama, A.: Drought sensitivity of the Amazon rainforest, Science, 323, 1344–1347, 2009.

Piao, S., Sitch, S., Ciais, P., Friedlingstein, P., Peylin, P., Wang, X., Ahlström, A., Anav, A., Canadell, J. G., Cong, N., Huntingford, C., Jung, M., Levis, S., Levy, P. E., Li, J., Lin, X., Lomas, M. R., Lu, M., Luo, Y., Ma, Y., Myneni, R. B., Poulter, B., Sun, Z., Wang, T., Viovy, N., Zaehle, S., and Zeng, N.: Evaluation of terrestrial carbon cycle models for their response to climate variability and to CO_2 trends, Glob. Change Biol., 19, 2117–2132, 2013.

Porada, P., Weber, B., Elbert, W., Pöschl, U., and Kleidon, A.: Estimating impacts of lichens and bryophytes on global biogeochemical cycles, Global Biogeochem. Cy., 28, 71–85, 2014.

Pos, W. H., Riemer, D. D., and Zika, R. G.: Carbonyl sulfide (OCS) and carbon monoxide (CO) in natural waters: evidence of a coupled production pathway, Mar. Chem., 62, 89–101, 1998.

Prentice, I. C., Harrison, S. P., and Bartlein, P. J.: Global vegetation and terrestrial carbon cycle changes after the last ice age, New Phytol., 189, 988–998, 2011.

Protoschill-Krebs, G. and Kesselmeier, J.: Enzymatic pathways for the consumption of carbonyl sulphide (COS) by higher plants. Botanica Acta 105, 206-212, 1992.

Protoschill-Krebs, G., Wilhelm, C., and Kesselmeier, J.: Consumption of carbonyl sulphide by Chlamydomonas reinhardtii with different activities of carbonic anhydrase (CA) induced by different CO_2 growing regimes, Plant Biol., 108, 445–448, 1995.

Protoschill-Krebs, G., Wilhelm, C., and Kesselmeier, J.: Consumption of carbonyl sulphide (COS) by higher plant carbonic anhydrase (CA), Atmos. Environ., 30(18), 3151–3156, 1996.

Raatikainen, M. and Kuusisto, E.: The number and surface area of the lakes in Finland, Terra, 102, 97–110, 1990.

Radford-Knoery, J. and Cutter, G. A.: Determination of carbonyl sulfide and hydrogen sulfide species in natural waters using specialized collection procedures and gas chromatography with flame photometric detection, Anal. Chem., 65, 976–976, 1993.

5   Radford-Knęry, J. and Cutter, G. A.: Biogeochemistry of dissolved hydrogen sulfide species and carbonyl sulfide in the western North Atlantic Ocean, Geochim. Cosmochim. Ac., 58, 5421–5431, 1994.

Rasmussen, R. A., Khalil, M. A., Dalluge, R. W., Penkett, S. A., and Jones, B.: Carbonyl sulfide and carbon disulfide from the eruptions of Mount St. Helens, Science, 215, 665–667, 1982.

Raz-Yaseef, N., Billesbach, D. P., Fischer, M. L., Biraud, S. C., Gunter, S. A., Bradford, J. A., and
10   Torn, M. S.: Vulnerability of crops and native grasses to summer drying in the U.S. Southern Great Plains, Agric. Ecosyst. Environ., 213, 209–218, 2015.

Read, J. S., Hamilton, D. P., Desai, A. R., Rose, K. C., MacIntyre, S., Lenters, J. D, Smyth,R .L, Hanson, P. C., Cole, J. J., Staehr, P. A., Rusak, J., A., Pierson, D. C., Brookes, J. D., Laas, A., Wu, C. H.: Lake-size dependency of wind shear and convection as controls on gas exchange, Geophys.
15   Res. Lett., 39, L09405, 2012.

Reichstein, M., Falge, E., Baldocchi, D., Papale, D., Aubinet, M., Berbigier, P., Bernhofer, C., Buchmann, N., Gilmanov, T., Granier, A., Grünwald, T., Havránková, K., Ilvesniemi, H., Janous, D., Knohl, A., Laurila, T., Lohila, A., Loustau, D., Matteucci, G., Meyers, T., Miglietta, F., Ourcival, J.-M., Pumpanen, J., Rambal, S., Rotenberg, E., Sanz, M., Tenhunen, J., Seufert, G., Vaccari, F.,
20   Vesala, T., Yakir, D., and Valentini, R.: On the separation of net ecosystem exchange into assimilation and ecosystem respiration: review and improved algorithm, Glob. Change Biol., 11, 1424–1439, 2005.

Reichstein, M., Bahn, M., Ciais, P., Frank, D., Mahecha, M. D., Seneviratne, S. I., Zscheischler, J., Beer, C., Buchmann, N., Frank, D. C., Papale, D., Rammig, A., Smith, P., Thonicke, K., van der
25   Velde, M., Vicca, S., Walz, A., and Wattenbach, M.: Climate extremes and the carbon cycle, Nature, 500, 287–295, 2013.

Restrepo-Coupe, N., Levine, N. M., Christoffersen, B. O., Albert, L. P., Wu, J., Costa, M. H., Galbraith, D., Imbuzeiro, H., Martins, G., da Araujo, A. C., Malhi, Y. S., Zeng, X., Moorcroft, P., and Saleska, S. R.: Do dynamic global vegetation models capture the seasonality of carbon fluxes in the Amazon
30   basin? A data-model intercomparison, Glob. Change Biol., 23, 191–208, 2017.

Rice, H., Nochumson, D. H., and Hidy, G. M.: Contribution of anthropogenic and natural sources to atmospheric sulfur in parts of the United States, Atmos. Environ., 15, 1–9, 1981.

Richards, S. R., Kelly, C. A., and Rudd, J. W. M.: Organic volatile sulfur in lakes of the Canadian Shield and its loss to the atmosphere, Limnol. Oceanogr., 36, 468–482, 1991.

35   Richards, S. R., Rudd, J. W. M., and Kelly, C. A.: Organic volatile sulfur in lakes ranging in sulfate and dissolved salt concentration over five orders of magnitude, Limnol. Oceanogr., 39, 562–572, 1994.

Rinsland, C. P., Goldman, A., Mahieu, E., Zander, R., Notholt, J., Jones, N. B., Griffith, D., Stephen, T. M., and Chiou, L. S.: Ground-based infrared spectroscopic measurements of carbonyl sulfide: Free tropospheric trends from a 24-year time series of solar absorption measurements, J. Geophys. Res.-
40   Atmos., 107, doi: 10.1029/2002JD002522, 2002.

Rubino, M., Etheridge, D. M., Trudinger, C. M., Allison, C. E., Rayner, P. J., Enting, I., Mulvaney, R., Steele, L. P., Langenfelds, R. L., Sturges, W. T., Curran, M. A. J., and Smith, A. M.: Low

66

atmospheric CO_2 levels during the Little Ice Age due to cooling-induced terrestrial uptake, Nat. Geosci., 9, 691–694, 2016.

Saleska, S. R., Didan, K., Huete, A. R., and da Rocha, H. R.: Amazon forests green-up during 2005 drought, Science, 318, 612, 2007.

Sandoval-Soto, L., Stanimirov, M., Von Hobe, M., Schmitt, V., Valdes, J., Wild, A., and Kesselmeier, J.: Global uptake of carbonyl sulfide (COS) by terrestrial vegetation: Estimates corrected by deposition velocities normalized to the uptake of carbon dioxide (CO_2), Biogeosciences, 2, 125–132, 2005.

Schenk, S., Kesselmeier, J. and Anders, E.: How does the exchange of one oxygen atom with sulfur affect the catalytic cycle of carbonic anhydrase?, Chem.-Eur. J., 10, 3091–3105, 2004.

Sauze, J., Ogée, J., Maron, P.-A., Crouzet, O., Nowak, V., Wohl, S., Kaisermann, A., Jones, S. P. and Wingate, L.: The interaction of soil phototrophs and fungi with pH and their impact on soil CO_2, CO ^{18}O and OCS exchange, Soil Biol. Biochem., 115, 371–382, 2017.

Sawyer, G.M., Carn, S.A., Tsanev, V.I., Oppenheimer, C., and Burton, M.: Investigation into magma degassing at Nyiragongo volcano, Democratic Republic of the Congo, Geochem. Geophy. Geosy., 9, doi:10.1029/2007GC001829, 2008.

Schlesinger, W. H. and Bernhardt, E. S.: Biogeochemistry: An Analysis of Global Change, Academic Press, Waltham, 2012.

Schuh, A. E., Denning, A. S., Corbin, K. D., Baker, I. T., Uliasz, M., Parazoo, N., Andrews, A. E., and Worthy, D.: A regional high-resolution carbon flux inversion of North America for 2004, Biogeosciences, 7, 1625–1644, 2010.

Scurlock, J. M. O. and Hall, D. O.: The global carbon sink: a grassland perspective, Glob. Change Biol., 4, 229–233, 1998.

Seefeldt, L. C., Rasche, M. E. and Ensign, S. A.: Carbonyl sulfide and carbon dioxide as new substrates, and carbon disulfide as a new inhibitor, of nitrogenase, Biochemistry, 34, 5382–5389, 1995.

Seibt, U., Kesselmeier, J., Sandoval-Soto, L., Kuhn, U. and Berry, J. A.: A kinetic analysis of leaf uptake of COS and its relation to transpiration, photosynthesis and carbon isotope fractionation, Biogeosciences, 7, 333–341, 2010.

Simmons, J. S.: Consumption of atmospheric carbonyl sulfide by coniferous boreal forest soils, J. Geophys. Res., 104, 11569–11576, 1999.

Sitch, S., Friedlingstein, P., Gruber, N., Jones, S. D., Murray-Tortarolo, G., Ahlström, A., Doney, S. C., Graven, H., Heinze, C., Huntingford, C., Levis, S., Levy, P. E., Lomas, M., Boulter, B., Viovy, N., Zaehle, S., Zeng, N., Arneth, A., Bonan, G., Bopp, L., Canadell, J. G., Chevallier, F., Ciais, P., Ellis, R., Gloor, M., Peylin, P., Piao, S. L., Le Quéré, C., Smith, B., Zhu, Z., and Myneni, R. Recent trends and drivers of regional sources and sinks of carbon dioxide. Biogeosciences, 12, 653–679, 2015.

Smeulders, M. J., Barends, T. R. M., Pol, A., Scherer, A., Zandvoort, M. H., Udvarhelyi, A., Khadem, A. F., Menzel, A., Hermans, J., Shoeman, R. L., Wessels, H. J. C. T., van den Heuvel, L. P., Russ, L., Schlichting, I., Jetten, M. S. M., and Op den Camp, H. J. M.: Evolution of a new enzyme for carbon disulphide conversion by an acidothermophilic archaeon, Nature, 478, 412–416, 2011.

Smith, N. A. and Kelly, D. P.: Oxidation of carbon disulphide as the sole source of Energy for the autotrophic growth of *Thiobacillus thioparus* strain TK-m, Microbiology, 134, 3041–3048, 1988.

Spence, C., Rouse, W. R., Worth, D., and Oswald, C.: Energy budget processes of a small northern lake, J. Hydrometeorol., 4, 694–701, 2003.

Steinbacher, M., Bingemer, H. G., and Schmidt, U.: Measurements of the exchange of carbonyl sulfide (OCS) and carbon disulfide (CS_2) between soil and atmosphere in a spruce forest in central Germany, Atmos. Environ., 38, 6043–6052, 2004.

Steudler, P. A. and Kijowski, W.: Determination of reduced sulfur gases in air by solid adsorbent preconcentration and gas chromatography, Anal. Chem., 56, doi:10.1021/ac00272a051, 1984.

Steudler, P. A. and Peterson, B. J.: Contribution of gaseous sulphur from salt marshes to the global sulphur cycle, Nature, 311, 455–457, 1984.

Steudler, P. A. and Peterson, B. J.: Annual cycle of gaseous sulfur emissions from a New England Spartina alterniflora marsh, Atmos. Environ., 19, 1411–1416, 1985.

Stickel, R. E., Chin, M., Daykin, E. P., Hynes, A. J., Wine, P. H., and Wallington, T. J.: Mechanistic studies of the hydroxyl-initiated oxidation of carbon disulfide in the presence of oxygen, J. Phys. Chem., 97, 13653–13661, 1993.

Stimler, K., Nelson, D., and Yakir, D.: High precision measurements of atmospheric concentrations and plant exchange rates of carbonyl sulfide using mid-IR quantum cascade laser, Glob. Chang. Biol., 16(9), 2496–2503, 2010a.

Stimler, K., Montzka, S. A., Berry, J. A., Rudich, Y., and Yakir, D.: Relationships between carbonyl sulfide (COS) and CO_2 during leaf gas exchange, New Phytol., 186, 869–878, 2010b.

Stimler, K., Berry, J. A., Montzka, S. A., and Yakir, D.: Association between carbonyl sulfide uptake and 18Δ during gas exchange in C3 and C4 leaves, Plant Physiol., 157(1), 509–517, 2011.

Stimler, K., Berry, J. A., and Yakir, D.: Effects of carbonyl sulfide and carbonic anhydrase on stomatal conductance1[OA], Plant Physiol., 158, 524–530, 2012.

Stoy, P. C., Katul, G. G., Siqueira, M. B. S., Juang, J.-Y., McCarthy, H. R., Kim, H.-S., Oishi, A. C., and Oren, R.: Variability in net ecosystem exchange from hourly to inter-annual time scales at adjacent pine and hardwood forests: A wavelet analysis, Tree Physiol., 25, 887–902, 2005.

Stoy, P. C., Richardson, A. D., Baldocchi, D. D., Katul, G. G., Stanovick, J., Mahecha, M. D., Reichstein, M., Detto, M., Law, B. E., Wohlfahrt, G., Arriga, N., Campos, J., McCaughey, J. H., Montagnani, L., Paw U. K. T., Sevanto, S., and Williams, M.: Biosphere-atmosphere exchange of CO_2 in relation to climate: A cross-biome analysis across multiple time scales, Biogeosciences, 6, 2297–2312, 2009.

Suntharalingam, P., Kettle, A. J., Montzka, S. M., and Jacob, D. J.: Global 3-D model analysis of the seasonal cycle of atmospheric carbonyl sulfide: Implications for terrestrial vegetation uptake, Geophys. Res. Lett., 35, doi:10.1029/2008GL034332, 2008.

Sun, W., Maseyk, K., Lett, C. and Seibt, U.: A soil diffusion–reaction model for surface COS flux: COSSM v1, Geosci. Model Dev., 8, 3055–3070, 2015.

Sun, W., Maseyk, K., Lett, C., and Seibt, U.: Litter dominates surface fluxes of carbonyl sulfide in a Californian oak woodland, J. Geophys. Res.-Biogeosciences, 121, doi:10.1002/2015JG003149, 2016.

Sun, W., Kooijmans, L. M. J., Maseyk, K., Chen, H., Mammarella, I., Vesala, T., Levula, J., Keskinen, H., and Seibt, U.: Soil fluxes of carbonyl sulfide (COS), carbon monoxide, and carbon dioxide in a boreal forest in southern Finland, Atmos. Chem. Phys. Discuss., 1–24, 2017.

Symonds, R.B., Reed, M.H., and Rose, W.I.: Origin, speciation, and fluxes of trace-element gases at Augustine volcano, Alaska: insights into magma degassing and fumarolic processes, Geochim. Cosmochim. Ac., 56, 633-657, 1992.

Thornton, D. C., Bandy, A. R., Blomquist, B. W. and Anderson, B. E.: Impact of anthropogenic and biogenic sources and sinks on carbonyl sulfide in the North Pacific troposphere, J. Geophys. Res., 101, 1873–1881, 1996.

Turco, R. P., Whitten, R. C., Toon, O. B., Pollack, J. B., and Hamill, P.: OCS, stratospheric aerosols and climate, Nature, 283, 283–285, 1980.

Uher, G.: Distribution and air–sea exchange of reduced sulphur gases in European coastal waters, Estuar. Coast. Shelf S., 70, 338–360, 2006.

Uher, G. and Andreae, M. O.: Photochemical production of carbonyl sulfide in North Sea water: A process study, Limnol. Oceanogr., 42, 432–442, 1997.

Vacher, C., Hampe, A., Porté, A. J., Sauer, U., Compant, S., and Morris, C. E.: The Phyllosphere: Microbial Jungle at the Plant–Climate Interface, Annu. Rev. Ecol. Evol. S., 47, 1–24, doi:10.1146/annurev-ecolsys-121415-032238, 2016.

Van Diest, H., and Kesselmeier, J.: Soil atmosphere exchange of carbonyl sulfide (COS) regulated by diffusivity depending on water-filled spore space, Biogeosciences, 5, 475–483, 2008.

Velazco, V. A., Toon, G. C., Blavier, J.-F. L., Kleinböhl, A., Manney, G. L., Daffer, W. H., Bernath, P. F., Walker, K. A., and Boone, C.: Validation of the Atmospheric Chemistry Experiment by noncoincident MkIV balloon profiles, J. Geophys. Res., 116, D06306, 2011.

Vincent, R. A. and Dudhia, A.: Fast retrievals of tropospheric carbonyl sulfide with IASI, Atmos. Chem. Phys., 17, 2981–3000, 2017.

Von Clarmann, T., Glatthor, N., Grabowski, U., Höpfner, M., Kellmann, S., Kiefer, M., Linden, A., Tsidu, G. M., Milz, M., Steck, T., Stiller, G. P., Wang, D. Y., Fischer, H., Funke, B., Gil-López, S., and López-Puertas, M.: Retrieval of temperature and tangent altitude pointing from limb emission spectra recorded from space by the Michelson Interferometer for Passive Atmospheric Sounding (MIPAS), J. Geophys. Res.-Atmos., 108, doi: 10.1029/2003JD003602, 2003.

Von Hobe, M., Cutter, G. A., Kettle, A. J., and Andreae, M. O.: Dark production: A significant source of oceanic COS, J. Geophys. Res., 106, 31217–31226, 2001.

Vorholt, J. A.: Microbial life in the phyllosphere, Nat. Rev. Microbiol., 10, 828–840, 2012.

Wang, L., Zhang, F., and Chen, J.: Carbonyl sulfide derived from catalytic oxidation of Carbon disulfide over atmospheric particles, Environ. Sci. Technol., 35, 2543–2547, 2001.

Wang, Y., Deutscher, N. M., Palm, M., Warneke, T., Notholt, J., Baker, I., Berry, J., Suntharalingam, P., Jones, N., Mahieu, E., Lejeune, B., Hannigan, J., Conway, S., Mendonca, J., Strong, K., Campbell, J. E., Wolf, A., and Kremser, S.: Towards understanding the variability in biospheric CO_2 fluxes: Using FTIR spectrometry and a chemical transport model to investigate the sources and sinks of carbonyl sulfide and its link to CO_2, Atmos. Chem. Phys., 16, 2123–2138, 2016.

Watts, S. F.: The mass budgets of carbonyl sulfide, dimethyl sulfide, carbon disulfide and hydrogen sulfide, Atmos. Environ., 34, 761–779, 2000.

Wehr, R., Munger, J. W., McManus, J. B., Nelson, D. D., Zahniser, M. S., Davidson, E. A., Wofsy, S. C., and Saleska, S. R.: Seasonality of temperate forest photosynthesis and daytime respiration, Nature, 534, 680–683, 2016.

69

Wehr, R., Commane, R., Munger, J. W., McManus, J. B., Nelson, D. D., Zahniser, M. S., Saleska, S. R., and Wofsy, S. C.: Dynamics of canopy stomatal conductance, transpiration, and evaporation in a temperate deciduous forest, validated by carbonyl sulfide uptake, Biogeosciences, 14, 389, 2017.

Weisenstein, D. K., Yue, G. K., Ko, M. K. W., Sze, N.-D., Rodriguez, J. M., and Scott, C. J.: A two-dimensional model of sulfur species and aerosols, J. Geophys. Res.-Atmos., 102, 13019–13035, 1997.

Welte, C. U., Rosengarten, J. F., de Graaf, R. M., and Jetten, M. S. M.: SaxA-mediated isothiocyanate metabolism in phytopathogenic pectobacteria, Appl. Environ. Microb., 82, 2372–2379, 2016.

Whelan, M. E. and Rhew, R. C..: Carbonyl sulfide produced by abiotic thermal and photo-degradation of soil organic matter from wheat field substrate, J. Geophys. Res.-Biogeo., doi: 10.1002/2014JG002661, 2015.

Whelan, M. E. and Rhew, R. C.: Reduced sulfur trace gas exchange between a seasonally dry grassland and the atmosphere, Biogeochemistry, 128, 267–280, 2016.

Whelan, M. E., Min, D.-H., and Rhew, R. C.: Salt marshes as a source of atmospheric carbonyl sulfide, Atmos. Environ., 73, 131–137, 2013.

Whelan, M. E., Hilton, T. W., Berry, J. A., Berkelhammer, M., Desai, A. R., and Campbell, J. E.: Carbonyl sulfide exchange in soils for better estimates of ecosystem carbon uptake, Atmos. Chem. Phys., 16, 3711–3726, 2016.

White, M. L., Zhou, Y., Russo, R. S., Mao, H., Talbot, R., Varner, R. K., and Sive, B. C.: Carbonyl sulfide exchange in a temperate loblolly pine forest grown under ambient and elevated CO_2, Atmos. Chem. Phys., 10, 547–561, 2010.

Wilson, K. B., Hanson, P. J., Mulholland, P. J., Baldocchi, D. D., and Wullschleger, S. D.: A comparison of methods for determining forest evapotranspiration and its components: sap-flow, soil water budget, eddy covariance and catchment water balance, Agr. Forest Meteorol., 106, 153–168, 2001.

Wohlfahrt, G., Brilli, F., Hörtnagl, L., Xu, X., Bingemer, H., Hansel, A., and Loreto, F.: Carbonyl sulfide (COS) as a tracer for canopy photosynthesis, transpiration and stomatal conductance: potential and limitations, Plant Cell Environ., 35, 657–667, 2012.

Wohlfahrt, G., and Gu, L.: The many meanings of gross photosynthesis and their implication for photosynthesis research from leaf to globe, Plant Cell Environ., 38, 2500-2507, 2015.

Xie, H., Moore, R. M., and Miller, W. L.: Photochemical production of carbon disulphide in seawater, J. Geophys. Res., 103, 5635–5644, 1998.

Xie, H., Scarratt, M. G., and Moore, R. M.: Carbon disulphide production in laboratory cultures of marine phytoplankton, Atmos. Environ., 33, 3445–3453, 1999.

Xu, X., Bingemer, H. G., and Schmidt, U.: The flux of carbonyl sulfide and carbon disulfide between the atmosphere and a spruce forest, Atmos. Chem. Phys. Discuss., 2, 181–212, 2002.

Yamasaki, M., Matsushita, Y., Namura, M., Nyunoya, H., and Katayama, Y.: Genetic and immunochemical characterization of thiocyanate-degrading bacteria in lake water, Appl. Environ. Microb., 68, 942–946, 2002.

Yi, Z. and Wang, X.: Carbonyl sulfide and dimethyl sulfide fluxes in an urban lawn and adjacent bare soil in Guangzhou, China, J. Environ. Sci., 23, 784–789, 2011.

Yi, Z., Wang, X., Sheng, G., Zhang, D., Zhou, G., and Fu, J.: Soil uptake of carbonyl sulfide in subtropical forests with different successional stages in south China, J. Geophys. Res., 112, D08302, 2007.

Yi, Z., Wang, X., Sheng, G., and Fu, J.: Exchange of carbonyl sulfide (OCS) and dimethyl sulfide (DMS) between rice paddy fields and the atmosphere in subtropical China, Agr. Ecosyst. Environ., 123, 116–124, 2008.

Zhang, L., Walsh, R. S., and Cutter, G. A.: Estuarine cycling of carbonyl sulfide: production and sea–air flux, Mar. Chem., 61, 127–142, 1998.

Zumkehr, A., Hilton, T. W., Whelan, M. E., Smith, S., and Campbell, J. E.: Gridded anthropogenic emissions inventory and atmospheric transport of carbonyl sulfide in the U.S., J. Geophys. Res.-Atmos., 122, doi:10.1002/2016JD025550, 2017.
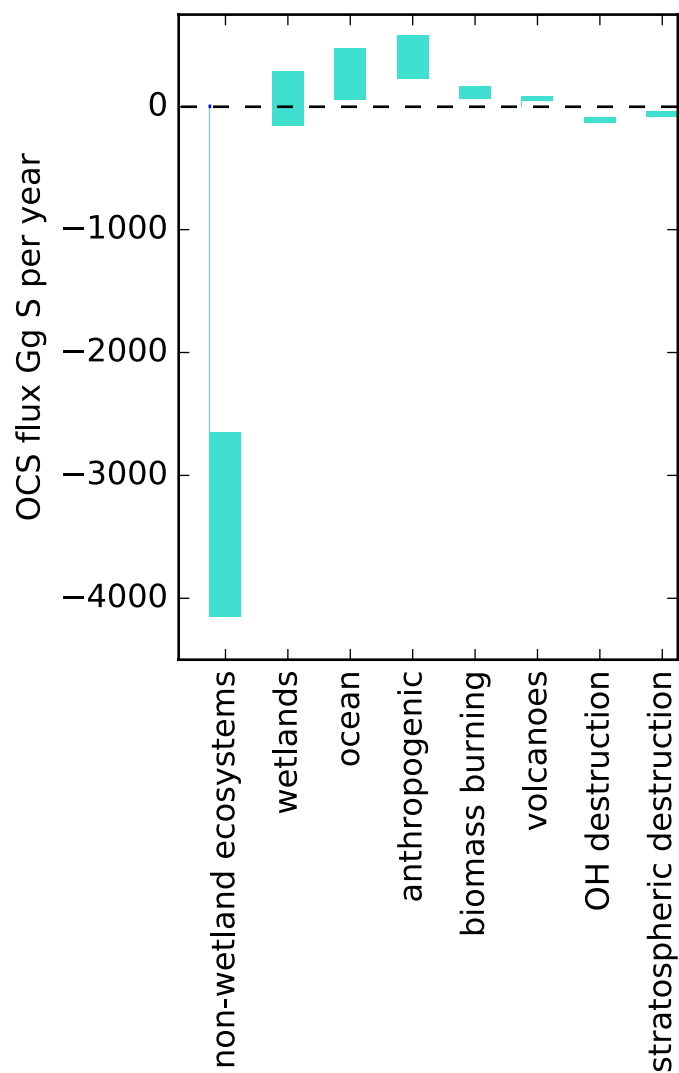
5

10

15

Figure 1. A bottom-up budget of OCS on the global scale developed. No attempt has been made to preserve mass balance.
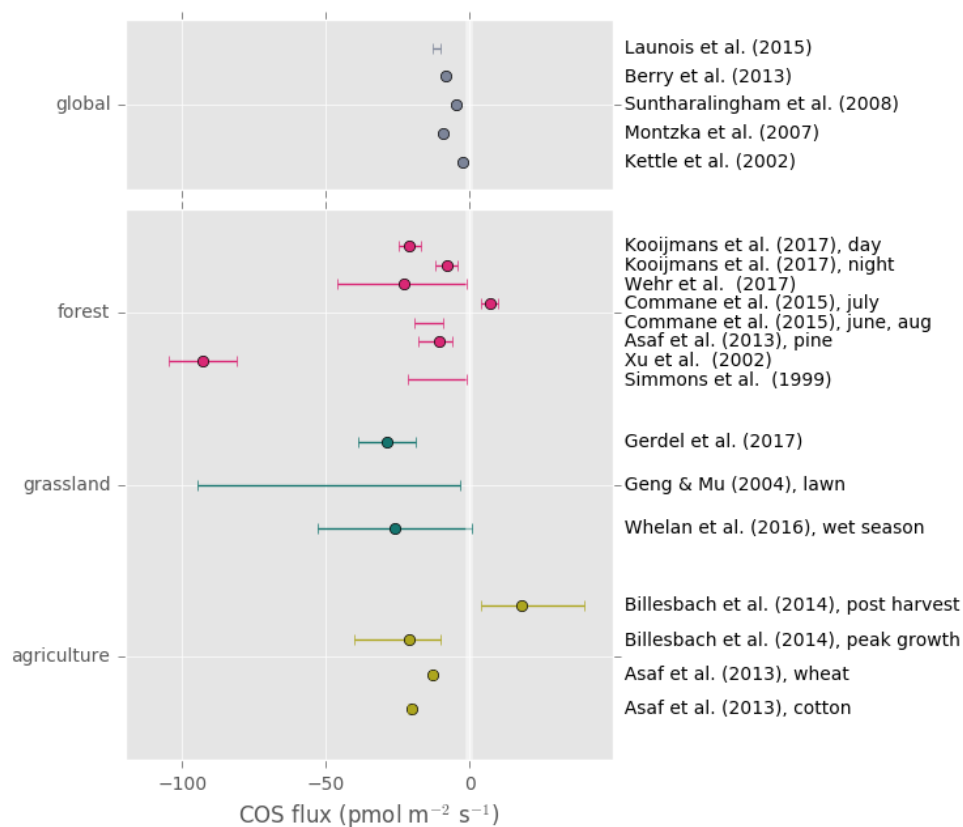
Figure 2. Top panel: Global average land OCS uptake from modeling studies. Bottom panel: reported averages and ranges of whole ecosystem, site-level OCS observations.
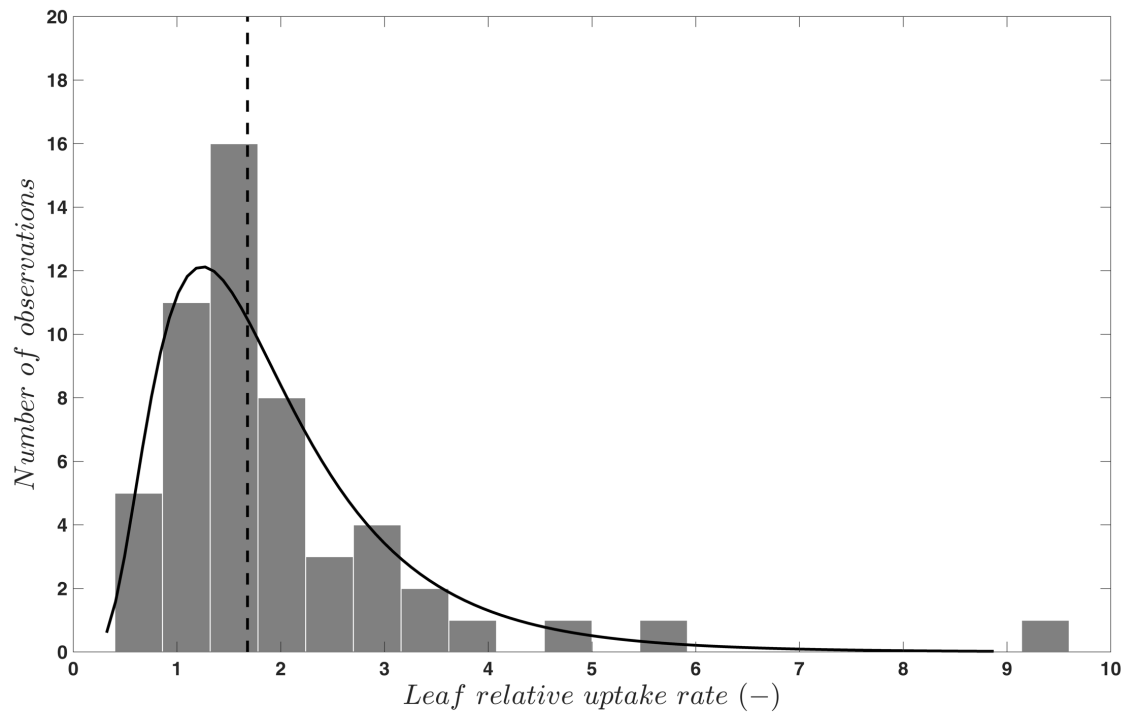
Figure 3. Frequency distribution (bars) of and log-normal fit (solid line) to published values (n = 53) of the leaf relative uptake rate of C3 species. The vertical line indicates the median (1.68). Published data are from: Berkelhammer et al., 2014; Sandoval-Soto et al., 2005; Stimler et al., 2010b, 2011, 2012.
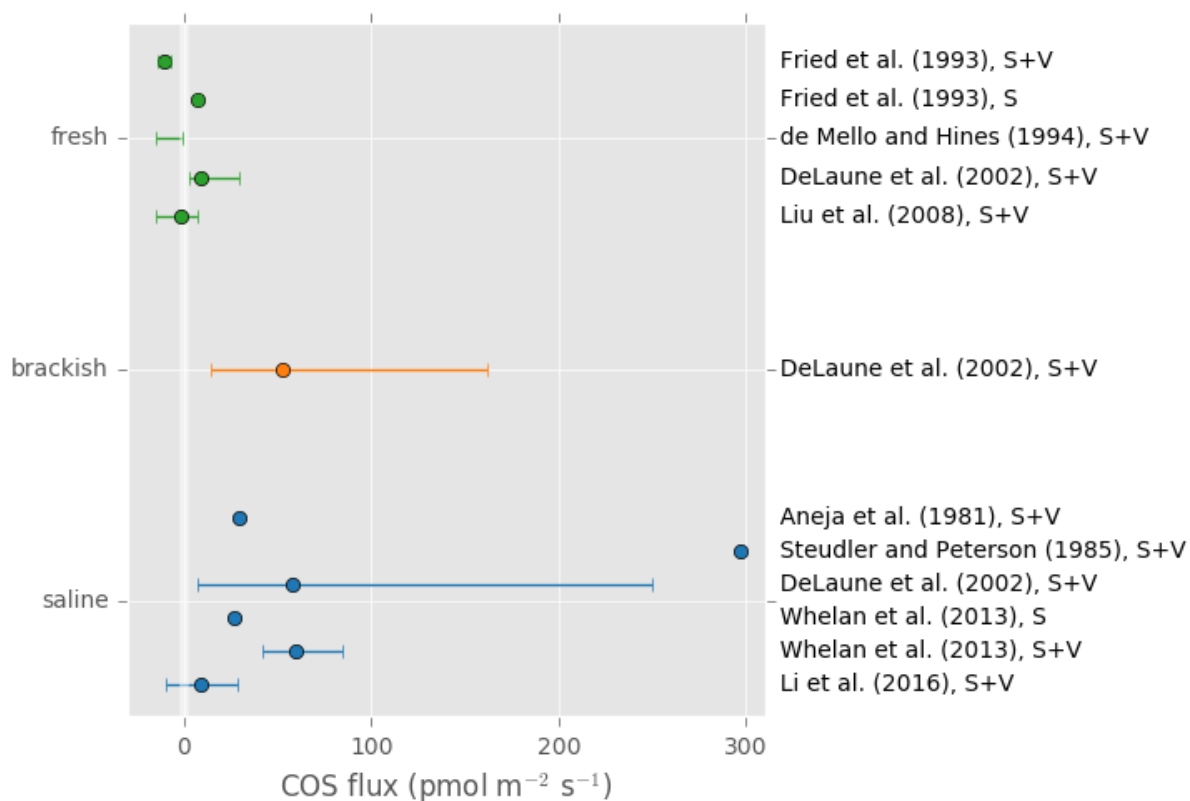
5

Figure 4. A summary figure for wetland OCS emissions. Lines indicate minimum to maximum ranges. Studies denoted "S" indicated a soil-only observation, and "S+V" denotes a soil and vegetation observation. Note that some earlier observations using sulfur-free air as chamber sweep air have been excluded due to overestimation (Castro and Galloway, 1991).
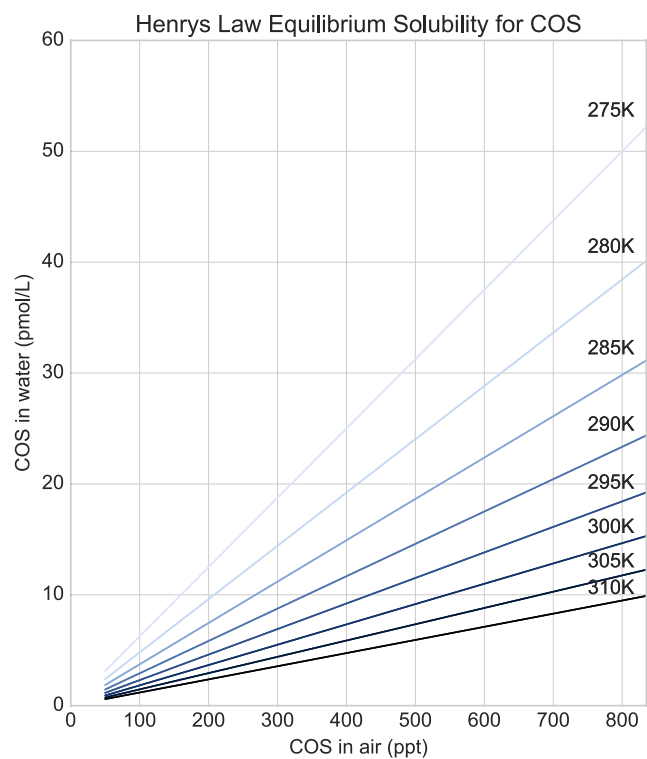
Figure 5. Solubility of OCS in water dependent on ambient OCS concentration and temperature.
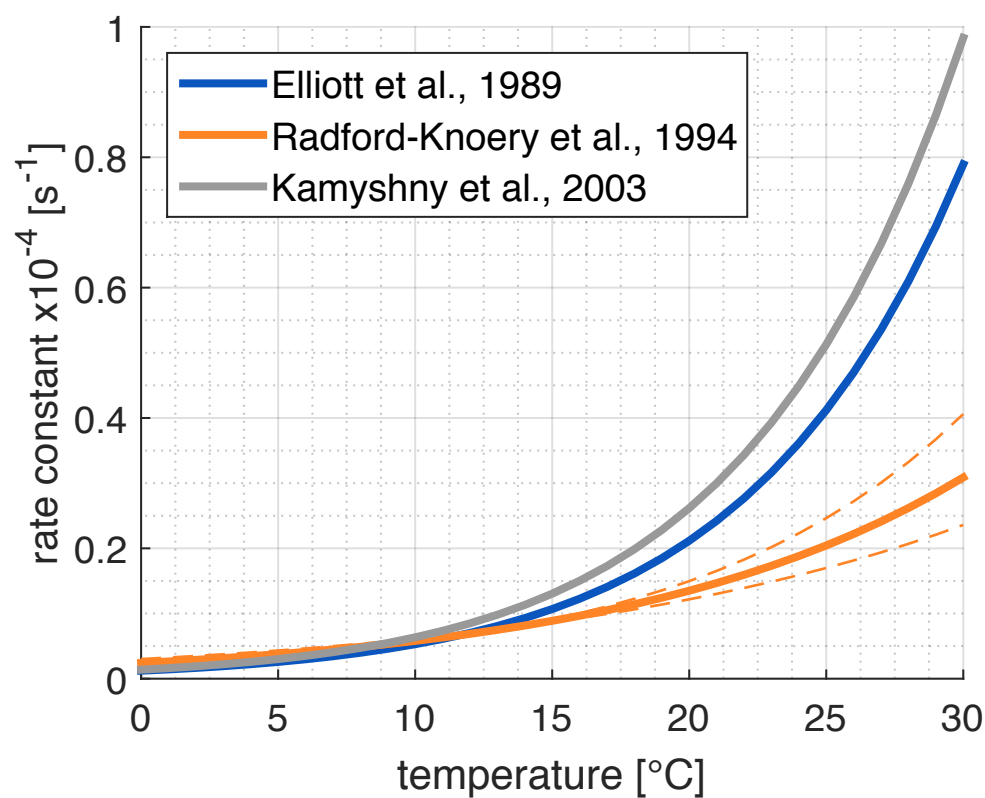
Figure 6. Comparison of published hydrolysis rates for OCS based on laboratory experiments with artificial waters (Elliott et al., 1989; Kamyshny et al., 2003), and under oceanographic conditions using filtered seawater (Radford-Knoery et al., 1994). The graph is replotted using equations from original papers at a pH of 8.2.
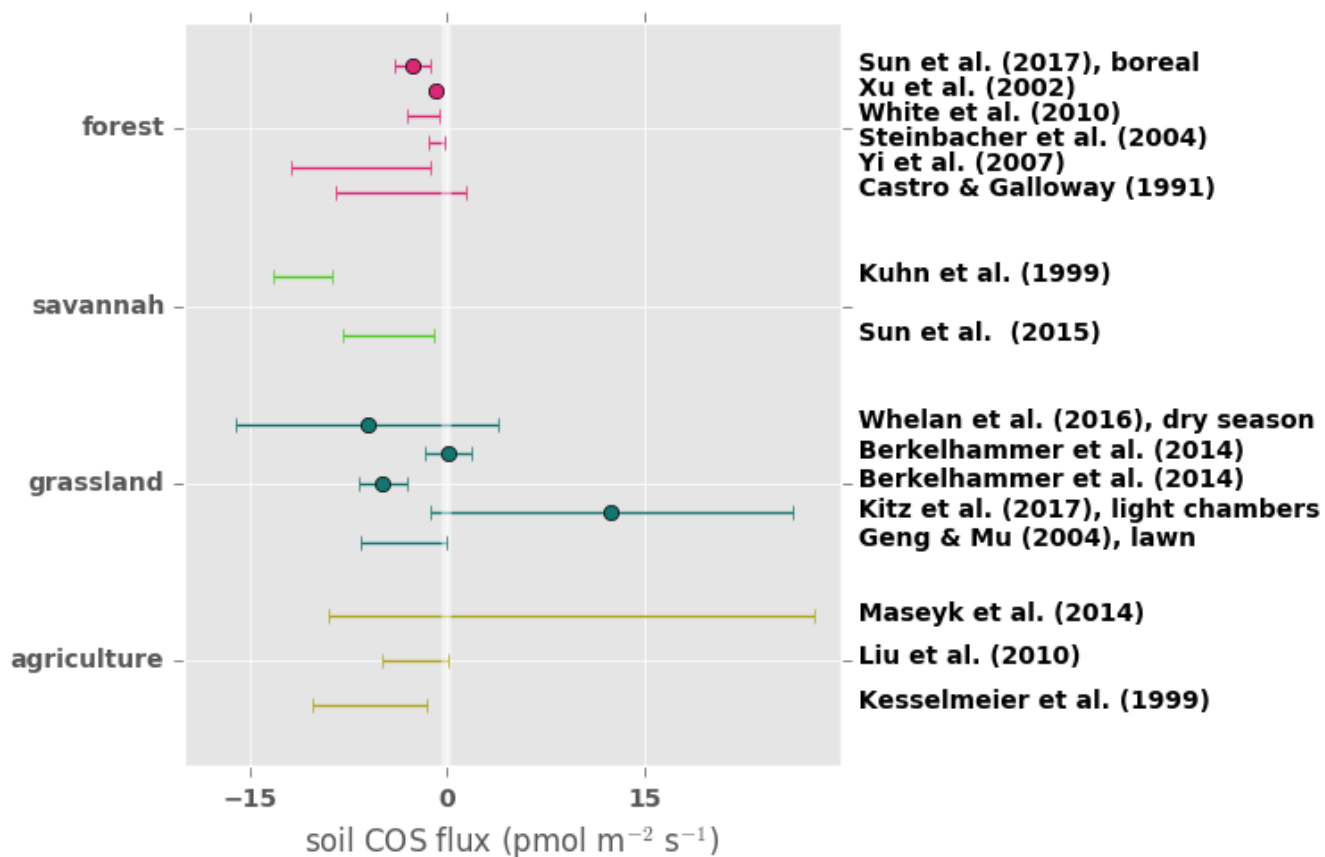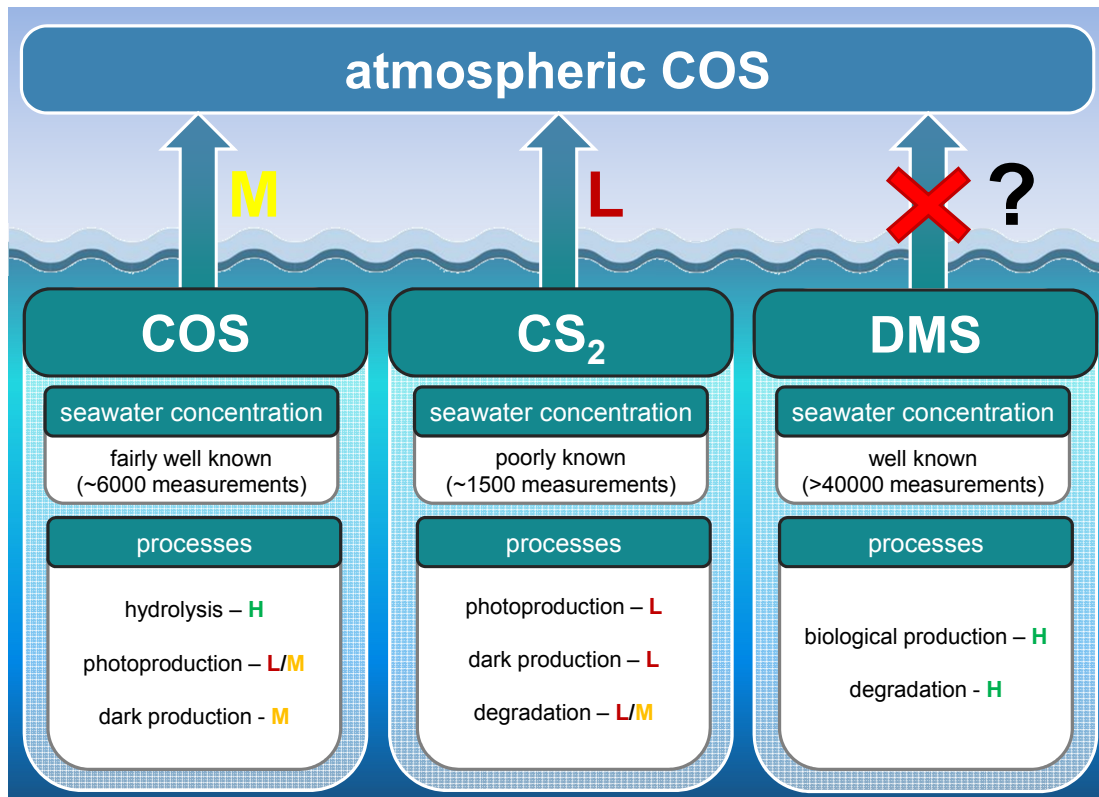
Figure 7. Field observations of soil OCS fluxes. Kuhn et al. 1999 represents an upper range due to under-pressurized soil chambers.

atmospheric COS

COS	CS$_2$	DMS
seawater concentration	**seawater concentration**	**seawater concentration**
fairly well known (~6000 measurements)	poorly known (~1500 measurements)	well known (>40000 measurements)
processes	**processes**	**processes**
hydrolysis – H	photoproduction – L	biological production – H
photoproduction – L/M	dark production – L	degradation - H
dark production - M	degradation – L/M	

Level of understanding: H – high, M – medium, L - low

Figure 8. Marine contribution to the atmospheric OCS loading from direct and indirect (CS$_2$) emissions. The sea surface concentration determines the magnitude of the oceanic emissions, and the uncertainty in global emissions decreases with increasing numbers of measurements. The understanding of processes is important to extrapolate from small-scale observations to a regional or global scale and varies between a low level of understanding for CS$_2$ (i.e. few process studies available) to a medium level of understanding for OCS (i.e. several process studies available, but considerable spread in quantifications across different locations). We recommend reconsidering the contribution of oceanic DMS emissions.
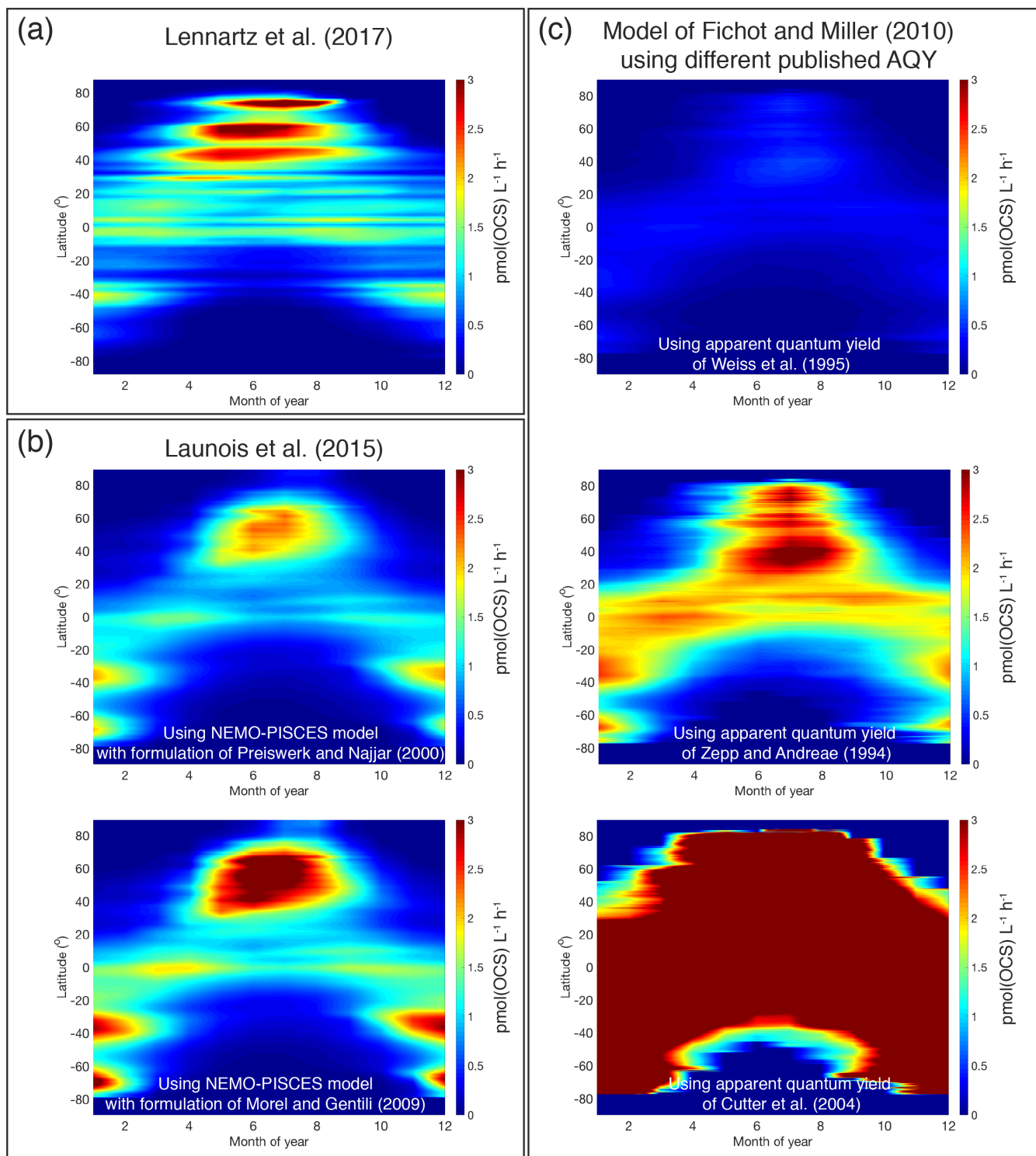
(a) Lennartz et al. (2017)

(b) Launois et al. (2015)

Using NEMO-PISCES model
with formulation of Preiswerk and Najjar (2000)

Using NEMO-PISCES model
with formulation of Morel and Gentili (2009)

(c) Model of Fichot and Miller (2010)
using different published AQY

Using apparent quantum yield
of Weiss et al. (1995)

Using apparent quantum yield
of Zepp and Andreae (1994)

Using apparent quantum yield
of Cutter et al. (2004)

Figure 9. Comparison of OCS photoproduction rates (averages for surface mixed layer, pmol(OCS) L^{-1} h^{-1}) modeled using different approaches and demonstrating discrepancies between methods: (A) Hovmöller (latitude-time) plot of rates calculated using the approach described in Lennartz et al. (2017). (B) Same Hovmöller plot generated with the approach described in Launois et al. (2015) and two

5   different formulations for CDOM absorption coefficients from Preiswerk and Najjar (2000) and Morel and Gentili (2004). (C) Same Hovmöller plots generated with the photochemical model of Fichot and Miller (2010) and the published spectral apparent quantum yields of Weiss et al. (1995), Zepp and Andreae (1994), and Cutter et al. (2004).
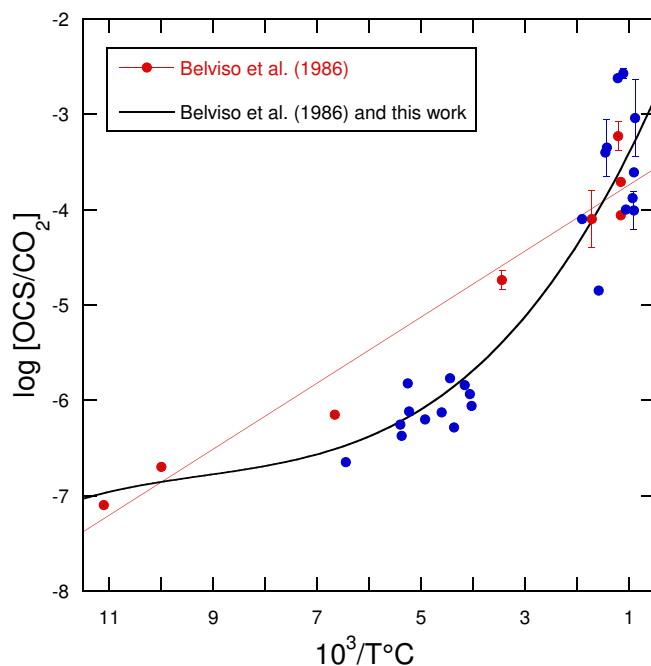
10

Figure 10. Decimal logarithm of the OCS/CO_2 ratios plotted against the reciprocal of the emission temperature of the gases for volcanos. The red dots refer to the analytical data published by Belviso et al. (1986) and the red line corresponds to the linear model used in that study to evaluate the volcanic

15   contribution to the atmospheric OCS budget. The blue dots refer to measurements published by others since 1986 (Chiodini et al., 1991; Notsu and Toshiya, 2010; Sawyer et al., 2008; Symonds et al., 1992). The better fit through all measurements is obtained using a polynomial of the third order ($R^2 = 0.89$, n = 31).
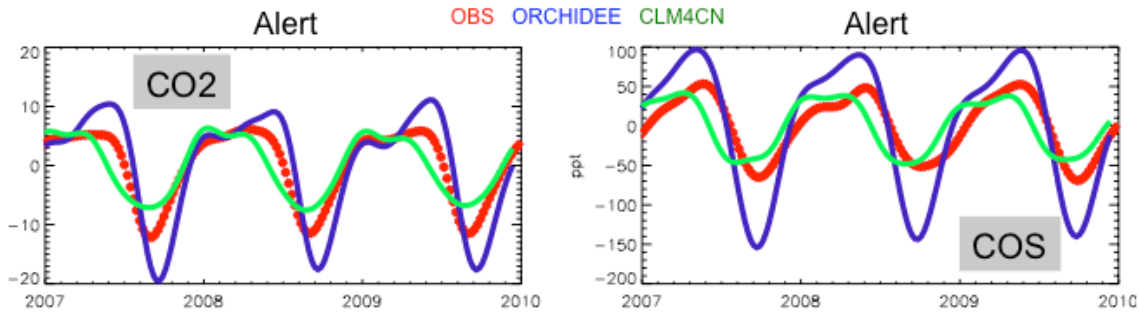
81

Figure 11. Smoothed seasonal cycles of OCS (right) and CO_2 (left) monthly mean mixing ratios, simulated at Alert station, Canada, obtained after removing the annual trends. Simulations are obtained with the LMDz transport model using two flux scenarios for the vegetation uptake of OCS, calculated with the GPP of ORCHIDEE and CLM4CN models; the other OCS flux components are identical (see Launois et al. (2015)). Observations (red) are from the NOAA-ESRL global monitoring network (Montzka et al., 2007) averaged from 2007 to 2010.
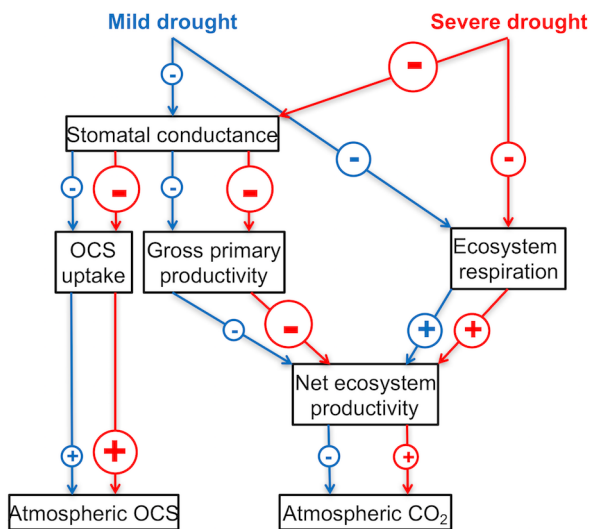

Figure 12. The impacts of droughts on biosphere processes and atmospheric CO_2 and OCS. Blue arrows show the impacts of mild droughts; red arrows show impacts of severe droughts. Plus signs show positive impacts; minus signs show negative impacts. The relative strength of the impacts is shown by the size of the signs.
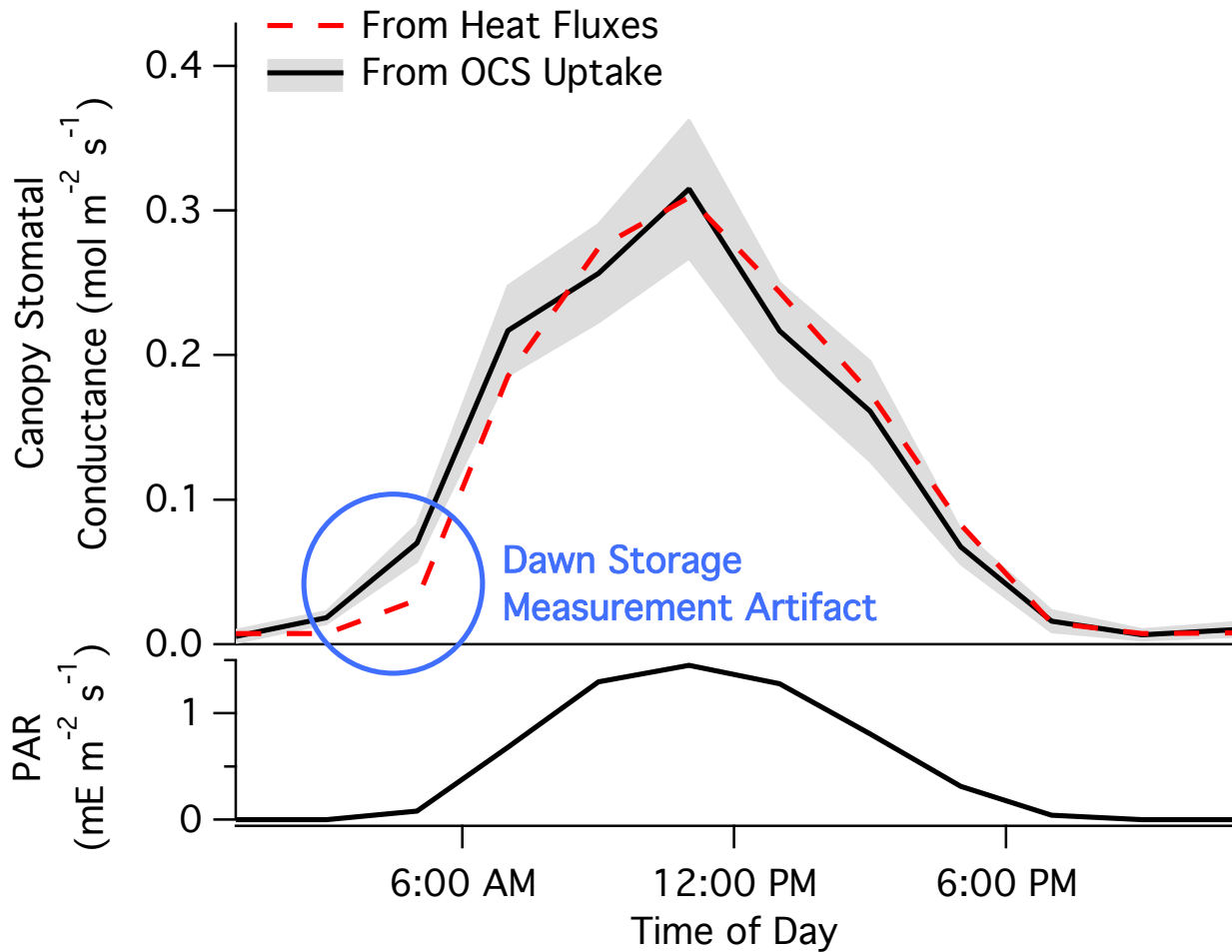
Figure 13. Composite diel cycles of stomatal conductance derived from the OCS uptake (solid black
line with grey bands) and from the sensible and latent heat fluxes (red dashed line), along with
photosynthetically active radiation (PAR, bottom panel) for context, including May through October of
2012 and 2013. Lines connect the mean values of each 2 h bin. The grey bands depict standard errors in
the means as estimated from the variability within each bin. Adapted from Wehr et al. (2017), which
discusses the dawn storage measurement artifact indicated here by the blue circle.
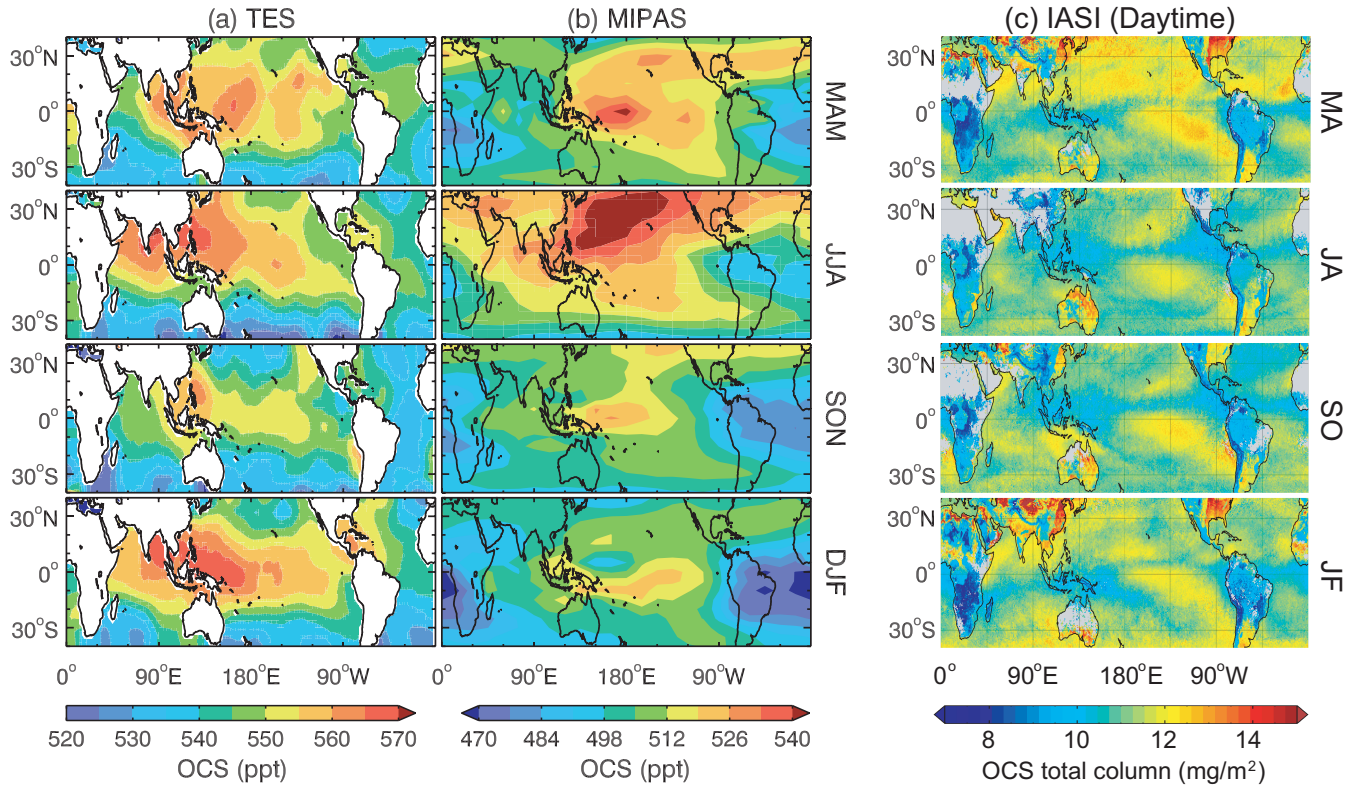
Figure 14. Comparisons of the seasonal horizontal distribution of retrieved OCS from (a) TES (averaged between 200–900 hPa), (b) MIPAS (250 hPa), and (c) IASI (total column). A 20° × 20° spatial smoothing has been applied to TES and MIPAS data. The IASI spatial patterns are of resolution 0.5° × 0.5° and are extracted from Vincent and Dudhia (2017). Missing data are represented by white areas in panels (a) and (b) and by gray areas in panel (c).
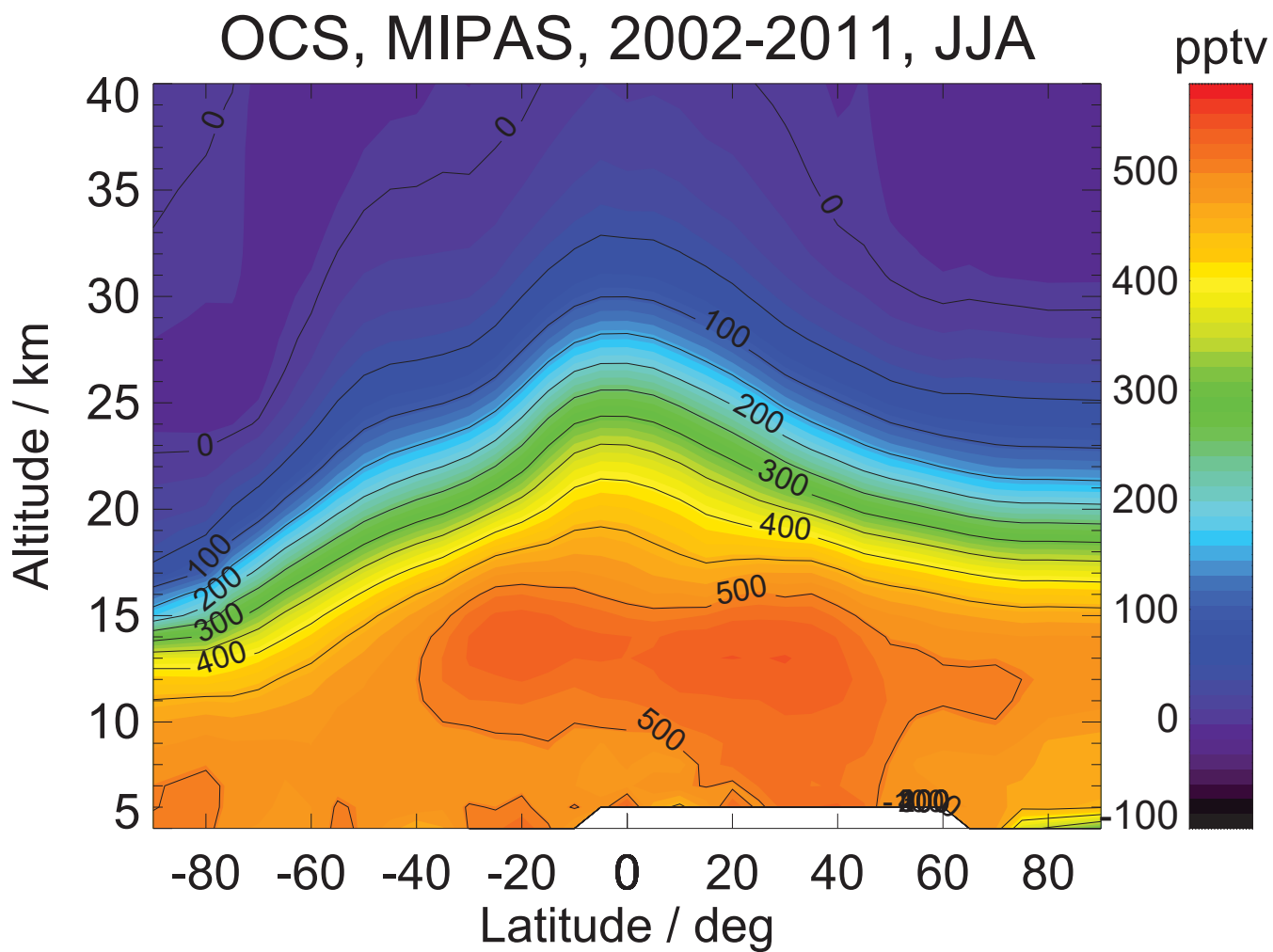
84

Figure 15. Latitudinal distribution of OCS, observed by MIPAS. Extracted from Glatthor et al. (2017).

5

Table 1. In situ fluxes of forest ecosystems. Some of this data is presented in Fig. 2.

Location; cover; time	Reported fluxes (pmol m^{-2} s^{-1})	Reference
Harvard Forest, Massachusetts, USA; red oak, red maple; Jan–Dec 2011, May–Oct 2012, May–Oct 2013	Near 0 in winter and at night to ~-50 at peak leaf area and light. Anomalous emissions in summer found in the 2015 study were not observed during subsequent summers.	Wehr et al. (2017) and Commane et al. (2015)
Niwot Ridge, Colorado, USA; populus and pinus; Aug 13–18, 2012	Leaf chamber flux near 0 at night to a peak at ~-50; soil flux between 0 and -7.	Berkelhammer et al. (2014)
Solling Mountains, Germany; spruce; summer, fall, 1997–1999	Relaxed eddy accumulation, -93±11.7 uptake; large nighttime emissions	Xu et al.(2002)
3 pine forests, Israel; pine; Growing season 2012	Eddy flux covariance, at 3 pine forests on a precipitation gradient, daylight averages were -22.9±23.5, -33.8±33.1, and -27.8±38.6.	Asaf et al. (2013)
Boreal forest, Hyytiälä, Finland; pine; June-November 2015	Nighttime fluxes -6.8 ± 2.2 (radon-tracer method) and -7.9 ± 3.8 (eddy covariance), daytime fluxes -20.8 (eddy covariance).	Kooijmans et al. (2017)

Table 2. OCS concentrations observed in rivers and lakes compared to ocean observations in Lennartz et al. (2017).

Location; time	OCS concentration	Reference
lake, surface, Canada	1.1 nmol L^{-1}	Richards et al. (1991)
lake, surface, China	910 ± 73 pmol L^{-1}	Du et al. (2017)
river, 0.25 m depth	636 ± 14 pmol L^{-1}	Radford-Knoery and Cutter (1993)
river, 3.84 m depth	415 ± 13 pmol L^{-1}	Radford-Knoery and Cutter (1993)
lake, whole water column, Canada	90 to 600 pmol L^{-1}	Richards et al. (1991)
lake, hypolimnion, Antarctica	233 to 316 pmol L^{-1}	Deprez et al. (1986)
Eastern Pacific Ocean	28.3 ± 19.7 pmol L^{-1}	Lennartz et al. (2017)
Indian Ocean	9.1 ± 3.5 pmol L^{-1}	Lennartz et al. (2017)

lake, hypolimnion, Switzerland	detected "occasionally"	Fritz and Bachofen (2000)

Table 3. Measurements of OCS water concentration at the ocean surface (0–5 m) in open ocean, coastal, shelf, and estuary waters. [a]Converted from ng L^{-1} with a molar mass of OCS of 60.07g. [b]Converted from ng S L^{-1} with a molar mass of S of 32.1g. [c]Continuous measurements.

References	Season	Region	Water concentration of OCS mean ±SD (pmol L^{-1})	No. of samples
Open ocean				
Mihalopoulos et al. (1992)	Mar/May 1986 Jul 1987	Indian Ocean	19.9 ±0.5[a] 19.9 ±1.0[a]	20 14
Staubes and Georgii (1993)	Nov–Dec 1990	Southern Ocean	109[b]	126
Ulshöfer et al. (1995)	Apr/May 1992 Jan 1994 Sep 1994	North Atlantic Ocean	14.9 ±6.9 5.3 ±1.6 19.0 ±8.3	118 120 235
Flöck and Andreae (1996)	Jan 1994	Northeastern Atlantic	6.7 (4–11)	120
Ulshöfer and Andreae (1998)	Mar 1995	Western Atlantic	8.1 ±7.0	323
Von Hobe et al. (1999)	Jun/Jul 1997	Northeastern Atlantic Ocean	23.6 ±16.0	940
Kettle et al. (2001)	Aug 1999	Atlantic (meridional transect)	21.7 ±19.1	783
Von Hobe et al. (2001)	Aug 1999	North Atlantic	8.6 ±2.8	518

87

Xu et al. (2001)	Oct/Nov 1997	Atlantic (meridional	14.8 ±11.4	306
	May/Jun 1998	transect)	18.1 ±16.1	440
Lennartz et al. (2017)	Jul/Aug 2014	Indian Ocean	9.1 ±3.5	[c]

Coastal, shelf and estuary waters

Cutter et al. (1993)	Jun/Jul 1990	Western North		
	Aug 1990	Atlantic	400	15
		Shelf	300–12,100	?
		Estuary		
Mihalopoulos et al. (1992)	Dec 1989-1990	Indian Ocean, Mediterranean Sea, French Atlantic Coast	400–70,300	336
	May 1987			
Andreae and Ferek (1992)	averages of several cruises	averages of several cruises (shelf+coast)	112	157
Ulshöfer et al. (1996)	Jul 1993	Mediterranean Sea (shelf)	43 ±24	34
Uher et al. (1997)	Sep 1992	North Sea (shelf)	49.1 ±11.7	69
Zhang et al. (1998)	Oct 1991– May 1994	Chesapeake Bay (coast)	320.0 ±351	23
Lennartz et al. (2017)	Oct 2015	Eastern tropical South Pacific (shelf)	40.5 ±16.4	[c]

5

Table 4. Total bottom-up atmospheric OCS budget. See text for description of calculations.

Component	OCS global flux Gg S year^{-1}	Data source
Forests	-2200 – -1800	
Grasslands	-1700 – -660	
Deserts	-170 (?)	See Table 5. No field data exists for deserts.
Agricultural, excluding rice	-66 – +18	
Freshwater	+0.8 – +12	
Fungus/Lichen/Mosses	-8 – -21	See calculation below
Wetlands	-150 – +290	
Ocean	Total: +265 ±210 OCS direct: +130 ± 80 OCS from oc. CS$_2$: +135 ±130 OCS from oc. DMS: 0 (+80)	Lennartz et al., (2017), see Sect. 2.3 for discussion
Anthropogenic	+400 ± 180	For the year 2012, Zumkehr et al. (in press)
Biomass Burning	+116 ± 52	Campbell et al. (2015)
Volcanoes	+25 – +43	See Sect. 2.6
Tropospheric destruction by OH radical	-82 – -130	Berry et al., (2013), Kettle et al., (2002) and Watts (2000)
Stratospheric destruction by photolysis	-30 – -80 or -50 ± 15	Barkley et al. (2008), Chin and Davis (1995), Crutzen (1976), Engel and Schmidt (1994), Krysztofiak et al. (2015), Turco et al. (1980), and Weisenstein et al. (1997)
Total	-4100 – -1200	

5

Table 5. GPP and OCS exchange estimates by biome.

[a]For the purpose of this estimate, we use the soil fluxes from temperate forests.

[b]Range of values from Castro and Galloway (1991), Steinbacher et al., (2004), White et al. (2010), and Yi et al. (2007).

5 [c]The average reported here is the average and one standard deviation from non-vegetated plots in a boreal forest, defined as plots having less than 10% vegetation cover (Simmons, 1999).

[d]Range from Whelan and Rhew (2016). The error estimate here is different from the one reported because a different LRU was used. Kitz et al. (2017) found soil-only OCS production of +60 pmol m^{-2} s^{-1} in an alpine grassland.

10 [e]In a laboratory incubation study, Whelan et al. (2016) found that desert soils exhibit a very small uptake. No field measurements have been published to our knowledge.

[f]The smaller production is from De Mello and Hines (1994). The larger production is an average estimate from Fried et al. (1993).

[g]Post-harvest soil exchange estimate from the wheat field (Billesbach et al., 2014) investigated further 15 in Whelan and Rhew (2015).

[h]See Table 1.

[i]From Simmons et al. (1999).

[j]Range from Whelan and Rhew (2016), encompassing observations of a grass field by Yi and Wang (2011).

20 [k]Range reported in DeMello and Hines (1994), encompassing values observed by a bog microcosm by Fried et al. (1993).

[l]High value for cotton, low value for wheat in Asaf et al. (2013). Daily fluxes for a wheat field investigated by Billesbach et al. (2014) were -21 during the growing season and +18 after harvest. Agricultural soils have been shown to emit a large portion of OCS compared to plant uptake under hot 25 and dry conditions (Whelan et al., 2016; Whelan and Rhew, 2015).

Biome	GPP estimated by Beer et al. (2010) in Pg C y^{-1}	Biome area (10^9 ha)	Anticipated F_{OCS}, plants from GPP estimate (pmol m^{-2} s^{-1})	F_{OCS}, soil (pmol m^{-2} s^{-1})	F_{OCS}, ecosystem By GPP method (pmol m^{-2} s^{-1})	F_{OCS}, ecosystem Field observations (pmol m^{-2} s^{-1})

Tropical forests	40.8	1.75	-102	No data[a]	-110 - -100	No data
Temperate forests	9.9	1.04	-42	-8 to 1.45[b]	-50 - -40	~0 to 93[h]
Boreal forests	8.3	1.37	-27	1.2 to 3.8[c]	-26 - -23	0 to -22[i]
Tropical savannas and grasslands	31.3	2.76	-32	No data	-57 - -25	No data
Temperate grasslands and shrublands	8.5	1.78	-21	-25 to 7.3[d]	-46 - -13	-26 growing season; +6.1 non-growing season[j]
Deserts	6.4	2.77	-6	0 (?)[e]	-6 (?)	No data
Tundra	1.6	0.56	-13	5.27 to 27.6[f]	-8 - 15	-15 to -1
Croplands	14.8	1.35	-48	-18 to 40[g]	-66 - -8	-22 to -16, +18 during non-growing season[l]
Total	121.7	13.38	-291	-44 to 80	-370 - -200	

Table 6. Components of the OCS budget and data gaps.

Component	Notes, critical data gaps
Vascular plant leaves	Vascular plant leaves have a well-established exchange of OCS that follows stomatal conductance. OCS is destroyed by both RuBisCO and CA in plant leaves, though it most often encounters CA first. The point of destruction is different for OCS and CO_2, though the correlation between their uptakes is consistent under high light conditions. Nocturnal uptake and role of phyllosphere is not well characterised and "mesophyll" conductance to COS is not well constrained
Non-vascular plants and lichen	Few studies have addressed non-vascular plants. Bryophytes and lichen have been found to take up OCS depending on their water content, sometimes regardless of light level.
Soil	Most soils are generally small sinks of OCS, making up less than 10% of the total ecosystem flux Non-desert soils exhibit large OCS emissions under hot and dry conditions. These OCS-emitting soils include both agricultural soils and some uncultivated soils. It is unknown what controls the magnitude of the soil source term.
Terrestrial ecosystem	Ecosystem-scale flux measurements are available only from a handful of studies on a limited number of ecosystems and during relatively short periods of time. No studies from the tropics and only one study in boreal forests have been published.
Regional terrestrial	The highly mechanistic leaf-enzyme kinetic approach to modeling plant-atmospheric OCS exchange yielded similar results to the mechanistically simple LRU approach when focusing on the peak of the North American growing season. However, laboratory studies demonstrate that LRU is not constant, and the minimum spatial and temporal scales at which the constant LRU approximation is viable are unknown. Uncertainties in non-plant OCS fluxes, particularly from soils, remain under-constrained at regional spatial scales.
Surface ocean	Consistent surface measurements using different detection methods are needed, but generally data are sparse for surface measurements of OCS (currently ca. ~6000 samples); more continuous measurements covering full diurnal cycles are needed especially for the Pacific, Indian, Southern, and Arctic oceans.
Deep ocean	Concentration profiles have been reported from only very

	few stations in the Atlantic Ocean (e.g. Cutter et al., 2004; Flöck and Andreae, 1996; Von Hobe et al., 2001).
Regional ocean	Surface measurements comprise different oceanic regimes including several meridional Atlantic transects and oligotrophic and upwelling regions. Especially, data from the Arctic and Southern oceans are missing.
Freshwaters	There are few, quite small datasets of OCS concentrations in lakes and rivers. No OCS fluxes from freshwater bodies currently exist.
Global, modern	Global satellite products currently lack coverage over the land, and the location of TCCON sites are purposely chosen to observe atmospheric background. A new satellite and data product would be necessary to use OCS to answer questions about climate-carbon feedbacks globally.
Global, paleo	Recent advances have allowed better interpretation of OCS in firn and ice air. There are still only a handful of cores that have been analyzed for OCS.

5